Thermodynamics and Mechanics of Freezing Soil Around a Pipeline

FINAL REPORT

for

EARTH PHYSICS BRANCH

ENERGY, MINES AND RESOURCES CANADA

INTERNAL REPORT - IR 51
GEOTECHNICAL SCIENCE LABORATORIES

CARLETON UNIVERSITY

OTTAWA, CANADA

K1S 5B6

NOV. 1986

DSS Contract Number: OST85-00285

Title: Investigation of Soil Freezing in Association with a Buried Chilled Pipeline in a Large-Scale Test Facility - Phase V

1 cm

Frontispiece: Sample of frozen soil from below pipeline at point of transition between Caen silt and SNEC sand. The non-heaving sand is to the far right. Note the ice lenses deformed by differential frost heave which in turn deforms the pipe. The photograph is of a preserved sample, and was taken at room temperature (see report for further details).

TABLE OF CONTENTS

		PAGE
FOREWORD		iii
LIST OF FIGURES		v
I	EXPERIMENTAL DESIGN	1
	1.1 General	1
II	EXPERIMENTAL CONDITIONS	3
	2.1 Test Facility	3
	2.2 Instrumentation	3
	2.3 Operating Conditions	6
III	EXPERIMENTAL OBSERVATIONS, SECOND THAW PERIOD	7
	3.1 General	7
	3.2 Thermal Regime	7
	3.3 Hydrologic Regime	7
	3.4 Pipe Settlement	10
	3.5 Surface Expression of Thaw and Surface Fissures	16
	3.6 Thaw Settlement from Telescopic Heave Rods and Magnetic Heave Device	24
	3.7 Stress in the Ground	24
IV	DISCUSSION OF FINDINGS - THAW PERIOD	31
	4.1 Conditions	31
	4.2 Non-reversible Displacement of Pipe	31
	4.3 Soil Cracking	32
	4.4 Total Stresses in Thawed Soil	33
V	INSTRUMENTATION AND CONDITIONS FOR THIRD FREEZE PERIOD	34
	5.1 General	34
	5.2 Details of Re-instrumentation	36
	5.2.1 Pipe Stress	36
	5.2.2 Thermal Regime	37
	5.2.3 Frost Heave	37
	5.2.4 Soil Stress	40
VI	EXPERIMENTAL OBSERVATIONS, THIRD FREEZE PERIOD	42
	6.1 General	42
	6.2 Thermal Regime	42
	6.3 Hydrologic Regime	47
	6.3.1 Phase Composition	47
	6.3.2 Volumes of Water Added	51

6.4 Pipe Heave 54
6.5 Frost Heave from Magnetic Heave Device 54
6.6 Surface Expression of Thaw and Surface Fissures 62
6.7 Pipe Stress 62
6.8 Stress in the Ground 65

VII EXAMINATIONS OF SOIL BEHAVIOUR MADE OFF SITE 70

7.1 Strain-Rate-Controlled Uniaxial Compression Tests with the Caen Silt 70
7.2 Introduction 70
7.3 Sample Preparation 71
7.4 Test Equipment and Procedure 71
7.5 Testing Programme and Results 74
7.6 Discussion of Test Results 87
7.6.1 Stress-strain Behaviour 87
7.6.2 Dilatancy 91
7.6.3 Strength Versus Strain Rate Curves (Rheological Curves) 91
7.6.4 Effect of Ice Lenses on Strength 92
7.6.5 Comparison with Previous Test Results .. 92
7.7 Conclusions 92

VIII STATUS OF CANADA-FRANCE PROJECT 94

IX CONCLUSIONS 96

REFERENCES 99

APPENDICES

I. Selected Temperature Data 100

II. Selected Heave Data 104

III. Notes on Petur Cell Assembly 109

FOREWORD

This report summarizes the findings of the Canada-France pipeline ground freezing project during the second thaw period and gives preliminary information from the third freeze period. The principle aim of the project is to study the effects of ground freezing and pipeline interactions in a controlled environment facility at Caen, Normandy. Over a five-year period, alternating periods of freezing and thawing have produced significant deformations of the buried 273 mm diameter steel pipe.

Although the contract period (one year) commenced on July 1, 1985, only results from September 18, 1985 to July 1, 1986 are reported and discussed in detail. The period July 1 to September 18, the last 172 days of a 700 day freeze cycle was reported previously in Geotechnical Science Laboratories (Report II 1985). The second thaw period started September 18, 1985 and ran for 19 weeks. The third freeze cycle began on March 3, 1986. Preliminary findings for this cycle are reported along with a discussion of changes in instrumentation which were installed in February 1986.

This report was prepared by D.E. Patterson (Project Manager, Ottawa), D.E. Lawrence (Project Manager, Caen) and Dr. P.J. Williams (Principal Investigator) with important contributions from Dr. M.W. Smith (Co-Principal Investigator), Dr. B. Ladanyi and P. Lebret (LCPC). The efforts of the members of the Centre du Geomorphologie and LCPC are greatly appreciated. Special thanks to A. Dupas (LCPC) whose untiring contribution to the project has ensured its viability.

The Canada-France project is comprised of a team of Canadian and French scientists, graduate students and technicians. The project as a whole is supervised by a scientific committee. The members and their affiliations are listed below.

M. Jaime Aguirre-Puente, Laboratoire d'Aerothermique, Centre National de la Recherche Scientifique

M. J-P. Lautridou, Centre National de la Recherche Scientifique

* M. Michel Fremond, Laboratoire Central des Ponts et Chaussees

Dr. A. Judge, Earth Physics Branch, Energy, Mines and Resources, Canada

M. Chantereau, Laboratoire Central des Ponts et Chaussees

M.S. Philippe, Laboratoire Central des Ponts et Chaussees

Dr. M.W. Smith, Geotechnical Science Laboratories, Carleton University

** Dr. P.J. Williams, Geotechnical Science Laboratories, Carleton University

* chairman France
** chairman Canada

D.E. Patterson

Project Manager, Ottawa Canada-France Ground Freezing Experiment

D.E. Lawrence

Project Manager, Caen
currently
Head, Environmental Operations Environment and Right-of-Way Branch, National Energy Board

P.J. Williams

Principal Investigator, Director, Geotechnical Science Laboratories

LIST OF FIGURES

Figure		
2.1	Longitudinal section of trough	4
2.2	Cross-section of trough	5
3.1	Soil temperatures in silt at BB section	8
3.2	Soil temperatures in silt at BB section, selected thermocouples	9
3.3	Unfrozen water content under pipe, BB section, 8 to 68 cm depths	11
3.4	Unfrozen water content under pipe, BB section, 73 to 88 cm depths	12
3.5	Pipe settlement along axis, second thaw	13
3.6	Surface settlement in silt during second thaw, section AA	14
3.7	Surface settlement in sand during second thaw, section BB	15
3.8	Pipe elevation at the start of freeze cycles	17
3.9	Pipe stress during second thaw	18
3.10	Surface elevation last day of second freeze	19
3.11	Surface elevation during second thaw, Day 37	20
3.12	Surface elevation during second thaw, Day 83	21
3.13	Surface fissures, day 30 second thaw	22
3.14	Heave rods at BB section in silt, second thaw: net settlement	25
3.15	Magnetic heave device at BB in silt, second thaw: net change from day 0	26
3.16	Magnetic heave device at sand/silt transition, second thaw: net change from day 0	27
3.17	Soil pressures at BB section in silt, second thaw	28
3.18	Soil pressures at AA section in sand, second thaw	30
5.1	Location of new instrumentation for third freeze	35
5.2	Magnetic heave device	38

6.1 Soil temperature in silt for selected dates, site 1 43

6.2 Depth of frost penetration, sites 1 and 10 44

6.3 Soil temperatures along pipe axis, day 52 third freeze 45

6.4 Soil temperatures along pipe axis, day 100 third freeze 46

6.5 Soil temperatures at section BB in silt, day 52 48

6.6 Soil temperatures at section BB in silt, day 100 49

6.7 Unfrozen water contents at section BB in silt for selected dates 50

6.8 Water added during third freeze 52

6.9 Pipe heave along axis, third freeze 55

6.10 Pipe heave comparison, day 99, second and third freeze: pipe elevations 56

6.11 Pipe heave comparison, day 99, second and third freeze: difference in elevation 57

6.12 Surface heave, section BB in silt, third freeze 58

6.13 Surface heave, section AA in sand, third freeze 59

6.14 Total heave at site 1 in silt, third freeze 60

6.15 Differential heave at various depths, site 1, third freeze 61

6.16 Surface elevation during third freeze, day 116 63

6.17 Pipe stress, third freeze 64

6.18 Pipe stress at the start of the three freeze cycles 66

6.19 Pipe stress comparison, day 99 during second and third freeze 67

6.20 Soil pressures at section BB in silt, third freeze 68

6.21 Soil pressures at section AA in silt, third freeze 69

7.1 Caen Silt: Grain size distribution curve 72

7.2 Caen Silt: Test 28, Stress-strain curves at -1 C and 5.52×10^{-2} min^{-1} 75

7.3 Caen Silt: Test 17, Stress-strain curves at -1 C and 5.02×10^{-3} min^{-1} 76

7.4 Caen Silt: Test 39, Stress-strain curves at -1 C and 9.25×10^{-4} min^{-1} 77

7.5 Caen Silt: Test 23, Stress-strain curves at -1 C and 1.55×10^{-4} min^{-1} 78

7.6 Caen Silt: Test 36, Stress-strain curves at -1 C and 2.86×10^{-5} min^{-1} 79

7.7 Caen Silt: Test 37, Stress-strain curves at -1 C and 5.64×10^{-6} min^{-1} 80

7.8 Caen Silt: Test 27, Stress-strain curves at -2 C and 5.51×10^{-2} min^{-1} 81

7.9 Caen Silt: Test 15, Stress-strain curves at -2 C and 4.83×10^{-3} min^{-1} 82

7.10 Caen Silt: Test 19, Stress-strain curves at -2 C and 1.59×10^{-4} min^{-1} 83

7.11 Caen Silt: Test 32, Stress-strain curves at -2 C and 2.85×10^{-5} min^{-1} 84

7.12 Caen Silt: Test 11, Stress-strain curves at -5 C and 4.93×10^{-3} min^{-1} 85

7.13 Caen Silt: Test 9, Stress-strain curves at -5 C and 1.60×10^{-4} min^{-1} 86

7.14 Caen Silt. Stress-strain curves in uniaxial compression obtained at -1 C and at different strain rates 88

7.15 Caen Silt. Stress-strain curves in uniaxial compression obtained at -2 C and at different strain rates 89

7.16 Caen Silt: Rheological curves for temperatures of -1, -2 and -5 C 90

I. EXPERIMENTAL DESIGN

1.1 General

Previous reports on this project have demonstrated that the freezing of soil around a buried chilled pipeline leads to heaving of the soil and the pipeline, the amount of heave being dependant upon soil type. When a pipeline traverses two soils with different heave susceptibilities, differential heave occurs. This leads to deformation of the pipeline and the creation of substantial stresses within the pipe. These stresses could deform the pipe and lead to possible failure if remedial action is not taken.

Various soil materials heave and thaw differently, resulting in variations in pipe settlement upon thawing. Data for the two freeze-thaw periods show that upon thawing the pipe does not settle back to its original position which results in a progressive jacking of the pipe upward toward the soil surface with each freeze-thaw cycle. During subsequent freezing, frost heave will further deform an already bent pipe. Repeated freeze-thaw cycles during the operating life of a chilled gas pipe could result in deformation which may render the pipeline inoperable.

The project at Caen is unique in that it permits precise control of the physical, thermal and hydrologic variables which is not possible in field experiments. This report presents data and observations from the second thaw period and preliminary findings of the third freeze period. Table 1 outlines the timetable of events since the start of the project.

Table 1 TIMETABLE OF EVENTS

Event	Date		Operating Conditions	
	from	to	Air/Ground (C)	Pipe temp.
First Freeze	09/21/82	08/06/83	-0.75	-2.0
Surface Thaw	08/06/83	17/10/83	+4.0	-2.0
Second Freeze	17/10/83	18/09/85	-0.75	-5.0
Second Thaw	18/09/85	01/02/86	4.0	ambient
Re-instru-mentation	01/02/86	- 03/03/86	-	-
Third Freeze	03/03/86		-0.5	-5.25

II EXPERIMENTAL CONDITIONS

2.1 Test Facility

The experiment is conducted in the "Station de Gel" at the Centre de Geomorpholgie du CNRS, Caen, France. The facility consists of a refrigerated hall 18m long by 8m wide with adjacent rooms to accommodate instrumentation and mechanical equipment. The base of the hall has been specially prepared in order to isolate the thermal and hydraulic regime of the soils and to ensure careful control of the experimental conditions. For a detailed description of the test facility and instrumentation refer to Burgess et al. 1982. Figures 2.1 and 2.2 show the longitudinal section and cross section of the facility respectively. A non-frost-susceptible sand and a frost susceptible silt have been placed in each half of the trough. An 18m long, 273 mm diameter steel pipe was buried at a depth of 30 cm within these soils. The pipe is connected to a refrigeration system to maintain pipe temperature. A separate system controls the air temperature within the hall.

2.2 Instrumentation

The thermal, hydrologic and heave characteristics of the soil are measured regularly. Information on pipe curvature and pipe stress are also gathered to examine the effects of frost heave on the pipe. Periodic measurements are made of soil density profiles and moisture content. Earlier reports give a detailed description of the instrumentation and a summary of the frequency of readings (see Geotechnical Science Laboratories, 1982, 1983, 1984a, b, 1985).

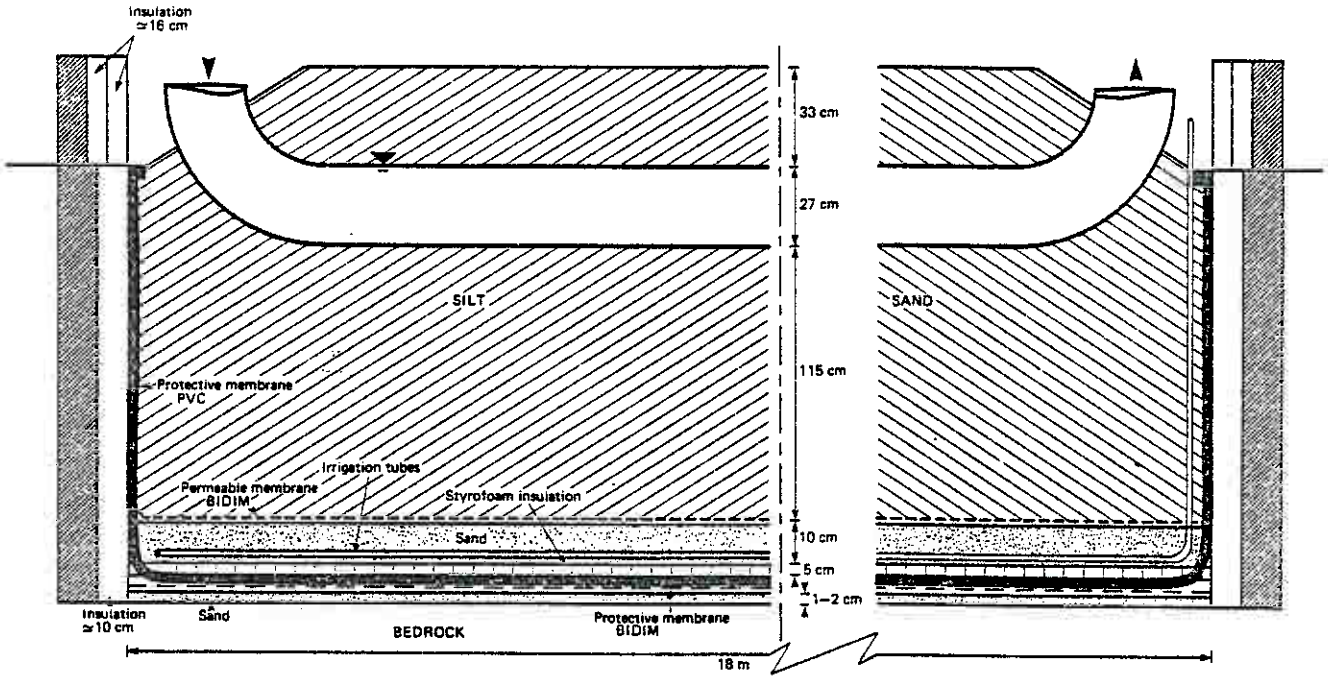

Figure 2.1 Longitudinal section of trough

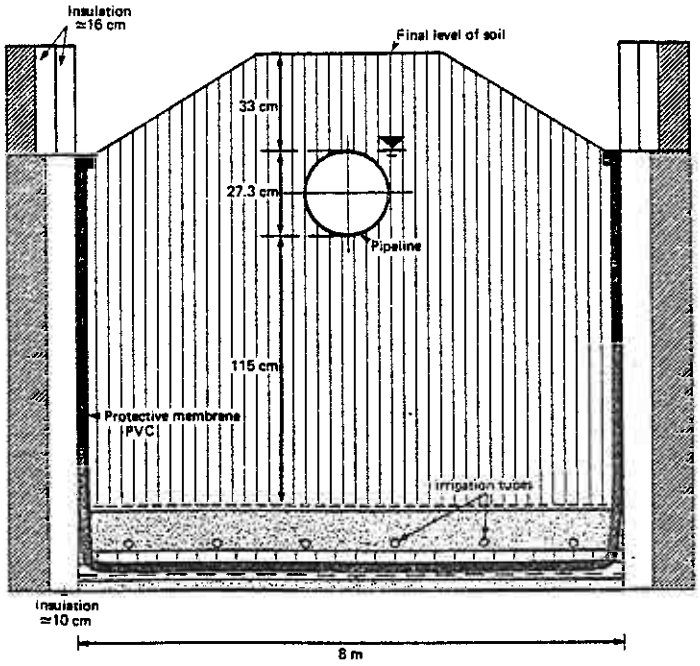

Figure 2.2 Cross-section of trough

2.3 Operating Conditions

During the second freezing period of 700 days, pipe temperature was maintained at -5.0 C and air temperature in the hall at -0.75 C. The cooling system was switched off during the subsequent 172 day period of thaw. The ground water table was maintained at approximately 30 cm below the ground surface.

III EXPERIMENTAL OBSERVATIONS, SECOND THAW PERIOD

3.1 General

Results from September 18, 1985 to March 3, 1986 are included in this section. During this period air was not circulated in the pipe and the temperature of the atmosphere was maintained at 4.0 C. The data for September 18, 1985 are the last observations for the second freeze period (day 700). This date is referred to as day 0 for the reported thaw.

3.2 Thermal Regime

The temperature profiles beneath the pipe in the silt are shown in Figures 3.1 and 3.2. These data were obtained from thermocouples and the indicated depths refer to original placement and are not corrected for heave. Figure 3.1 indicates that there was a gradual warming of the soil until thawing was complete and then a fairly rapid change at about day 80 whereby the soil warmed to ambient conditions (between 4 to 5 C). Figure 3.2 shows the change in temperature for selected thermocouples which illustrates the thaw progression of the frozen soil in more detail. Thaw progressed from the surface downwards and from the base of the pit upwards resulting in a shrinking frost bulb during the thaw period. The thaw settlement pattern of the soil and pipe is discussed in section 3.4.

3.3 Hydrologic Regime

Volumetric liquid water contents were determined from time-domain reflectometry (TDR) measurements of dielectric constant of the soil. The water content data are presented in Figures 3.3

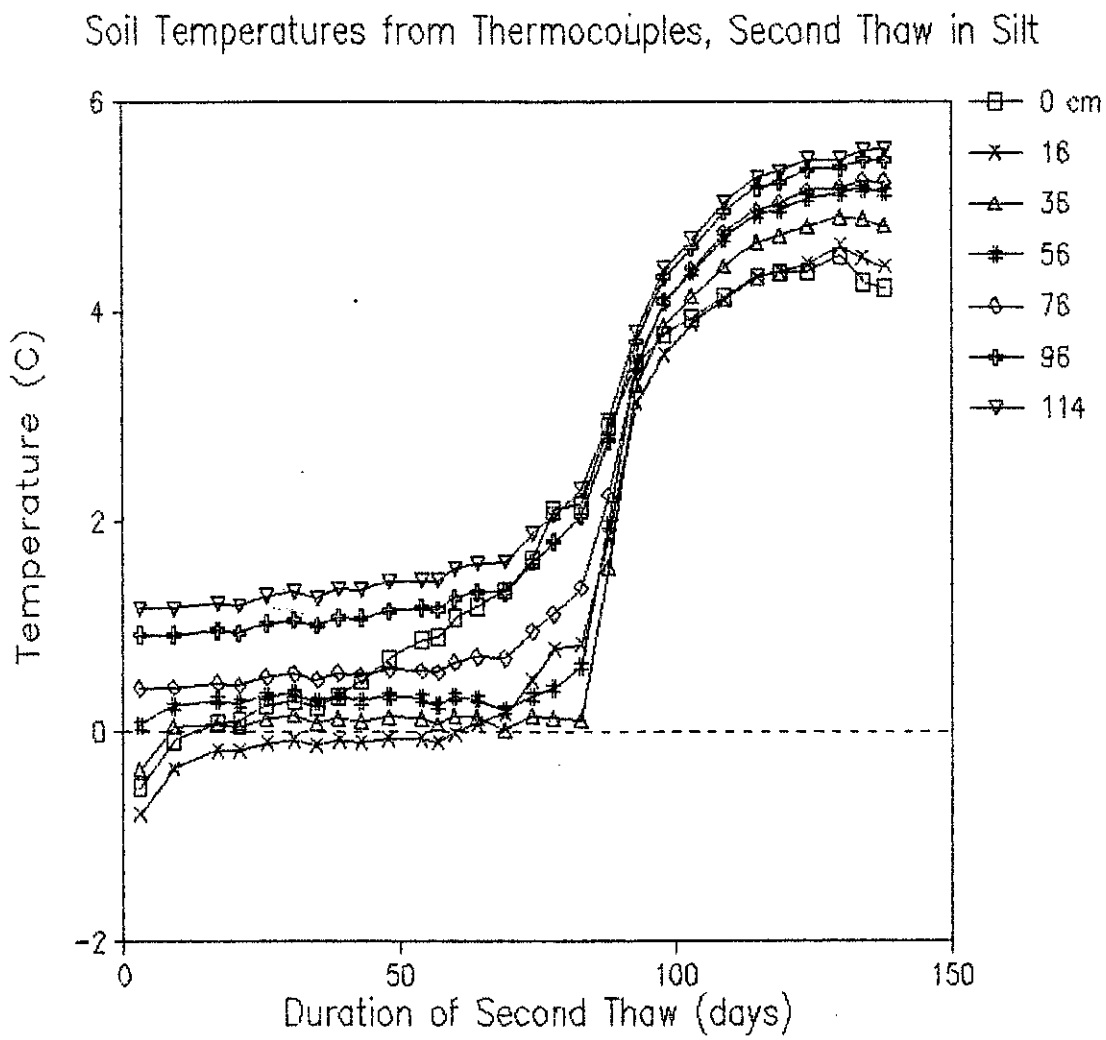

Figure 3.1 Soil temperatures beneath pipe in silt at BB section

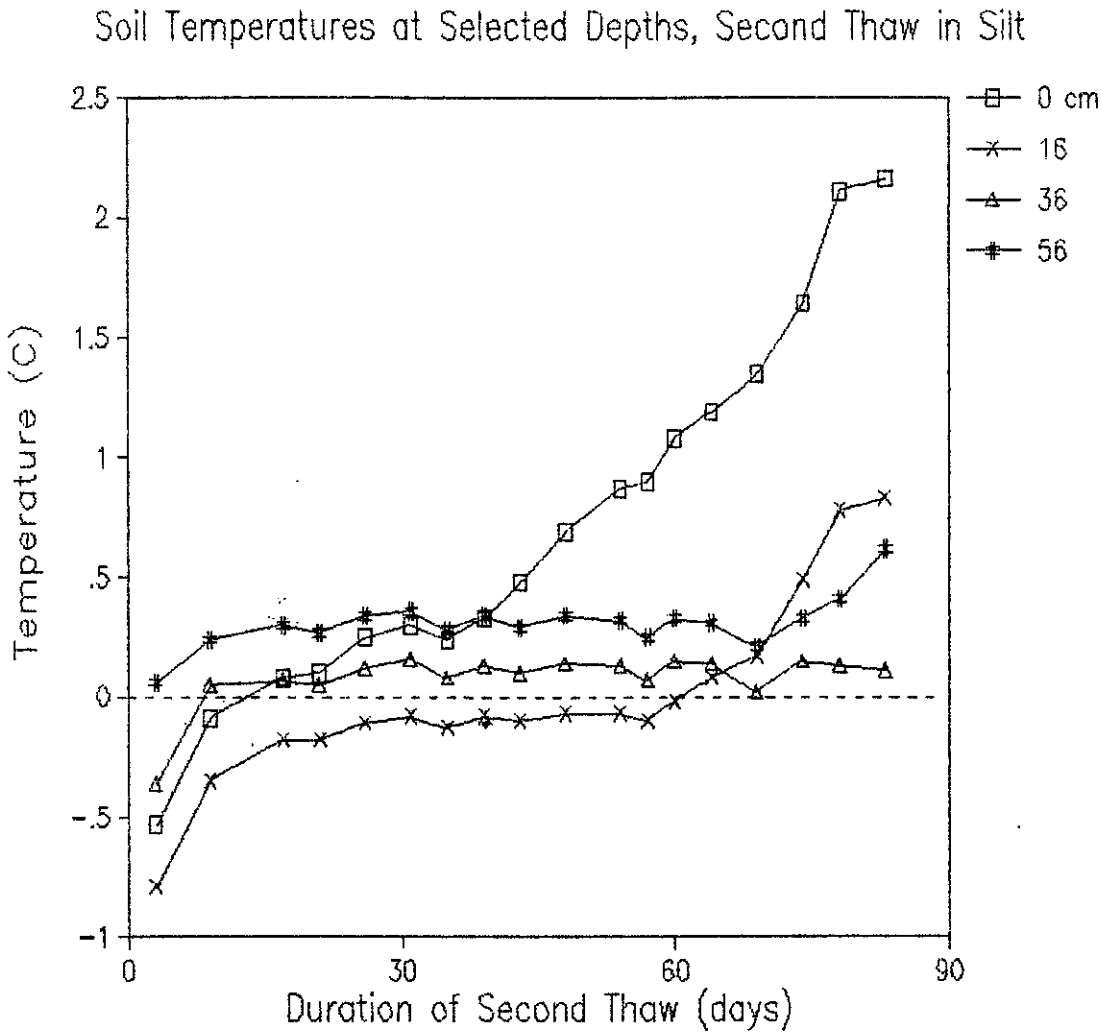

Figure 3.2 Soil temperatures beneath pipe in silt at BB section, selected thermocouples

and 3.4 for the silt section for various depths beneath the pipe. These data show the increase in volumetric (unfrozen) water content at all depths as the thaw period progresses.

It should be noted that the values for water content at 8 cm beneath the pipe are uncharacteristically low which suggests that a cavity may have formed beneath the pipe at that location. During the installation of instruments for the third freeze period it was found that cavities beneath the pipe had formed as the soil settled around the pipe. If a cavity exists, the electrical field around the TDR probe at this depth would extend into air rather than moist soil resulting in a lower value of dielectric constant (hence volumetric water content) than would normally be experienced.

3.4 Pipe Settlement

The longitudinal position and shape of the buried pipe is shown in Figure 3.5 for several dates during the thaw period. Day 0 represents the position and shape for the last day of the second thaw period (day 700). The data were obtained from optical levelling of rods affixed to the pipe which extend above the ground surface.

Figures 3.6 and 3.7 show the change in surface elevation at right angles to the pipe in the silt (section BB) and sand (section AA) respectively. The data were obtained from optical surveying of the soil surface. Both figures suggest that thaw was essentially complete around day 80.

The change in shape and position of the pipe since the start of the experiment on September 21, 1982 is shown in Figure

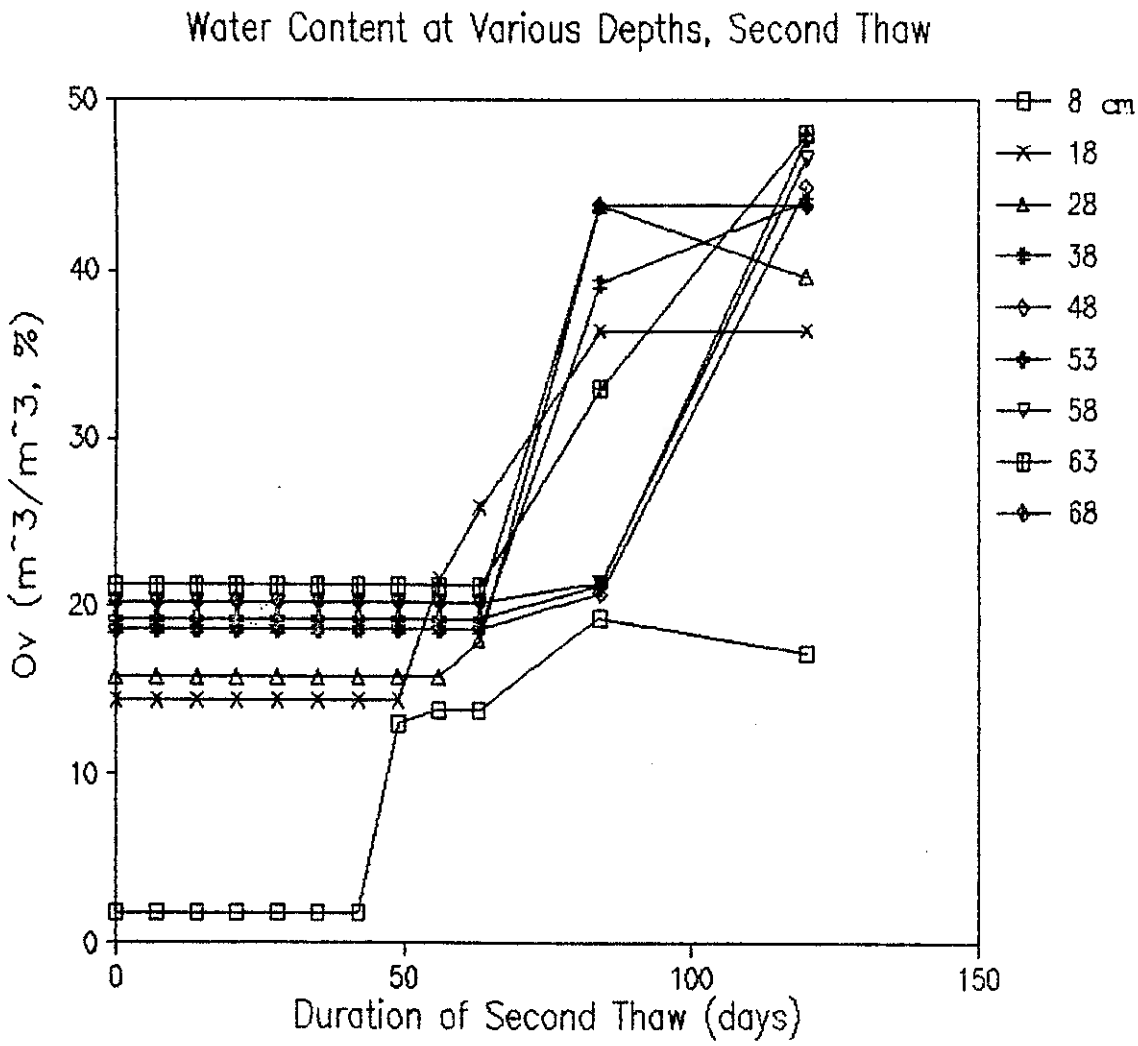

Figure 3.3 Unfrozen water content under pipe, BB section, 8 to 68 cm depths

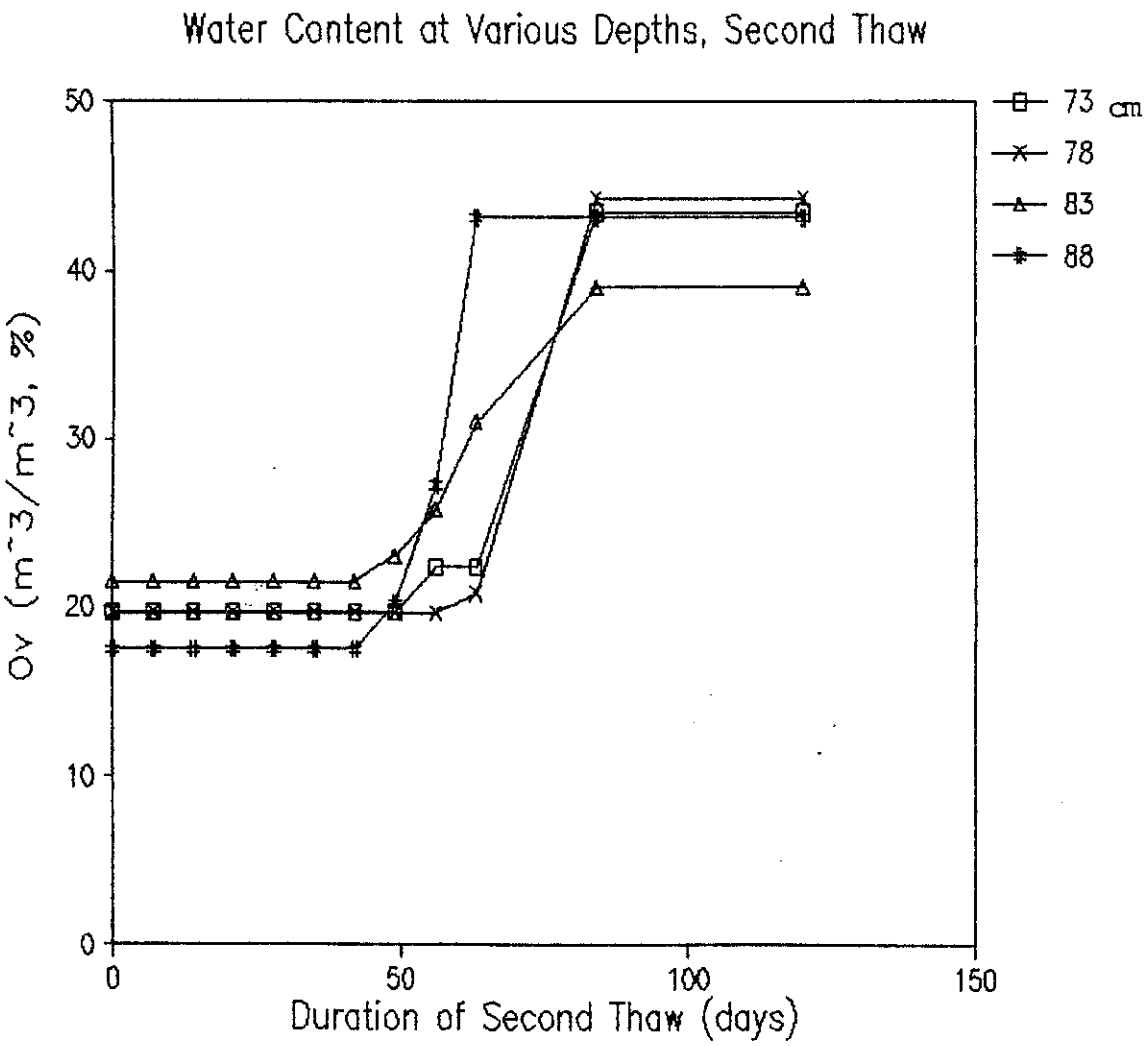

Figure 3.4 Unfrozen water content under pipe, BB section, 73 to 88 cm depths

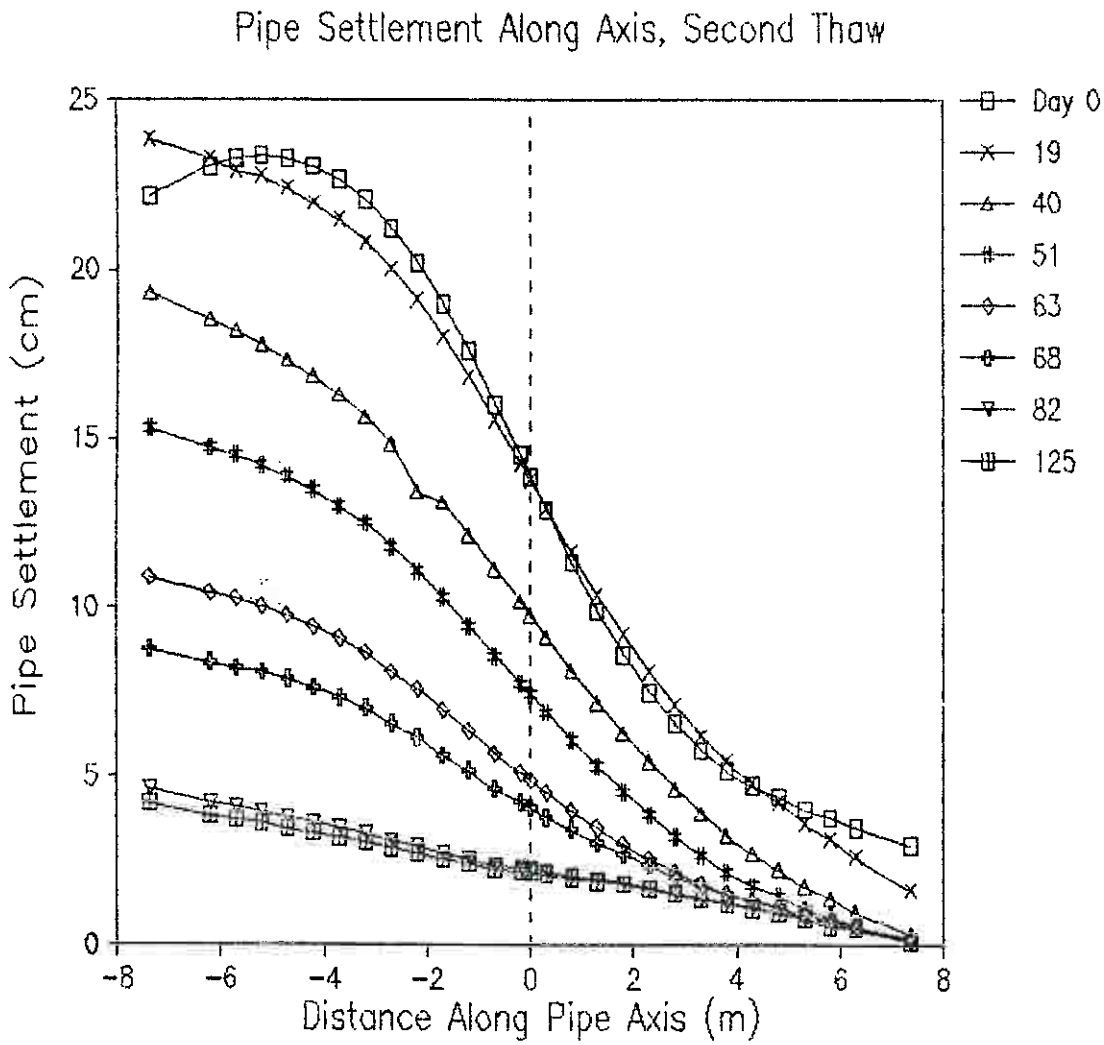

Figure 3.5 Pipe settlement along axis, second thaw

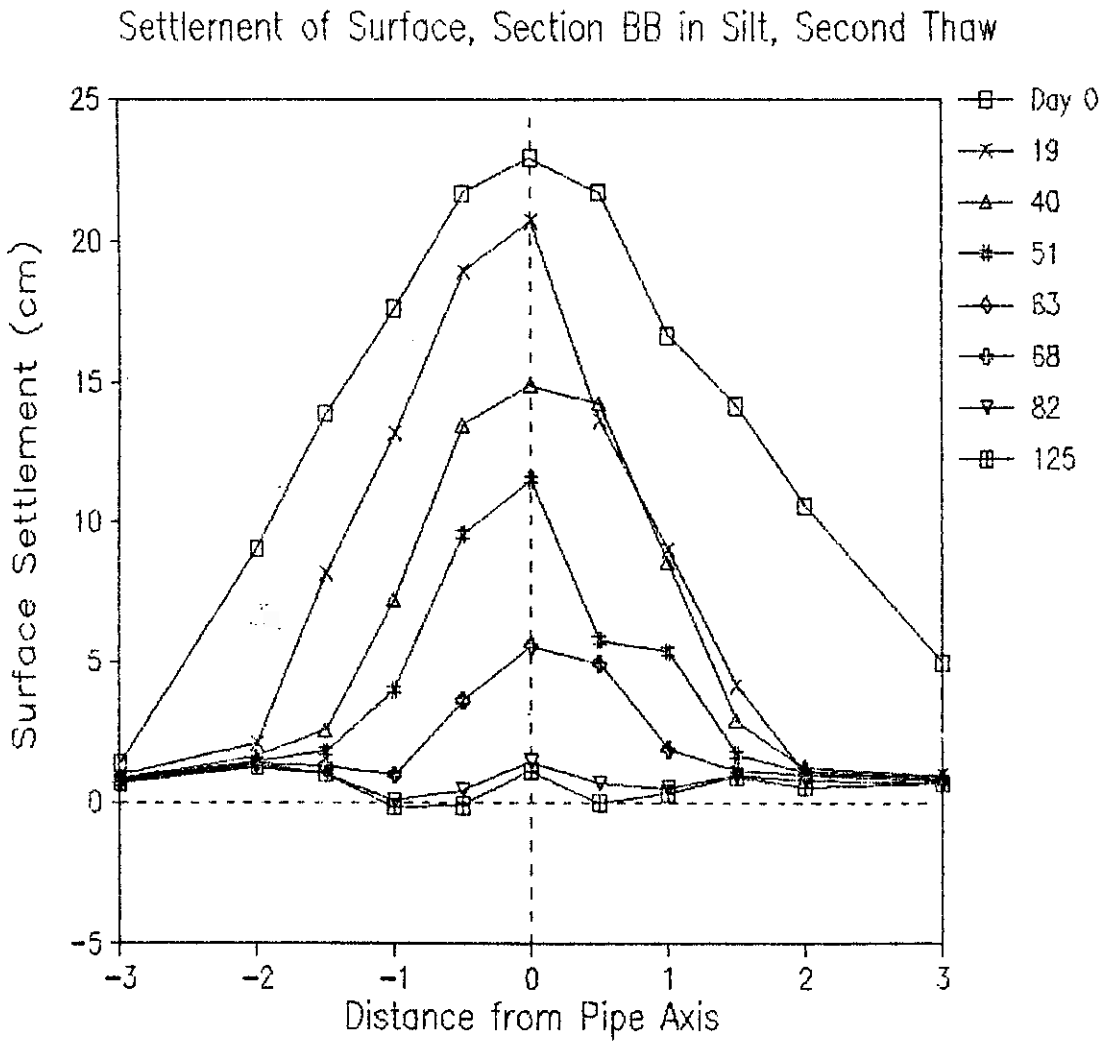

Figure 3.6 Surface settlement in silt during second thaw, section AA

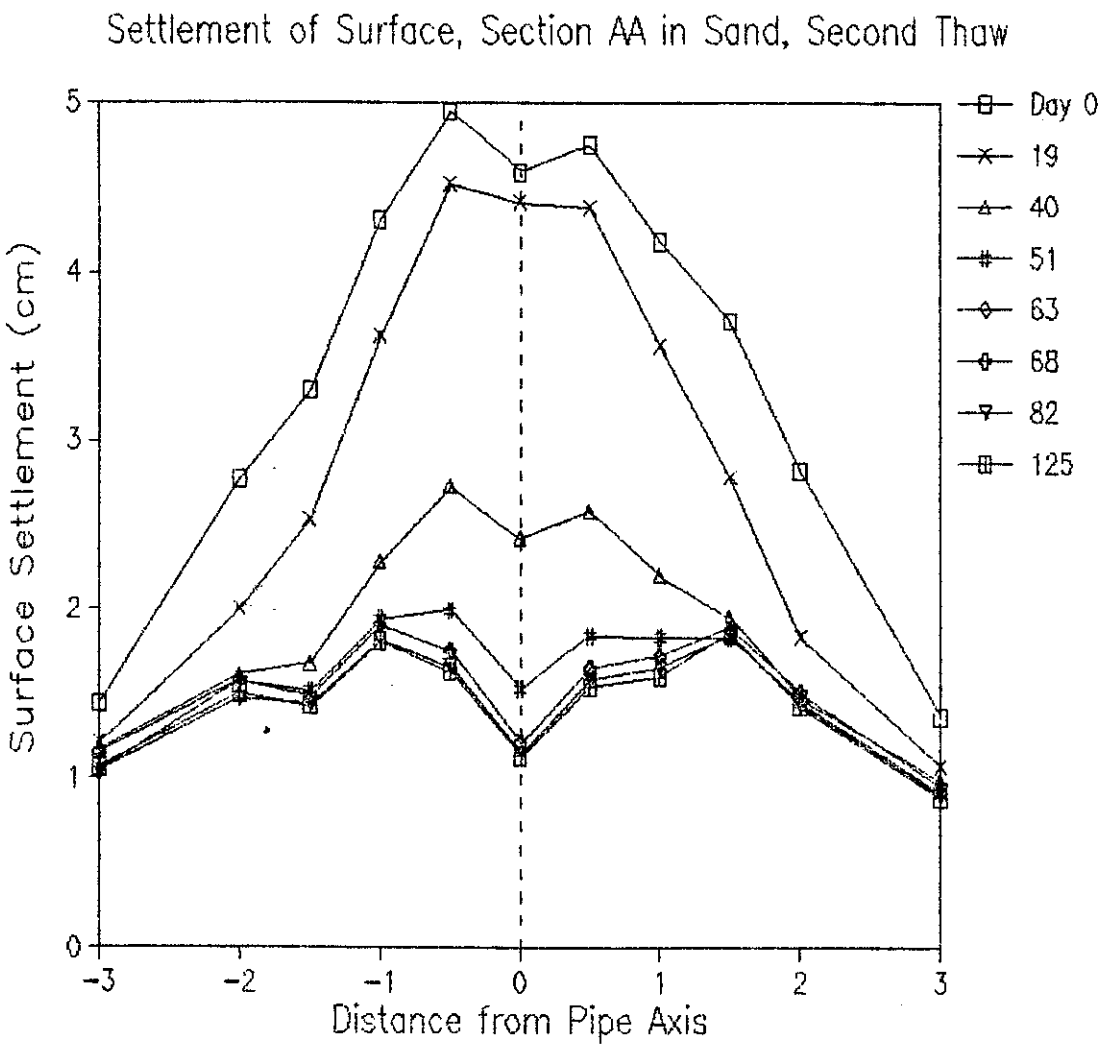

Figure 3.7 Surface settlement in sand during second thaw, section BB

3.8. This indicates that the pipe is progressively being jacked upward in the silt section relative to that of the sand section.

Figure 3.9 Shows the change in pipe stress as monitored by the strain gauges attached to the pipe. The first two strain gauges in the silt section broke between day 10 and 20 resulting in an unfortunate loss of data. Since the gauges have operated satisfactorily since 1982, it can only be surmized that the gauges or connecting cables were broken during settlement.

The remaining guage readings show the reduction in pipe stress during the thaw, effectively stabilizing between day 74 and 99.

3.5 Surface expression of Thaw and Surface Fissures

Figures 3.10 to 3.12 show the change in surface elevation observed during the second thaw period. The last day of the second freeze cycle (day 700) corresponds to the first day of the second thaw cycle. By about day 83, the thaw cycle is essentially complete.

Figure 3.13 indicates the fissured nature of the soil surface as it appeared on October 18 (day 30 of thaw). By this date, the fissures were in the order of 1 to 2 cms wide and 9 to 25 cms deep in the silt section. Most fissures paralleled the pipe and were concentrated along the pipe axis. It should also be reiterated that cavities were found beneath the pipe when equipment was being installed for the third freeze cycle.

Table 2 indicates the progressive change in depth and length of the fissures. The location numbers are referenced to Figure 3.13.

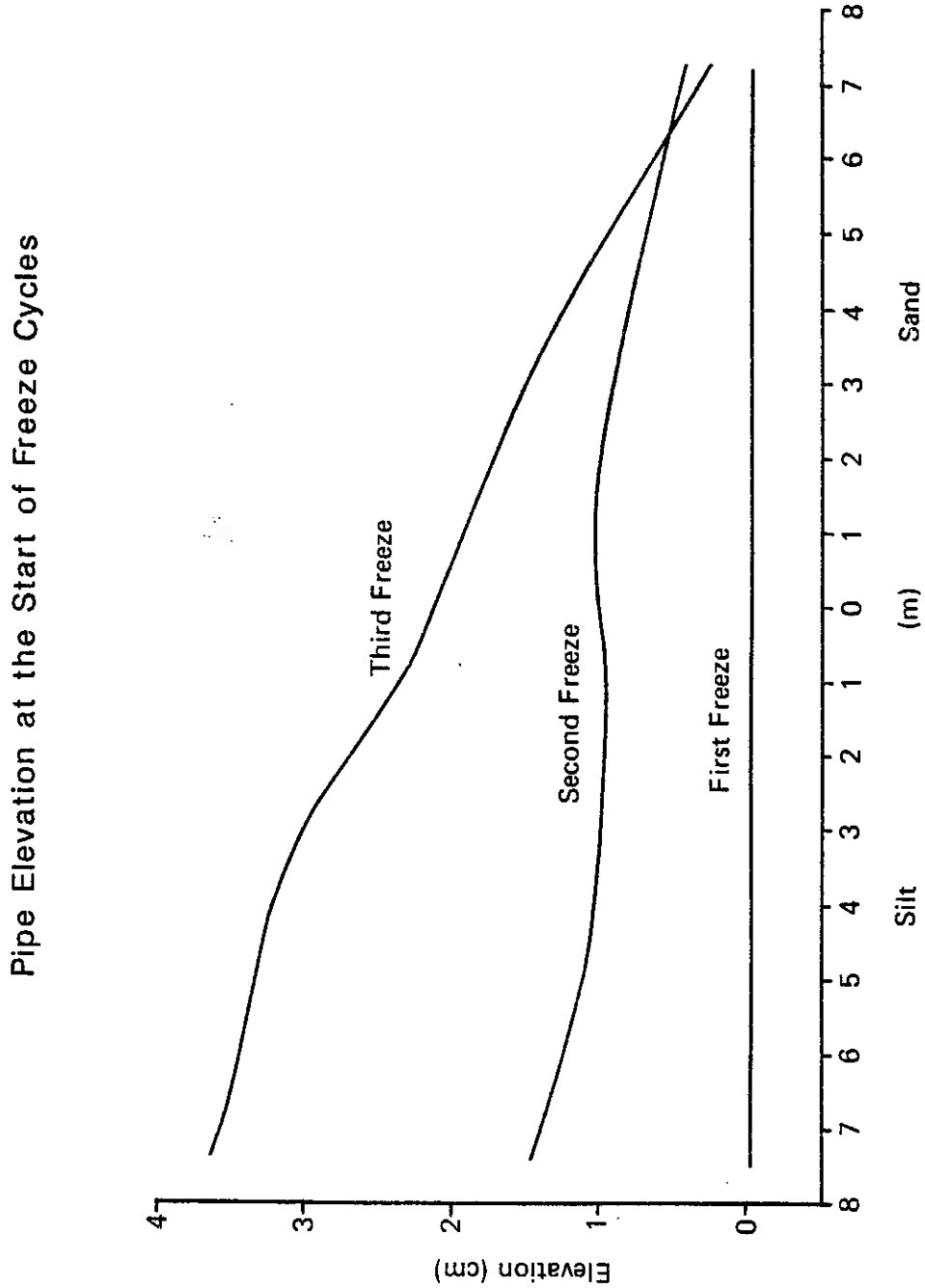

Figure 3.8 Pipe elevation at the start of the freeze cycles

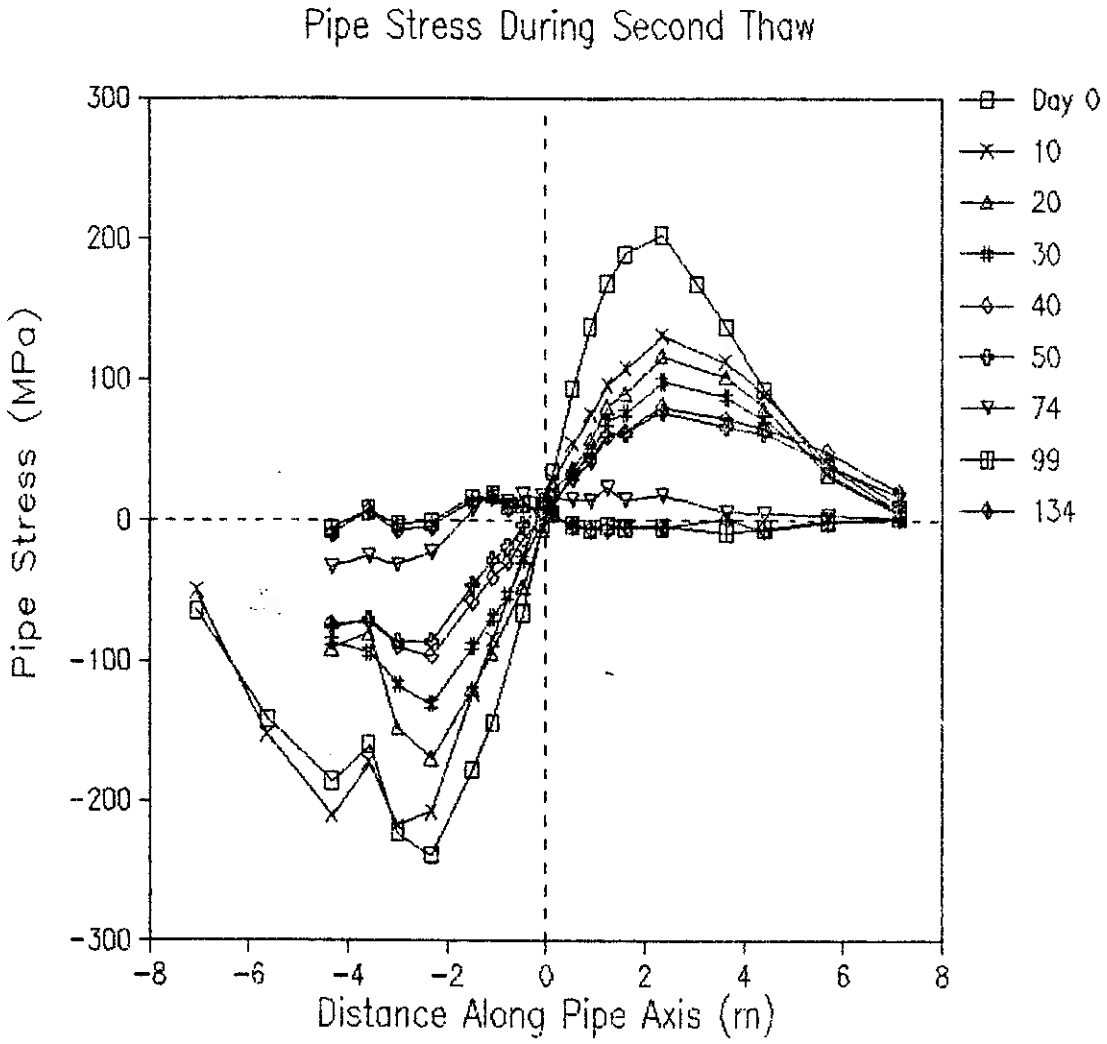

Figure 3.9 Pipe stress during second thaw

Last Reading Before Second Thaw
Sept.17 1985.

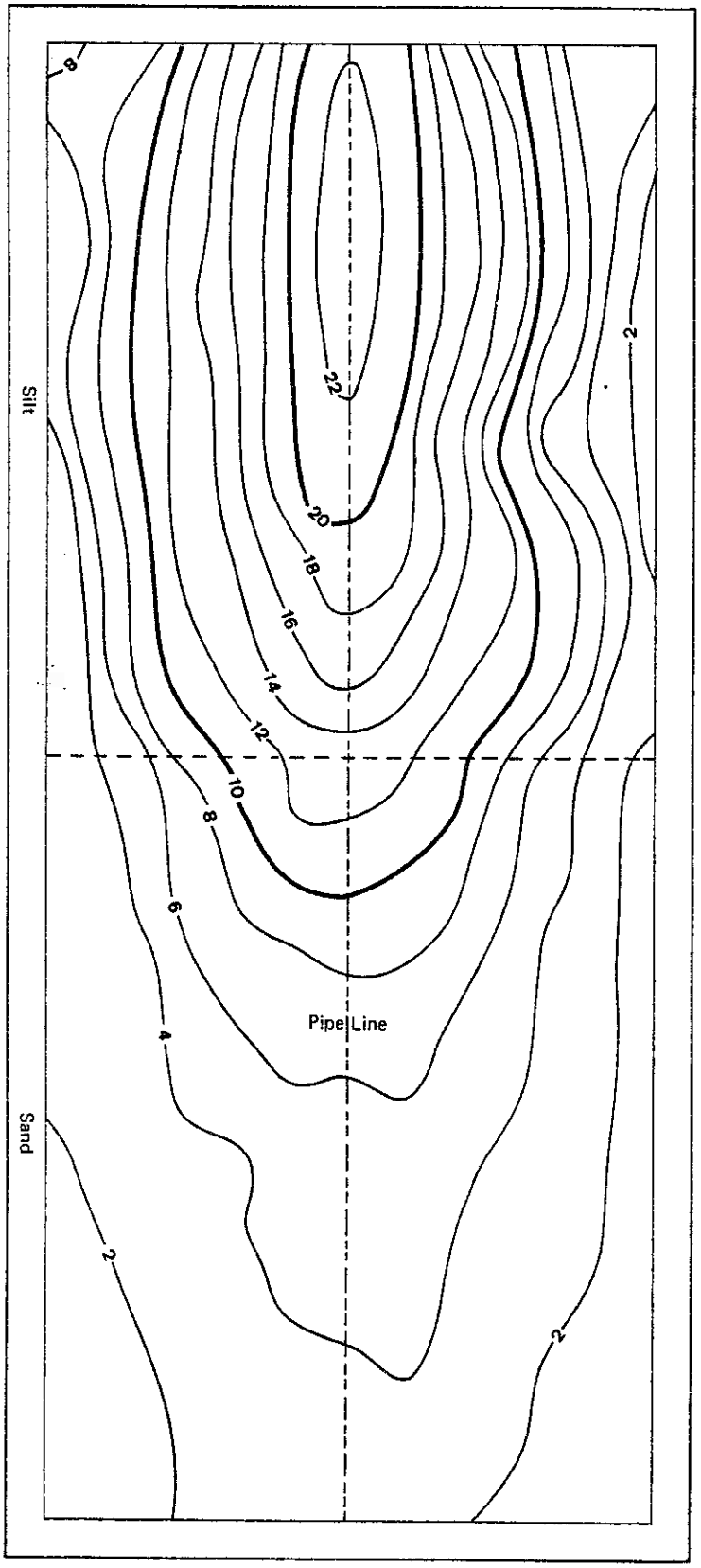

Contour Interval - 2 cm

Drawn by Kevin Roberts
October 1986

Figure 3.10 Surface elevation last day of second freeze

Day 37 Second Thaw

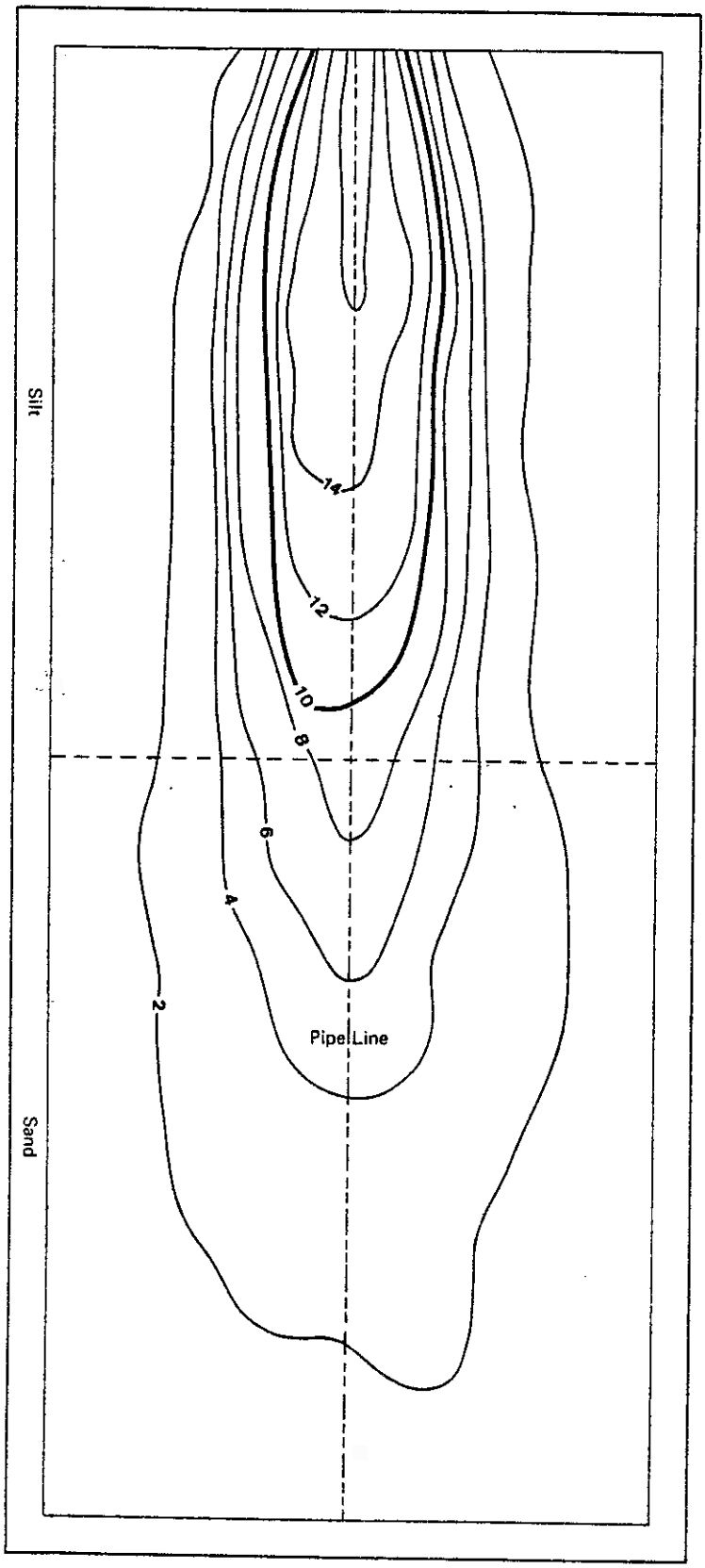

Contour Interval - 2 cm.

Drawn by Kevin Roberts
October 1986

Figure 3.11 S--face elevation during second
', Day 37

Day 83 Second Thaw

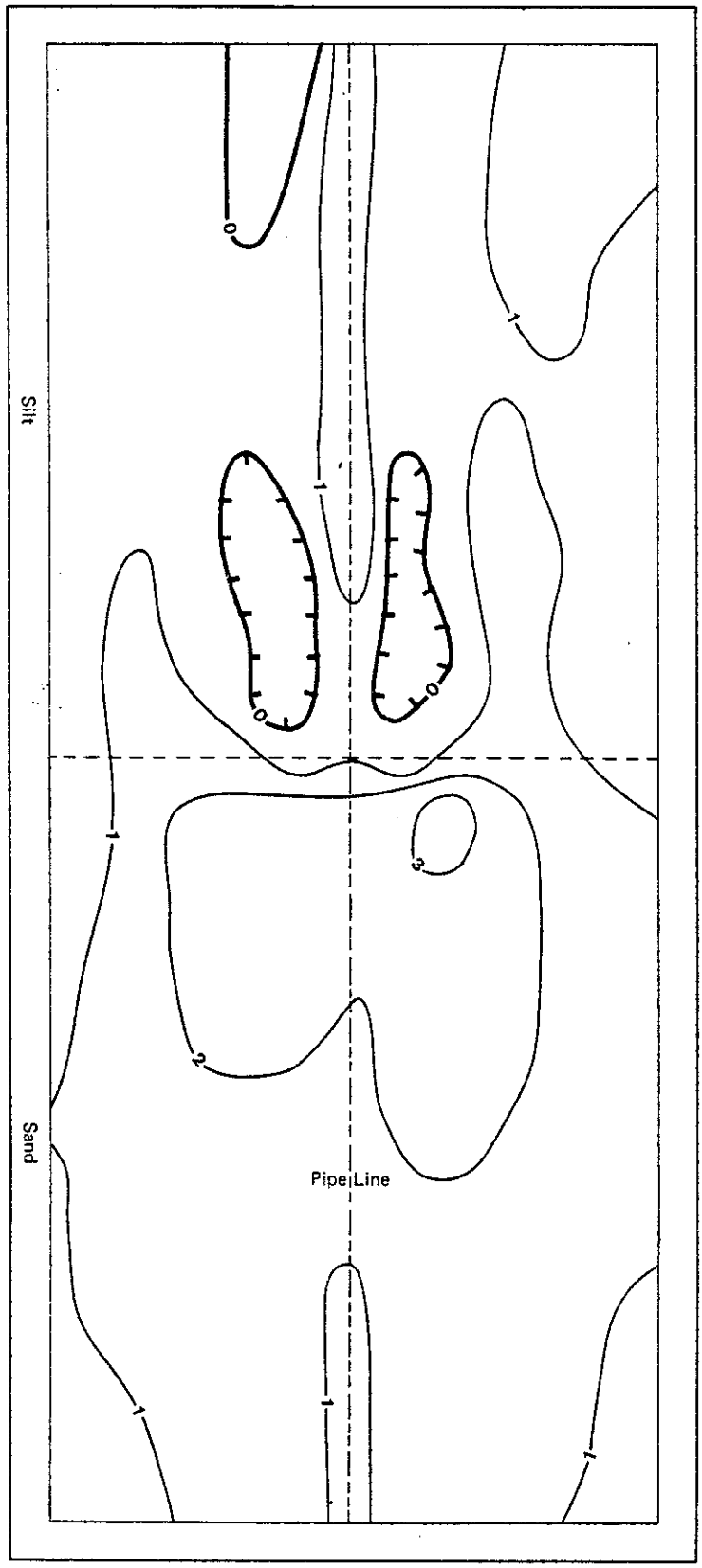

Contour Interval - 1 cm.

Drawn by Kevin Roberts
October 1986

Figure 3.12 Surface elevation during second haw, Day 83

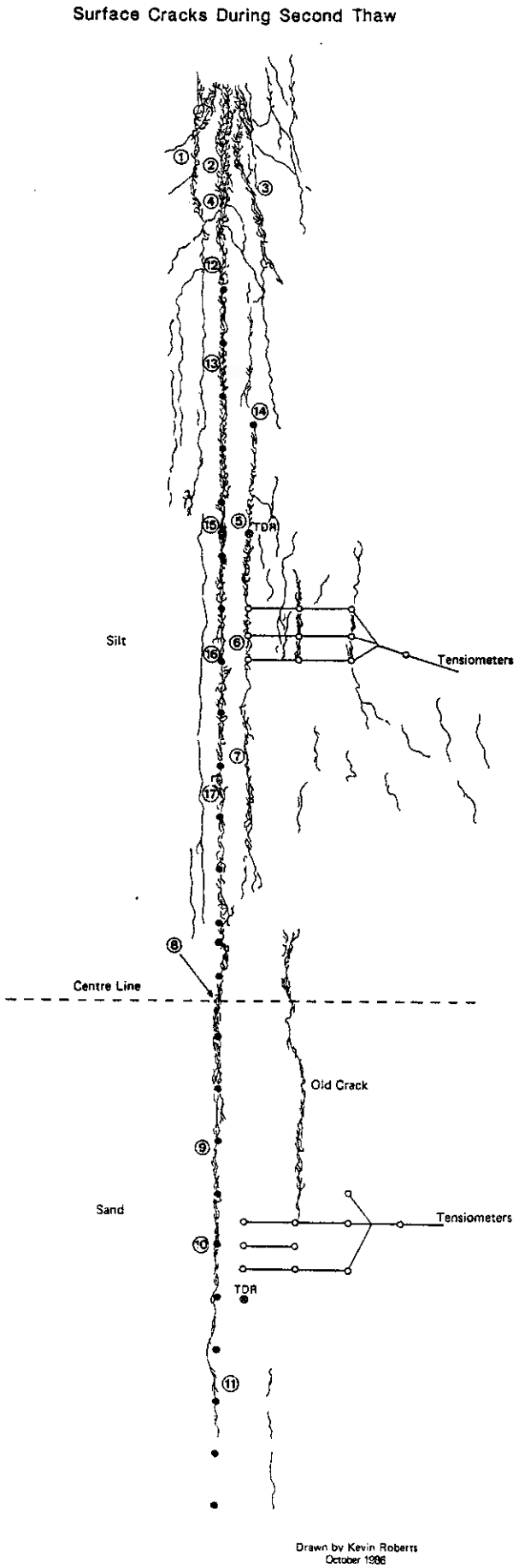

Figure 3 Surface fissures, day 30 second thaw

Table 2 Surface Fissures During Second Thaw

Day	12		16		30	
Location	Width (cm)	Depth (cm)	Width (cm)	Depth (cm)	Width (cm)	Depth (cm)
1	8.5	1.5	9.4	1.0	-	-
2	24.8	1.5	24.5	4.0	24.0	9.5
3	9.8	2.0	9.8	1.7	26.0	3.0
4	15.3	1.4	26.9	4.2	26.0	9.5
5	10.5	1.4	11.0	2.0	13.0	1.5
6	9.8	0.9	17.1	1.3	19.8	1.4
7	4.1	1.0	10.0	1.1	11.5	1.0
8	7.4	0.8	13.6	0.9	13.5	1.2
9	2.1	0.5	3.5	0.7	7.8	0.7
10	-	-	6.3	0.4	2.5	0.4
11	-	-	1.1	0.3	-	-
12	new fissures	-	15.0	1.0	25.0	5.0
13					27.5	4.0
14					24.5	1.3
15					27.0	1.8
16					26.5	1.5
17					20.0	0.8

3.6 Thaw Settlement from Telescopic Heave Rods and Magnetic Heave Device

The interpretation of the telescopic heave rod and magnetic heave device data is complicated by the fact that the frozen soil was thawing from above and below. Figure 3.14 shows the net settlement of the telescopic heave rods during the thaw at the BB section. This figure shows the thawing of the soil from two directions.

Figures 3.15 and 3.16 show similar patterns of settlements obtained from the magnetic heave device near the BB transition and the sand-silt transition respectively.

3.7 Stress in the Ground

Glotzl cells were installed at differents depths beneath and along the pipe to obtain information on total stress within the soil. From the previous freeze cycles, it has been noted that if a Glotzl cell is enclosed in unfrozen soil, the only pressures noted can be ascribed to the weight of overburden. If the cell is enclosed in frozen soil, the observed pressure will generally show a sharp rise at the onset of freezing followed by a slow discipation of pressure.

The data obtained from the Glotzl cells at the BB section in the silt section during the second thaw period, Figure 3.17, show a rapid drop in total soil pressure at 10 cm beneath the pipe on day 15. At 46 cm beneath the pipe, the drop began on about day 70 while the readings for the 86 cm depth change little during the thaw period.

Similar large drops in total pressure were noted in the sand

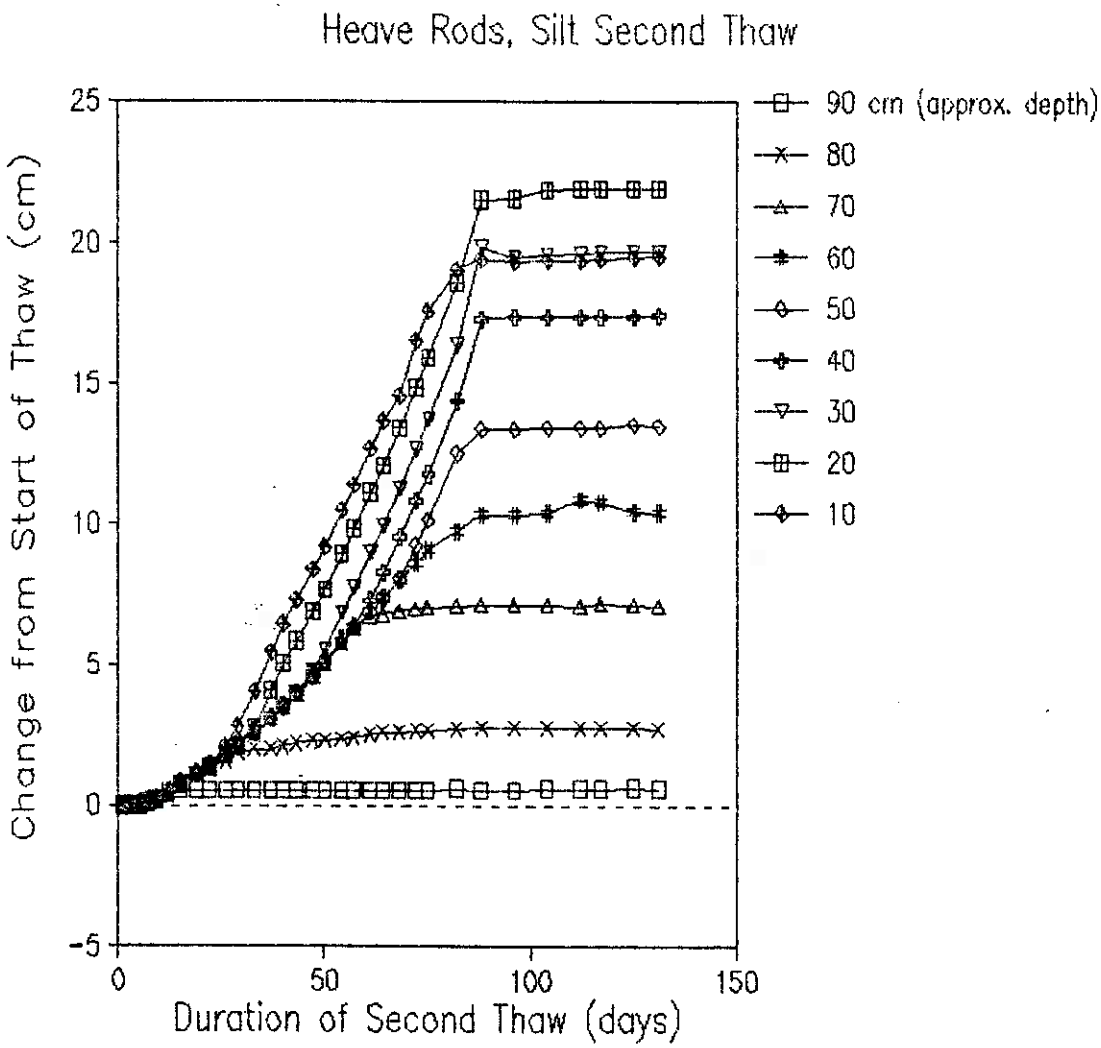

Figure 3.14 Heave rods at BB section in silt, second thaw: net settlement

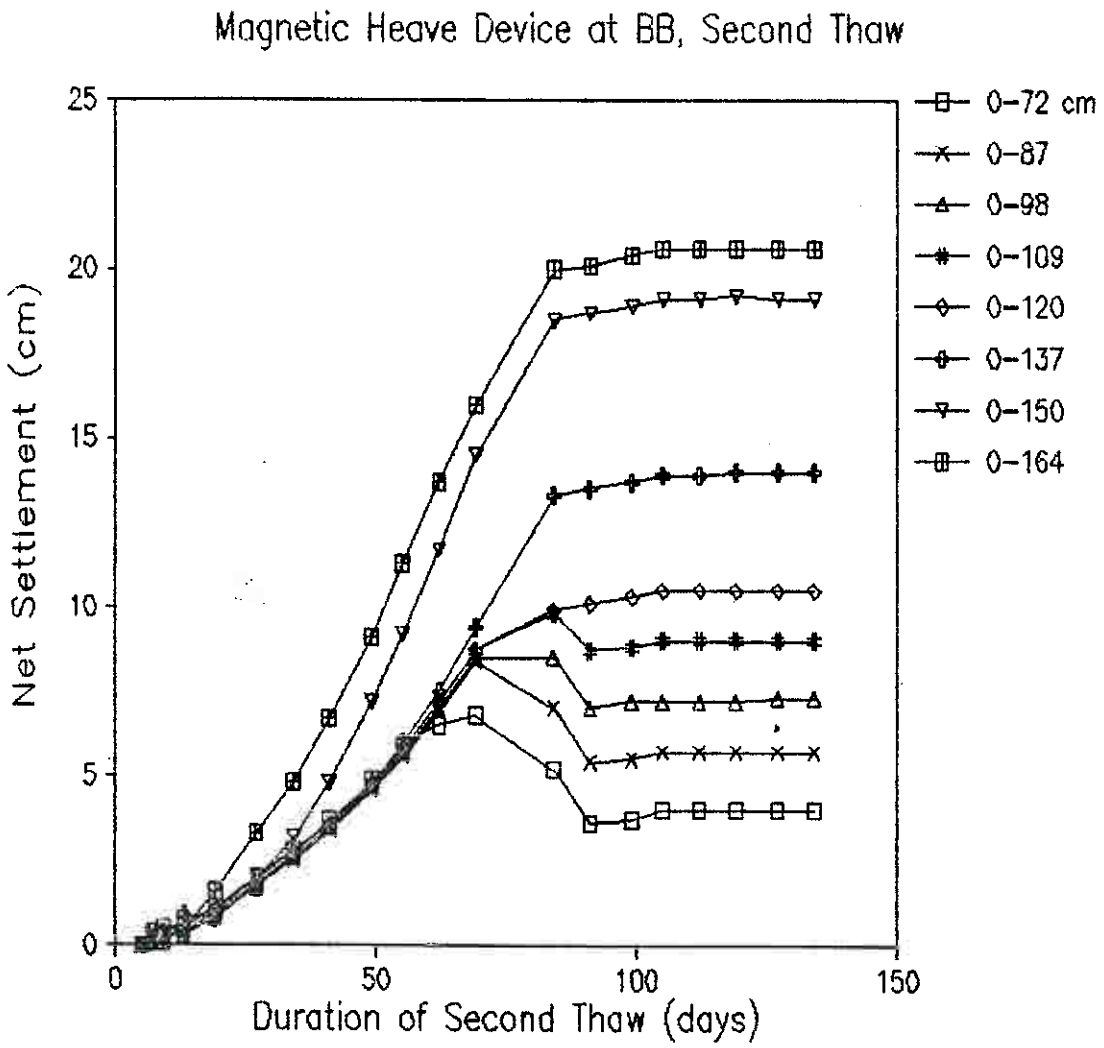

Figure 3.15 Magnetic heave device at BB in silt, second thaw: net change from day 0

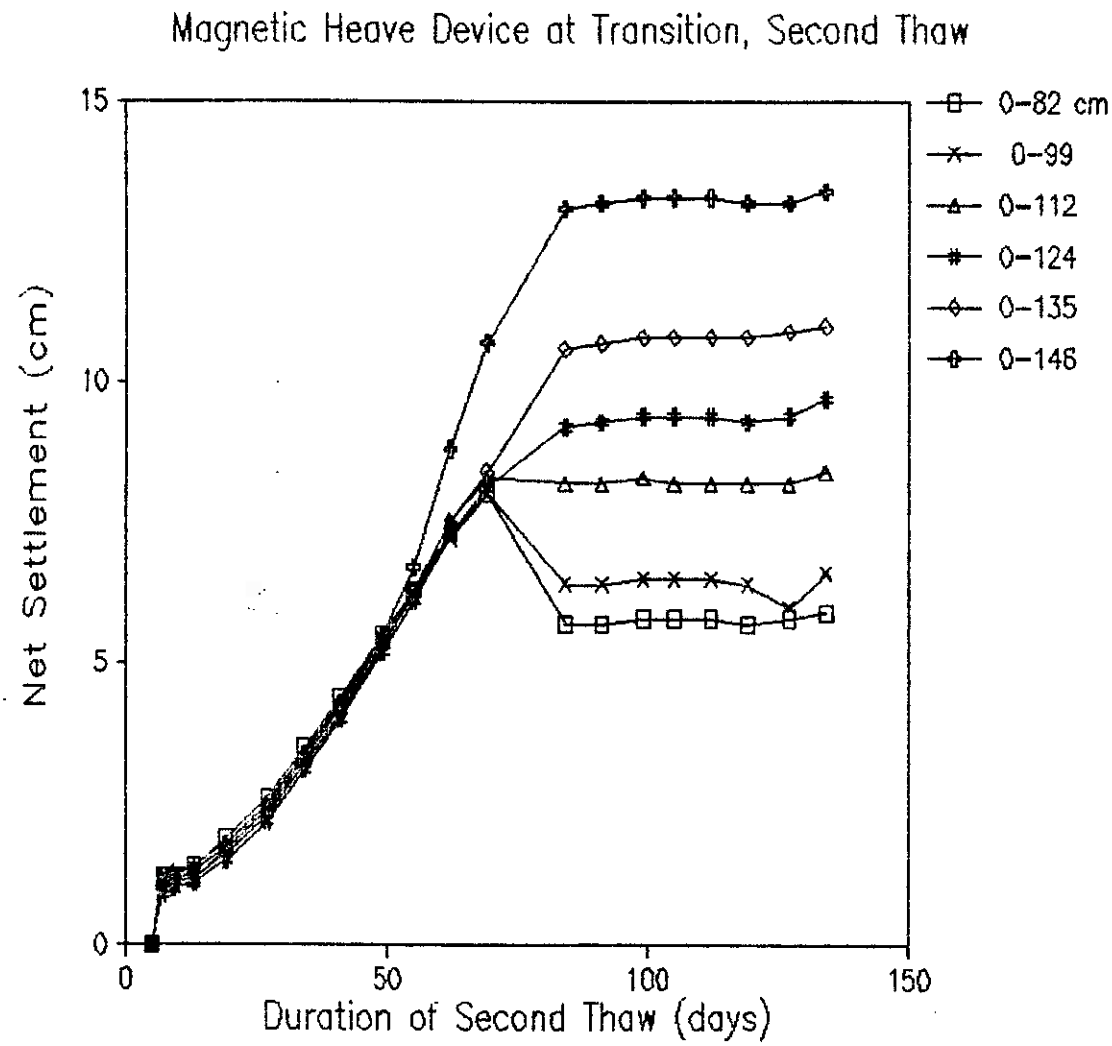

Figure 3.16 Magnetic heave device at sand/silt transition, second thaw: net change from day 0

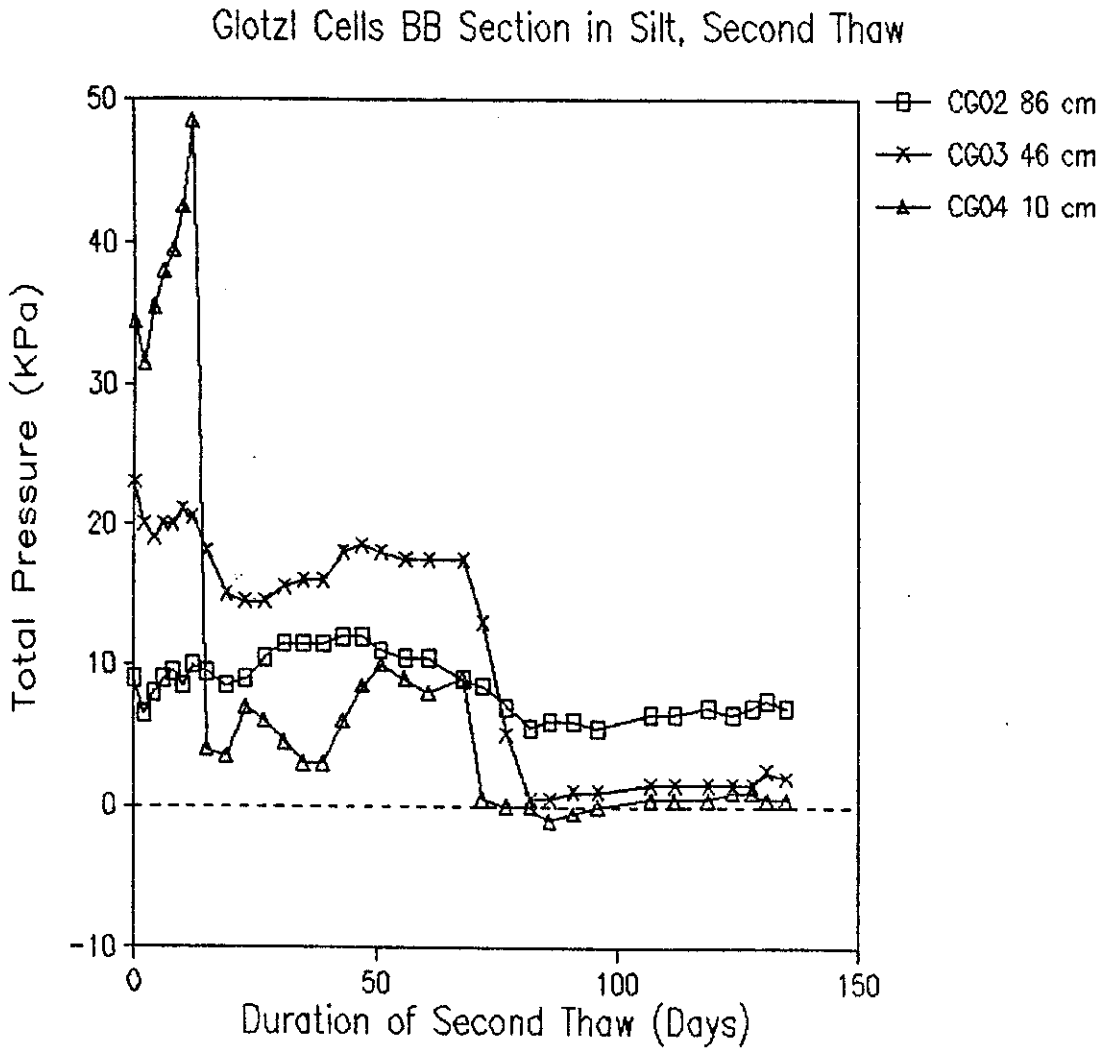

Figure 3.17 Soil pressures at BB section in silt, second thaw

section (see Figure 3.18), however, all gauges attained a lower pressure about day 47 due to a more rapid thaw.

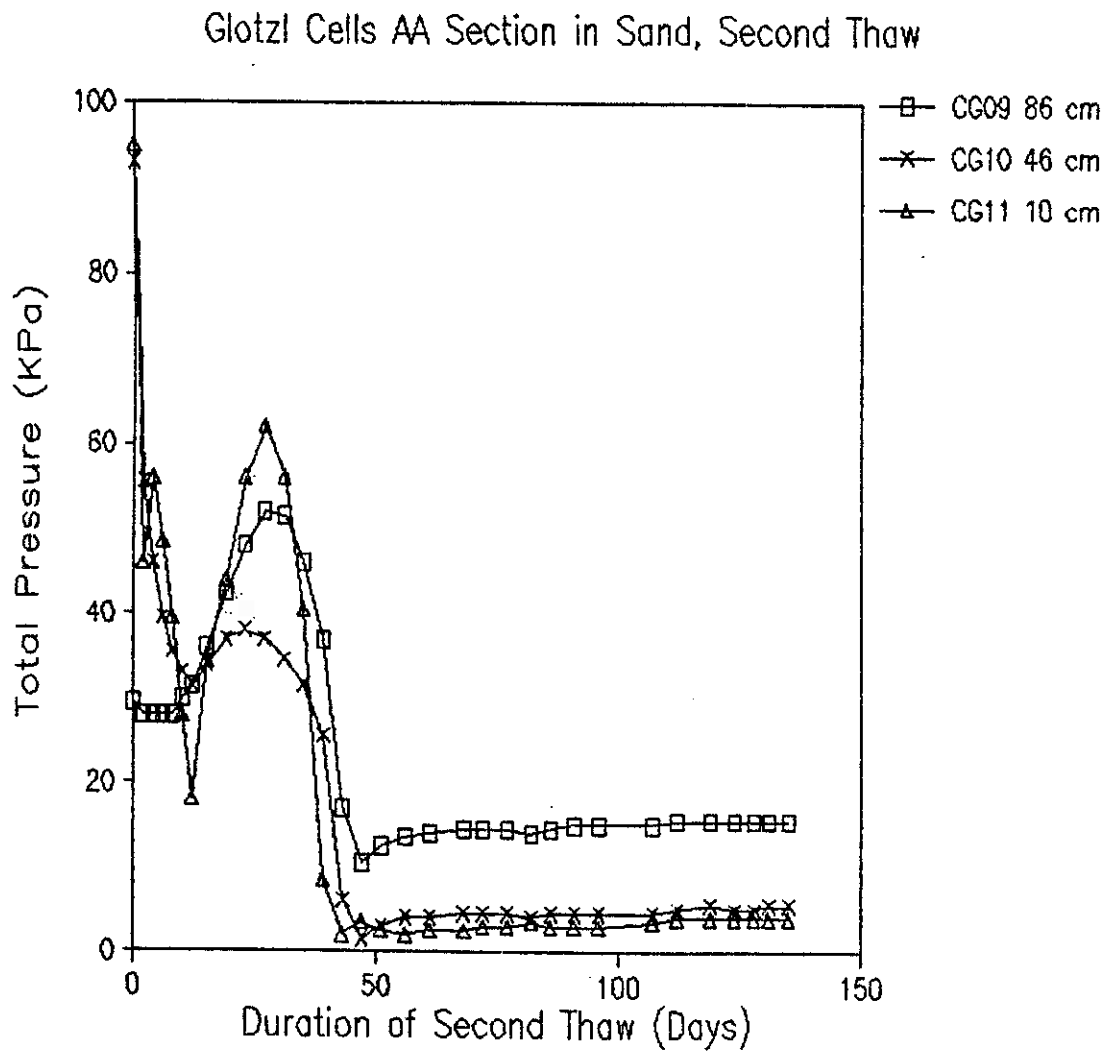

Figure 3.18 Soil pressures at AA section in sand, second thaw

IV DISCUSSION OF FINDINGS

4.1 Conditions

During the thaw period, 18 September 1985 to 1 January 1986, the air temperature in the hall was maintained at +4 C. This led to the first total thaw of the soil in the facility. No air was circulated in the pipe during the period so that the pipe temperature was dictated by that of the surrounding soil.

4.2 Non-reversible Displacement of the Pipe

During the earlier partial thaw (the period of June 8, 1983 to October 17, 1983 - see Geotechnical Science Laboratories, 1984) it had been observed that the pipe did not return exactly to its original position (prior to heave). At the end of the partial thaw a few centimeters of frozen ground remained below the pipe (Geotechnical Science Laboratories 1984 fig. 3.4). The pipe was elevated one to two centimeters above its original position in the silt and for the first two meters into SNEC sand, with a smaller amount further along the pipe.

At the end of the total thaw period, the pipe was elevated further - by an amount roughly equal to that following the partial thaw. At the maximum, therefore, the pipe was now five centimeters above its position at the time of construction.

Were this part of a continuous pipe, the maximum displacement might have been somewhat less due to restraint exerted by the adjacent pipe length. However, it is equally possible that the maximum would have been greater if the adjacent soils were more prone to heave.

Irreversible displacement shows that the pipe is susceptible

to the same repetitive uplift processes that cause uplift of boulders, formation of patterned ground and other natural phenomena. These phenomena are not fully understood, but frost heave and creep of the frozen soil are involved, as well as "infilling" or "blockage" of cavities formed below the raised object. A cavity several centimetres high, below the pipe, was observed in a small excavation during re-instrumentation in February 1986.

The residual deformation gives only small stresses in the pipe, because the displacements do not include sharp curvatures. The residual displacement, however, apparently will accumulate rapidly (some 2.5 cm per year). If conditions were such that the pipe was anchored at some point, the consequent bending (that is corresponding to a differential displacement of 2.5 cm per year) could lead to significant, persistent longitudinal stresses in the pipe.

4.3 Soil Cracking

The conspicuous fissures developed at the ground surface parallel to and to the side of the axis of the pipe during thaw were probably associated with this residual displacement of the pipe. As thawing is followed by consolidation, soil to the sides of the pipe moved downwards relative to the pipe. This tends to produce shear stresses in a roughly vertical direction, near to the pipe and parallel to its axis. This is probably the cause of the cracks, particularly as there is to be expected a component of movement of soil laterally from above the pipe.

4.4 Total Stresses in Thawed Soil

The glotzl cells installed at various points in the ground and below the pipe showed a rapid increase in pressure during the freezing period, as soon as they became enclosed in the freezing soil. This important observation was not entirely unexpected, but it was of particular interest to observe the pressures recorded as the soil around the cells thawed completely. Figure 3.17 shows that a sharp drop in the pressure was recorded in each case (except the deepest cell (at 86 cm) in the silt which was probably never enclosed in frozen material). Subsequently the readings remained stable and had values corresponding to the depths of overburden.

The observations during the thaw period thus confirm that the glotzl cells are functioning normally and that, accordingly, the observations of the internal pressures in the frozen ground are likely to be valid (the internal presures in the frozen ground are considered further in chapter 5). The internal pressures of the frozen ground are ascribed to the thermodynamic processes of ice accumulation (secondary heave, see Williams and Wood, 1986). It would be of interest to establish whether the pressures fall as the frozen ground is warmed prior to complete thawing. The pressures are quite unstable and this fact coupled with the intervals between reading did not allow any firm conclusion on this point. A fortuitous day-long warming of the frozen ground during the freezing period has, however, provided interesting data on this question (p. 65).

V INSTRUMENTATION AND CONDITIONS FOR THIRD FREEZE PERIOD

5.1 General

New instrumentation was installed at the facility for the third freeze period in order to gather more information on the thermal state, heave characteristics and stresses within the soil during freezing. Specifically, a new configuration of thermistor cables (soil temperature) and magnetic heave sensors were installed in two arrays, one parallel to the pipe and one 25 cm off axis and normal to the pipe in the silt near section BB, as shown in Figure 5.1. Excavations for these instruments were made with a 10 cm soil auger.

Petur pressure cells were also installed in four vertical profiles directly beneath the pipe in the silt section to obtain information on soil stress during freezing. The installation required the excavation of pits approximately 2m deep and 70 by 70 cm cross-section. Although these pits were large and the soil disturbance was considerable, it was felt that this was easier than attempting to bore a number of inclined holes beneath the pipe. This excavation also offered the opportunity to examine the soil structure and the pipe following two freeze cycles. In addition, oriented undisturbed frozen samples were obtained from each pit. These samples were resin impregnated to permit further detailed examination of soil structure. Other samples were taken for moisture content determinations.

Several of the vertical TDR probes were relocated. Information on the new instrumentation is presented in subsequent

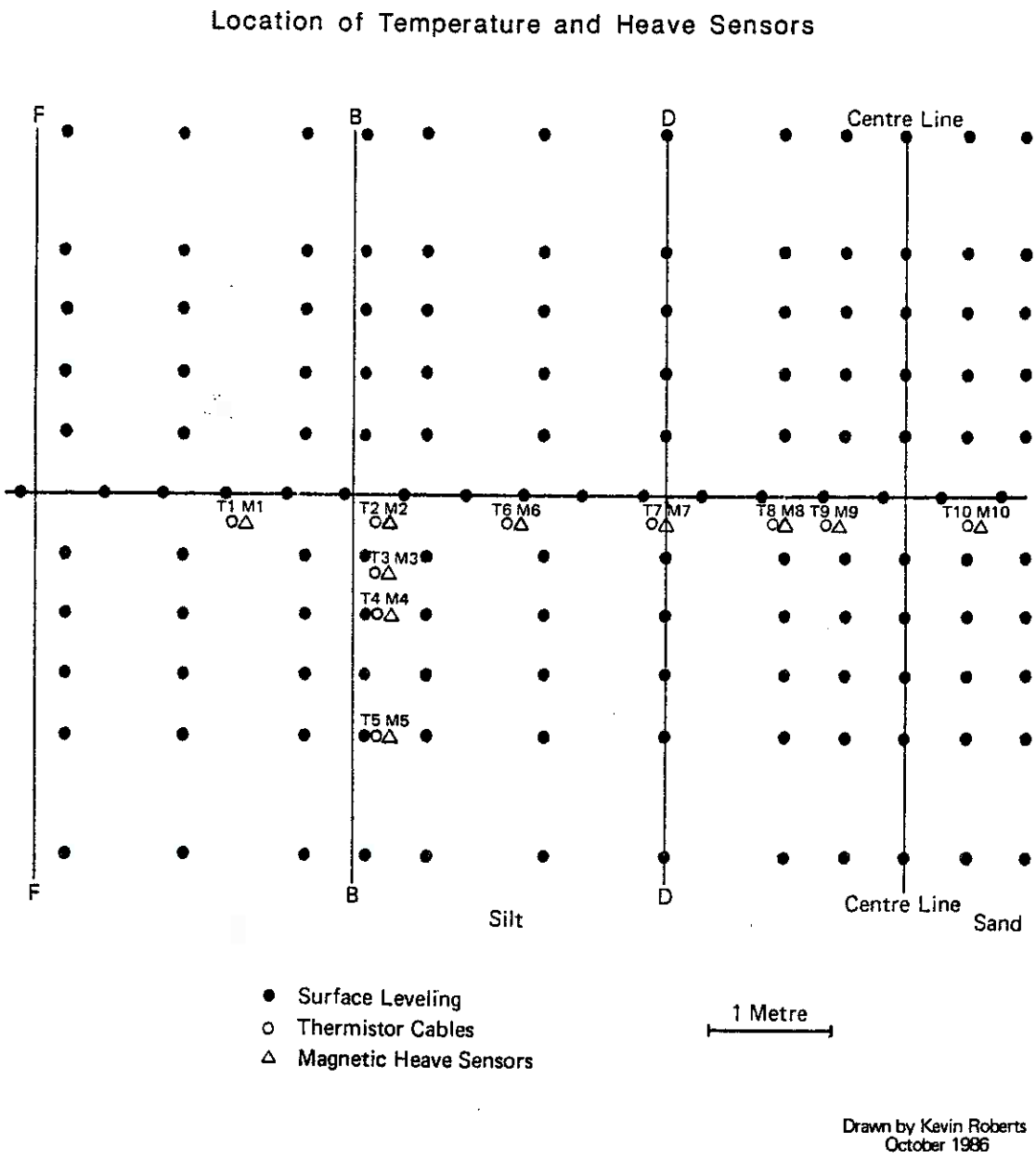

Figure 5.1 Location of new instrumentation for third freeze

sections.

5.2 Details of Re-instrumentation

Refurbishing and re-instrumentation took place during the latter part of January and February 1986 following completion of the second thaw period. During this time all systems were checked especially those which could not be shut down or altered during the experiment.

The refrigerator for both the atmosphere and pipe were serviced. This included changing the motor on one compressor and recharging the coolant systems. The electro-mechanical systems were cleaned and checked.

A review of the frequency of data acquisition was made for all instrumentation, some minor changes were made.

5.2.1 Pipe Stress

The Bowes device permits determination of pipe curvature from which pipe stress can be calculated. This instrument was tested during the first and second freeze cycles and results have been reported previously. At present, the instrument requires upgrading in the micrometer system and measurements could be resumed if it were desirable to test an improved prototype. Currently the data provided by the strain gauges gives a more reliable picture of the stress state of the pipe. Two strain gauges near the end of the pipe in the silt section broke during the second thaw period, however, the remainder of the gauges are still operational providing a picture of the strain pattern along the pipe.

5.2.2 Thermal Regime

Sets of thermistor cables were installed in the soil at ten locations as shown in Figure 5.1. The new temperature sensors were installed to augment the existing thermocouple sensors and to provide better resolution of soil temperature with depth. The thermistors used are YSI 44004 which have been individually calibrated. The thermistors were installed in multiconductor cables which in turn were placed in oil-filled tubes extending from the soil surface to about 165 cm depth.

The thermistors are located at 0, 15, 30, 45, 60, 75, 90, 105, 120, 135 and 160 cm from the soil surface. The tubes in which the thermistors are installed are optically surveyed on a regular basis to ensure that the position of each thermistor is known exactly.

Each thermistor string is located adjacent to a set of magnetic heave sensors so that an improved correlation between heave and temperature could be obtained. The thermistors are read three times a week.

5.2.4 Frost Heave

The potential use of magnetic sensors to measure soil heave was suggested by J.R. MacKay (per. comm.) as an alternative to telescopic heave rods. The basic principle of the apparatus has been used in geotechnical engineering for some time. The device is shown in Figure 5.2 and was developed and constructed in the Geotechnical Science Laboratories. This device is an improvement on the earlier prototype.

The apparatus consists of three parts: a magnetic indicator

Figure 5.2 Magnetic heave device

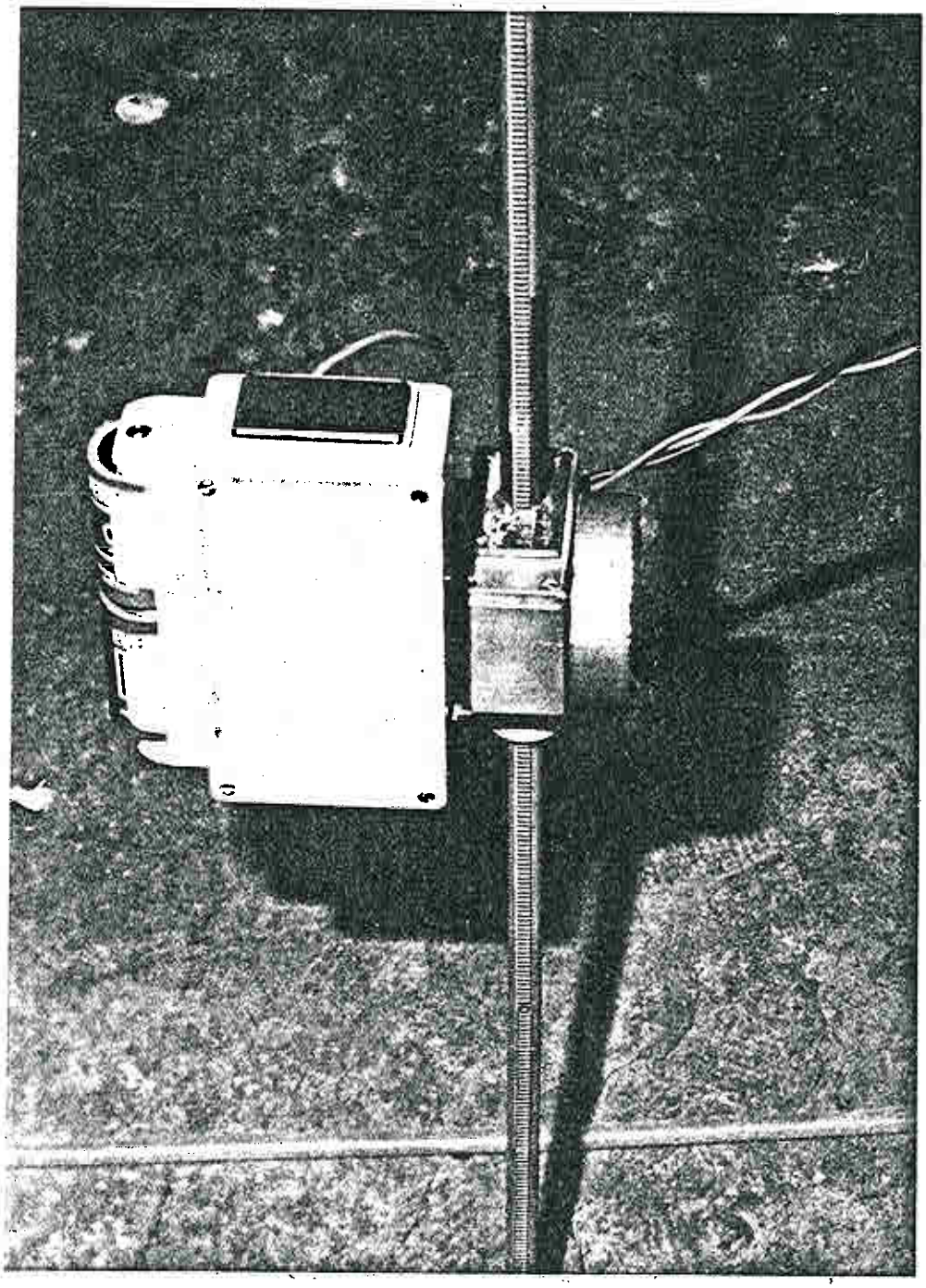

ring; a magnet sensing device and a plastic access tube. The magnetic indicator is comprised of three small magnets installed in a plexiglass disc through which the access tube passes. The magnet sensing device is attached to the end of an aluminum rod which is lowered into the tube on a rack and pinion device. The rack and pinion assembly can move freely up and down the access tube.

A pilot hole about 10 cm in diameter was augered to permit installation of the magnetic indicators and the access tube. Magnetic indicators are dropped over the access tube to lie at selected depths, approximately 20 cm apart. After an indicator is installed, the augered hole is backfilled to the depth where the next indicator will be installed. When the hole was completely backfilled a final magnetic disc was installed at the surface to provide a zero point for the profile.

To obtain the position of the magnetic heave sensors, the detector is lowered in the access tube. A digital readout indicates the position of the detector and an audible signal indicates when a magnetic disc is encountered. The position of the magnetic indicators in a profile are measured with reference to the surface magnetic disc. The position of this disc is determined monthly by optical surveying.

The accuracy and reproducability of data obtained with this device represents an order of magnitude improvement over the previous design. The new digital readout reads to 0.1 mm. Normally, magnetic discs can be located to within 0.2-0.3 mm. Backlash in the rack and pinion is in the order 0.1-0.2 mm. Therefore, it is estimated that the location of the dics is to

within +/-0.5 mm.

5.2.3 Soil Stress

A new array of soil pressure meters was installed to determine values of soil stress during freezing. Petur cells were utilized since they were physically smaller than Glotzl cells and could provide greater flexibility in obtaining total or directional stress data.

The Petur soil pressure meters were installed in four vertical profiles under the pipe. These devices can measure total soil pressure or pressure in a single direction depending upon their design configuration. In each profile there are four devices for measuring total pressure. These are located at 20, 40, 60 and 80 cm below the pipe. In addition, in two of the profiles, two directional measurement devices were installed at the 40 cm level to monitor lateral and vertical pressures.

The principle of operation for the Petur soil pressure system is the same as the Glotzl cells. The same manometer and gas pressuring system is used for both Glotzl and Petur cells:

More complete details of the construction of the sensing device is given in Appendix III.

Laboratory tests prior to installation suggested the new devices would operate satisfactorily. However, it was subsequently found that the rubber bulb, where stretched over the metal extension, was extremely susceptible to puncturing or pinching. The effect was possibly made worse by extended contact of the bulb with water. As a result a number of the bulbs have developed pin-holes making pressure measurements impossible and

casting suspicion on the results from remaining sensors. Subsequently, tests have been made on a replacement bulb which will not deteriorate. These, however, will not be installed until after the third thaw period.

VI EXPERIMENTAL OBSERVATIONS, THIRD FREEZE PERIOD

6.1 General

The data reported in this section covers the period March 3, 1986 (day 0) to July 1, 1986 (day 120). The raw data is given in appendices to this report.

6.2 Thermal Regime

Figure 6.1 shows representative temperature data for selected dates for thermistor string # 1 located 5.6 m along the pipe axis in the silt section and 25 cm off the pipe axis. The data are referenced to the soil surface and differences between soil heave and access tube heave are accounted for. At site 1, about 2.3 cm of soil heave occurred before the thermistor access tube was grasped by the frozen ground and began to heave. This means that the '0 cm' thermistor is actually 2.3 cm beneath the soil surface. The temperature pattern shown in Figure 6.1 is typical of the thermistor strings located along the pipe axis. The bulge in the 25 to 55 cm zone reflects the presence of the pipe which is buried about 30 cm beneath the soil surface.

The depth of frost penetration for this site is shown in Figure 6.2. The apparent rate of frost penetration from day 0 to day 14 is due to the fact that the soil is freezing laterally from the pipe axis as well as freezing downward. The depth of frost penetration for site 10 is also shown in Figure 6.2. Site 10 is located 0.25 m off the pipe axis and 0.55 m from the transition in the sand. As expected, the frost penetration in the sand is greater than that of the silt.

Figures 6.3 and 6.4 show soil temperatures parallel to the

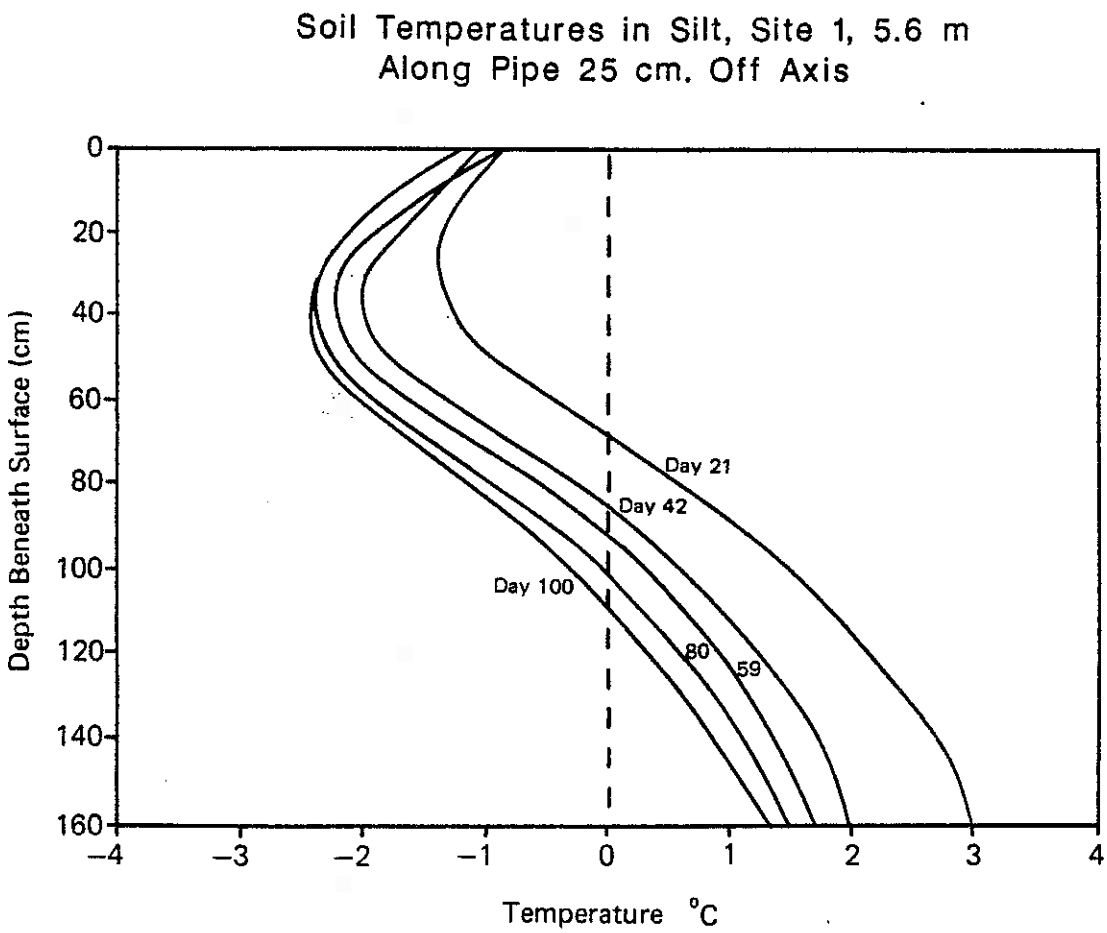

Figure 6.1 Soil temperature in silt for selected dates, site 1

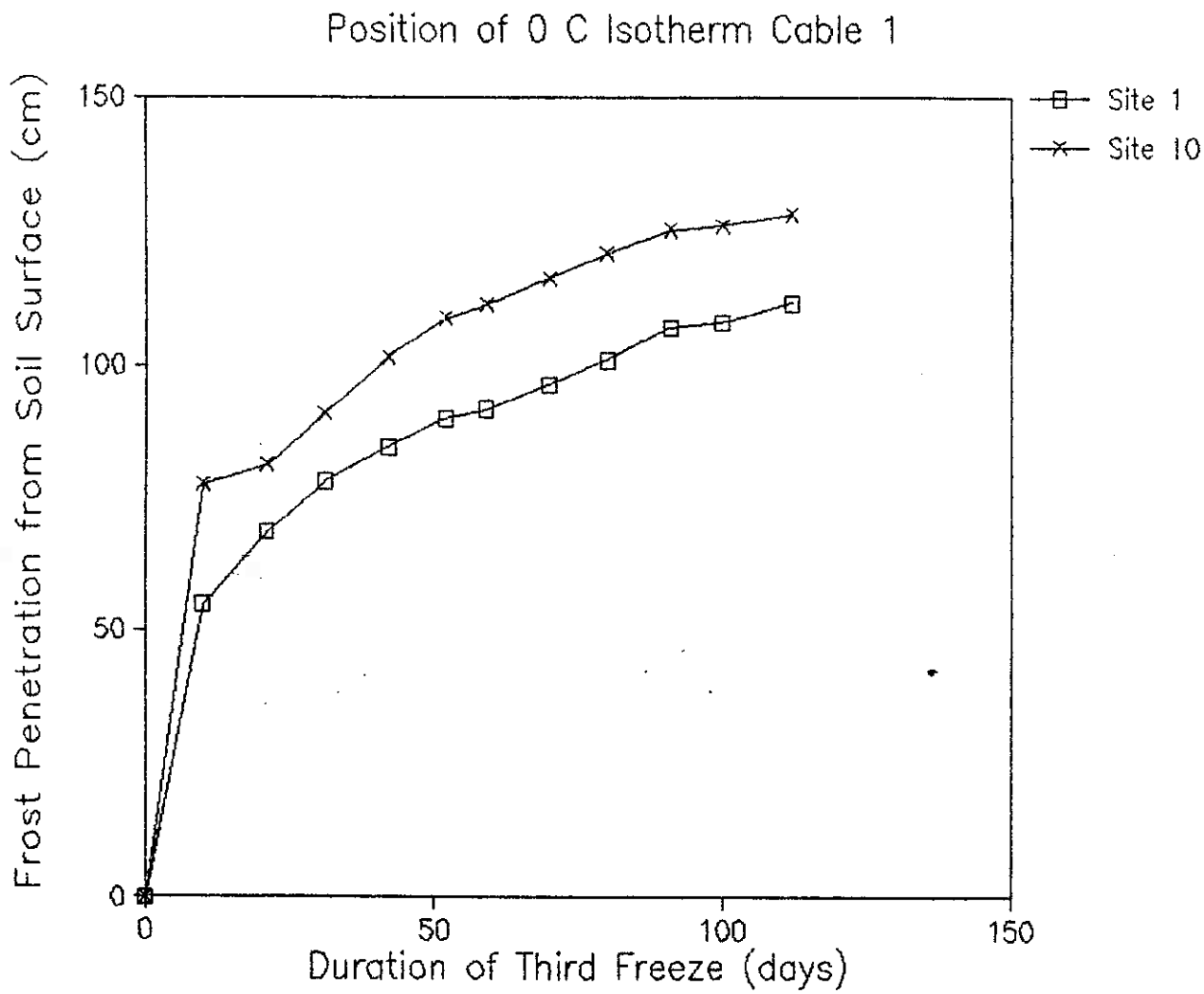

Figure 6.2 Depth of frost penetration, sites 1 and 10

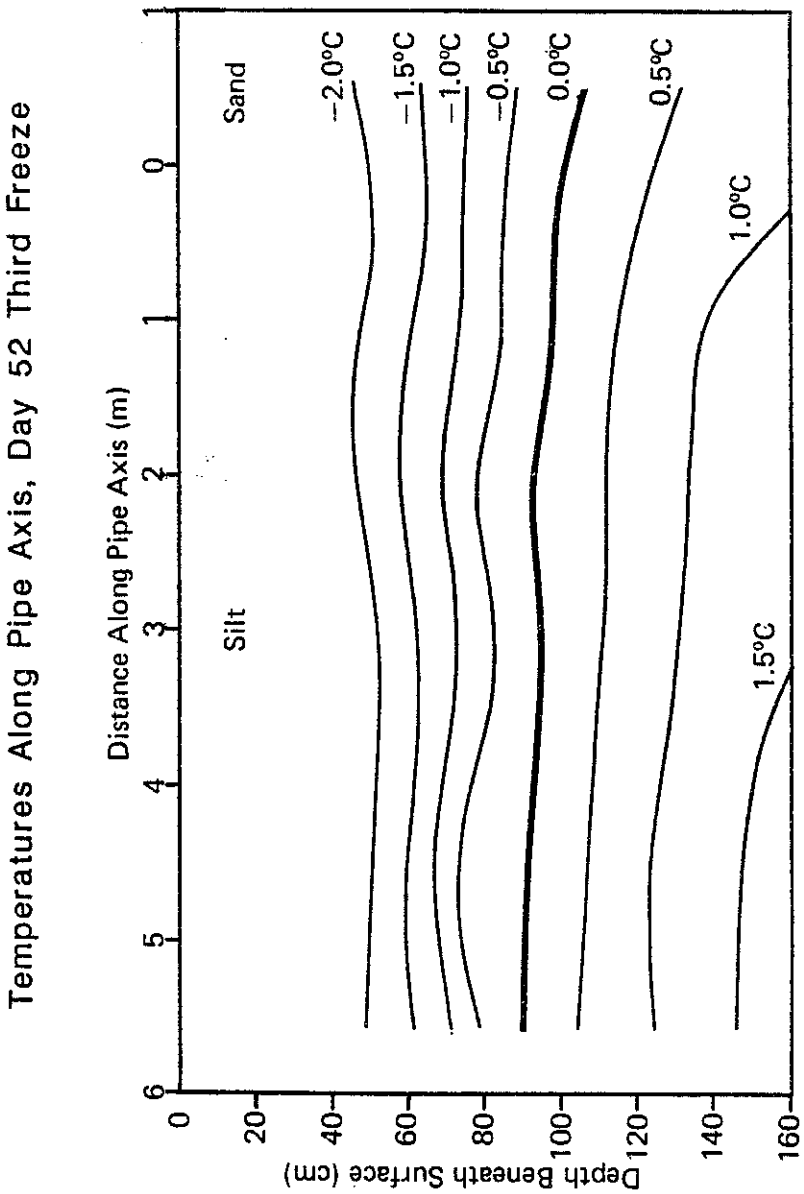

Figure 6.3 Soil temperatures along pipe axis, day 52 third freeze

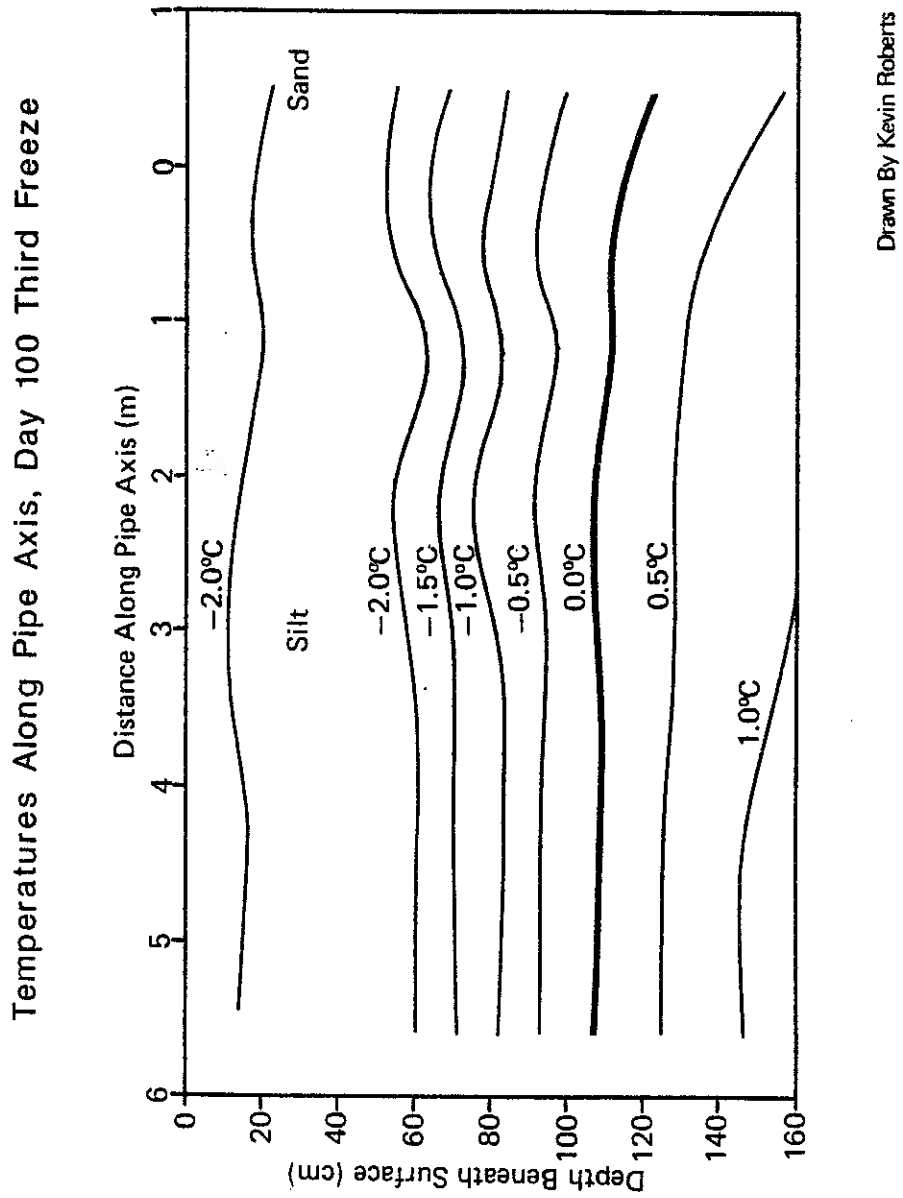

Figure 6.4 Soil temperatures along pipe axis, day 100 third freeze

pipe axis 25 cm off axis for days 52 and 100 respectively. Both figures show that the penetration of the 0 C isotherm is greater in the sand section and in the silt near the transition zone and is fairly uniform from 2 to 6 m along the pipe in the silt section.

Figure 6.5 and 6.6 show soil temperatures across the BB cross-section (located about 4.4 m from the sand-silt transition in the silt section) for days 52 and 100 respectively. These data were obtained from thermistor strings (2 to 6) located 0.25, 0.65, 1.0 and 2.0 m off axis located on one side of the pipe. It should be noted that the ground surface and pipe position in the figures has been corrected to reflect soil heave. These figures show the increased thickness of the frozen zone in the vicinity of the pipe as well as the greater soil heave in the material surrounding the pipe compared to soil at distance from the pipe axis.

6.3 Hydrologic Regime

6.3.1 Phase Composition from TDR

Figure 6.7 presents unfrozen water content data determined by Time Domain Reflectometry (TDR) for selected dates during the third freeze. The TDR probes are located on a frame situated beneath the pipe at the BB cross-section. The distance between probes is known exactly since they are fixed, however, it is difficult to determine the actual depth of each probe since the various freeze thaw cycles may have altered the pipe-TDR frame spacing. Initially the first TDR probe was located 8 cm below the pipe (65 cm beneath the soil surface).

Figure 6.5

Soil Temperatures at Section BB in Silt, Day 52.

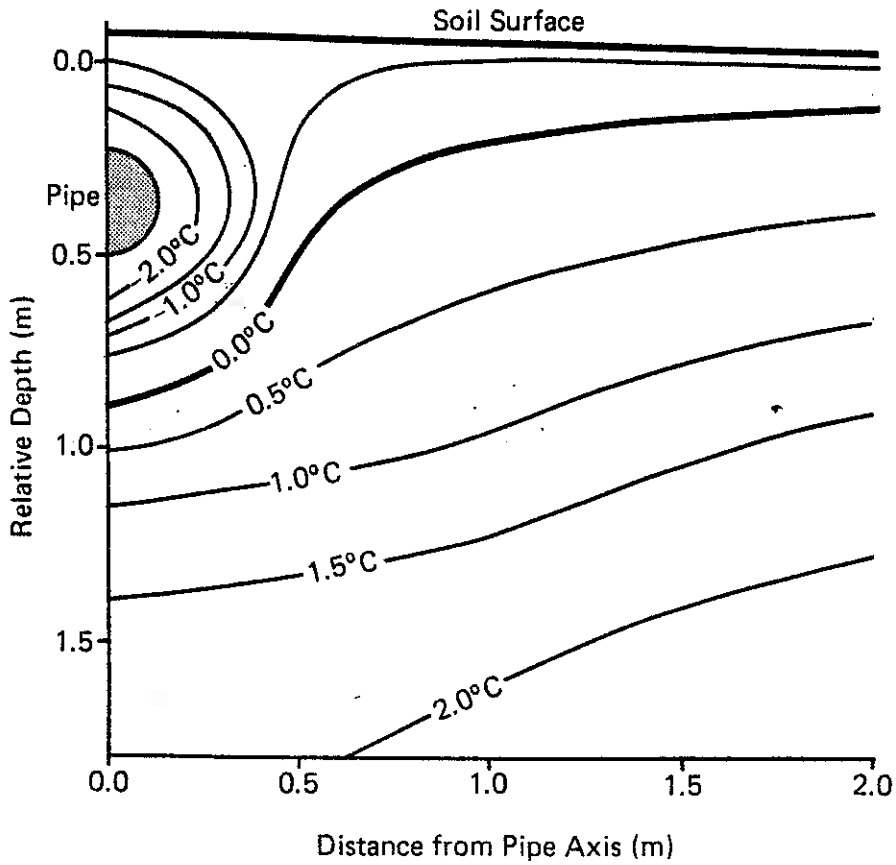

Figure 6.6

Soil Temperature at Section BB in Silt, Day 100

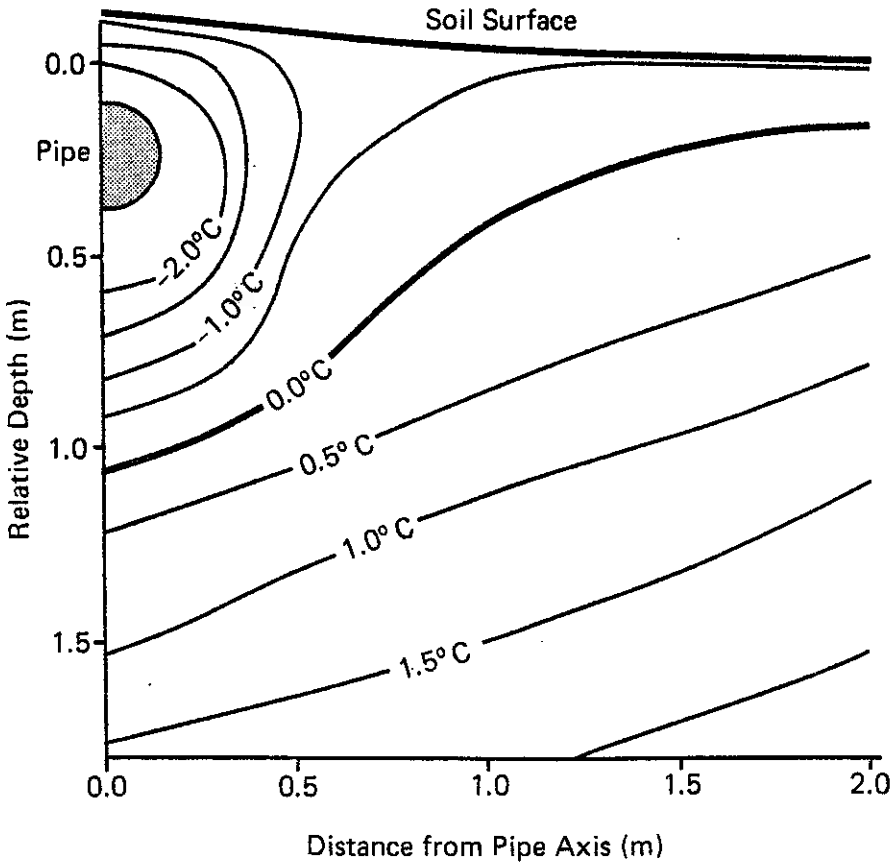

Drawn by Kevin Roberts

Figure 6.7

Unfrozen Water Contents Third Freeze, BB Section in Silt

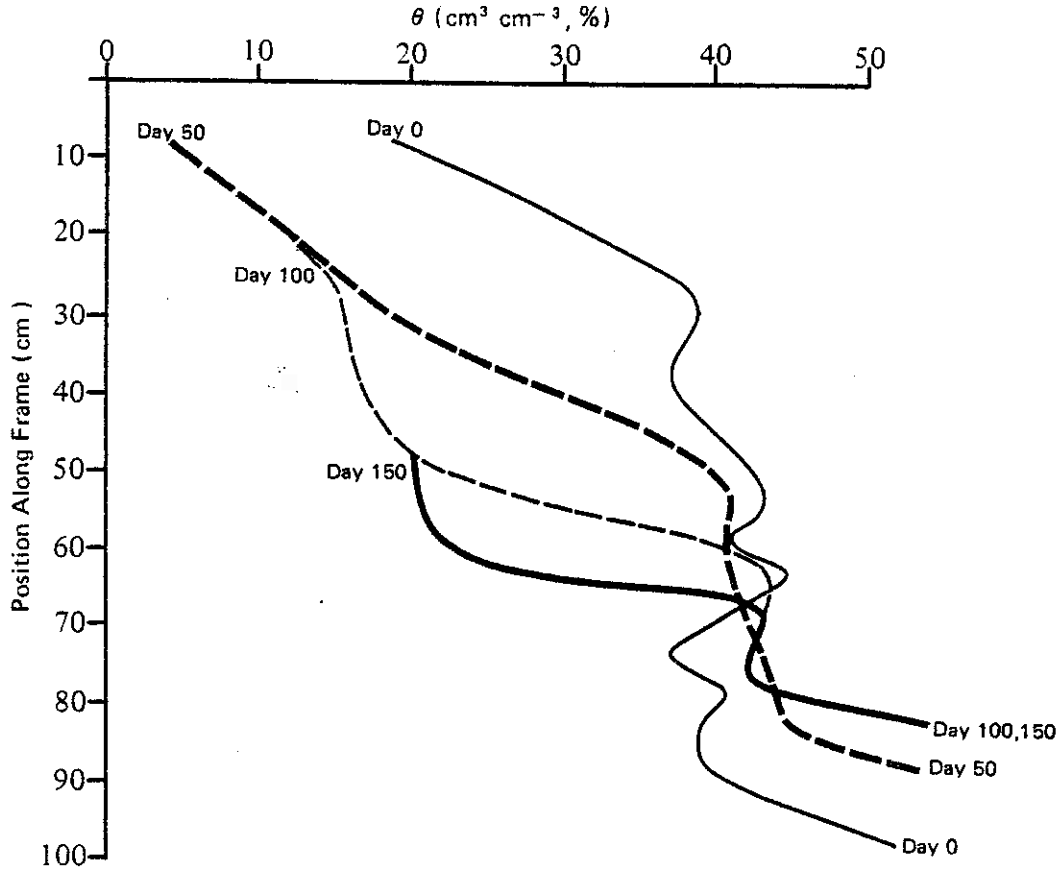

Drawn By Kevin Roberts

The data shows the progressive decrease in liquid water accompanying soil freezing. It should be noted that the TDR probes at 83, 88 and 98 cm along the TDR frame show a marked increase in water content on days 50, 100 and 150. This suggests that the TDR frame is being heaved upward in the soil as freezing progresses possibly resulting in gaps between the probe and soil at these depths. Since these probes are beneath the water table, water would accumulate resulting in higher water contents than the initial porosity would suggest.

6.3.2 Volumes of Water Added

Water levels were checked daily in order to keep the water table approximately 90 cm below the surface of the soil or 30 cm below the pipe. Figure 6.8 shows the cumulative amount of water added during the third freeze cycle.

Following the start of freezing, no water was added for 3 days. After this, water was added at approximately 100 l/day for 5 days. The rate of water consumption has very gradually decreased over the first 90 days as outlined below.

Table Volumes of Water Added to Maintain Water Table

Time (days)	Water Added (l/day)
0 - 10	57.0
20 - 30	42.5
30 - 60	45.8
60 - 90	35.6

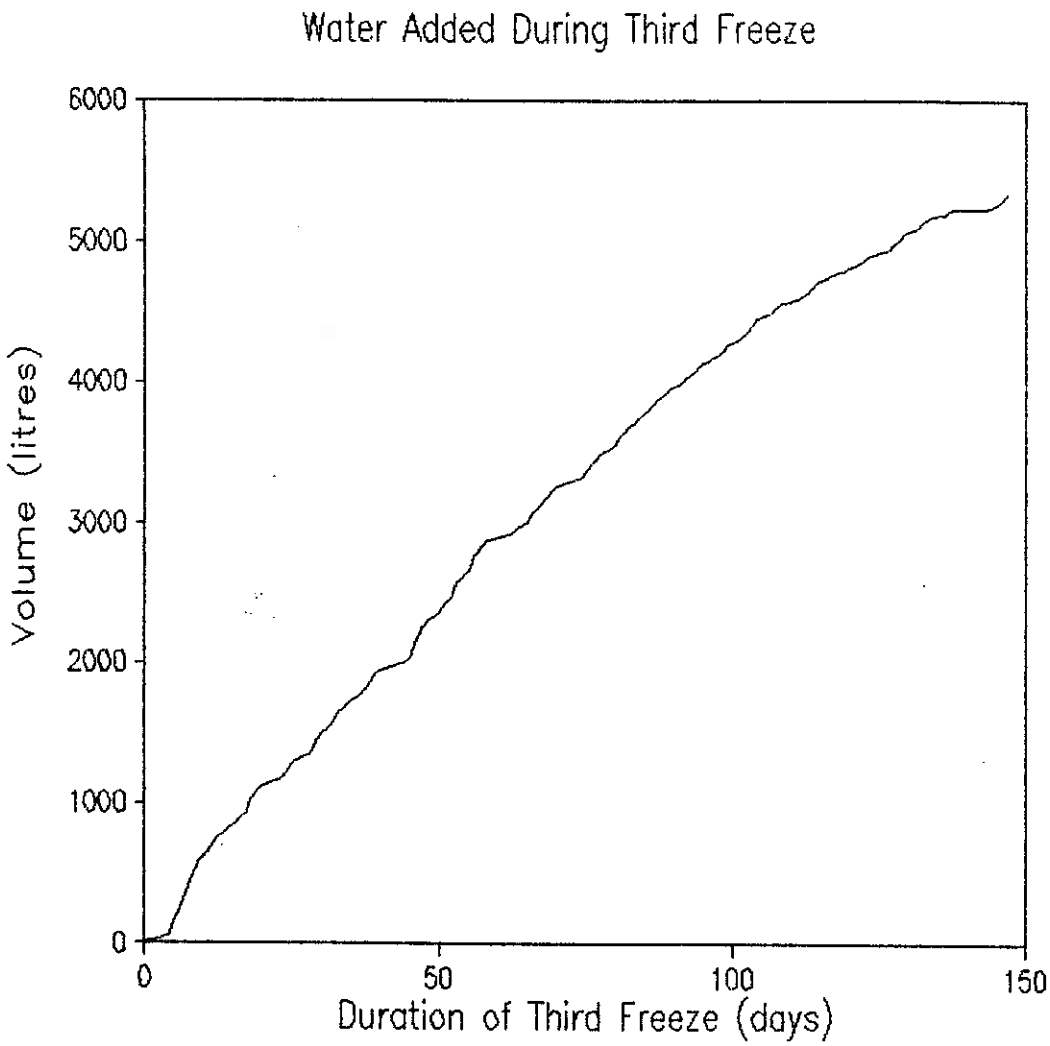

Figure 6.8 Water added during third freeze

Water consumption is usually fairly regular over short periods of say 5 - 10 days followed by a 2 - 5 day period where no additional water is required. Some of these plateaux correspond to heavy rainfall events and thus additional water is assumed to have leaked into the system from outside. Note days 20 - 23 at which time water levels in the piezometers went up by 10 cm representing approximately 200 l additional water. No water was added during this 3 day period. At other times, days 40 - 44, days 58 - 62 and the period day 69 - 75 only 100 l was added and no unusual rainfall event was recorded. It is assumed therefore that the rate of ice lens growth is not constant but proceeds in a somewhat irregular fashion with periods of growth separated by periods of little growth.

The total volume of water added during the first 90 days of this freeze cycle was slightly more than for the previous freezing cycle and the rate of addition of water was only marginally greater as shown below:

Table Rates and Amount of Water Added During Second and Third Freeze Period

Freeze Cycle	Time Period (days)					
	0 - 30		30 - 60		60 - 90	
	Total	Rate	Total	Rate	Total	Rate
Second	1176	39.2	2303	37.5	3348	34.8
Third	1550	51.1	2925	45.8	3993	35.6

Total is in litres and Rate is in litres per day

6.4 Pipe Heave

Figure 6.9 shows the pipe shape for selected dates during the third freeze. One should note that the pipe position on Day 0 shows the pipe at a higher elevation than at the start of the second freeze cycle. This indicates that the pipe has been slowly jacked upward in the soil profile during successive freeze-thaw cycles (see Figure 3.8).

Figure 6.10 shows the pipe heave at day 99 for the second and third freeze. The figure shows that heave in the silt section is greater during the third freeze than during the second and that the sand is heaving less. This aspect is further illustrated in Figure 6.11. The differences in heave are difficult to attribute to any one factor since the thermal and hydrologic conditions are the same for both freeze cycles.

Figures 6.12 and 6.13 shows the surface elevation across the pipe in the silt section (BB profile) and sand section (AA profile) respectively.

6.5 Frost Heave from Magnetic Heave Device

The total heave observed for site # 1 (5.6 m along axis in silt, 25 cm off axis) is presented in Figure 6.14. On day 115 the total heave was about 12 cm.

Figure 6.15 shows the differential heave occuring between the magnet rings at site # 1. The depths for each curve refer to the original position of the magnets within the soil. The heave noted in the 70-82 and 82-92 cm layers corresponds approximately to 17-28 and 28-38 cm beneath the pipe (although offset from the pipe axis). The amount of heave noted in each layer is

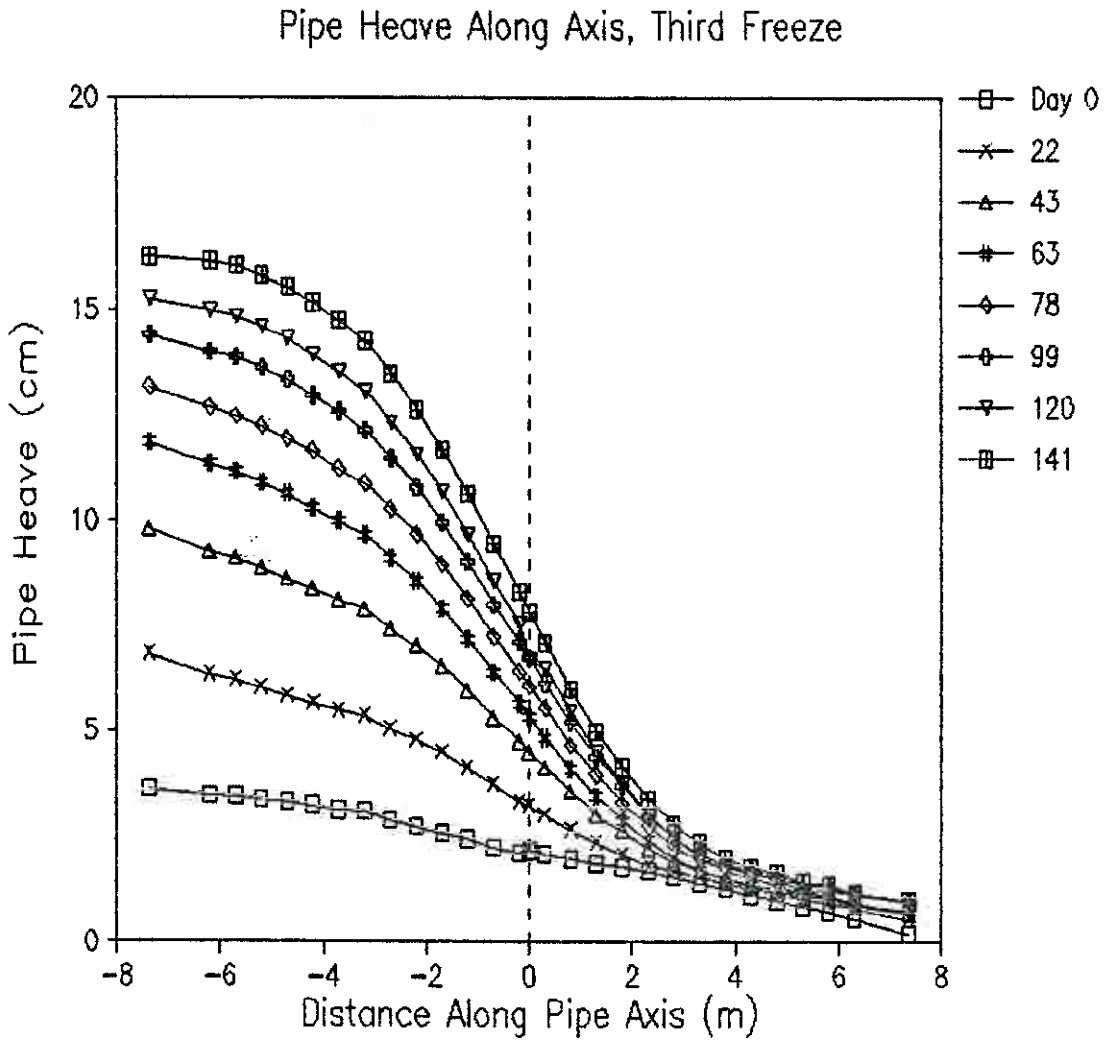

Figure 6.9 Pipe heave along axis, third freeze

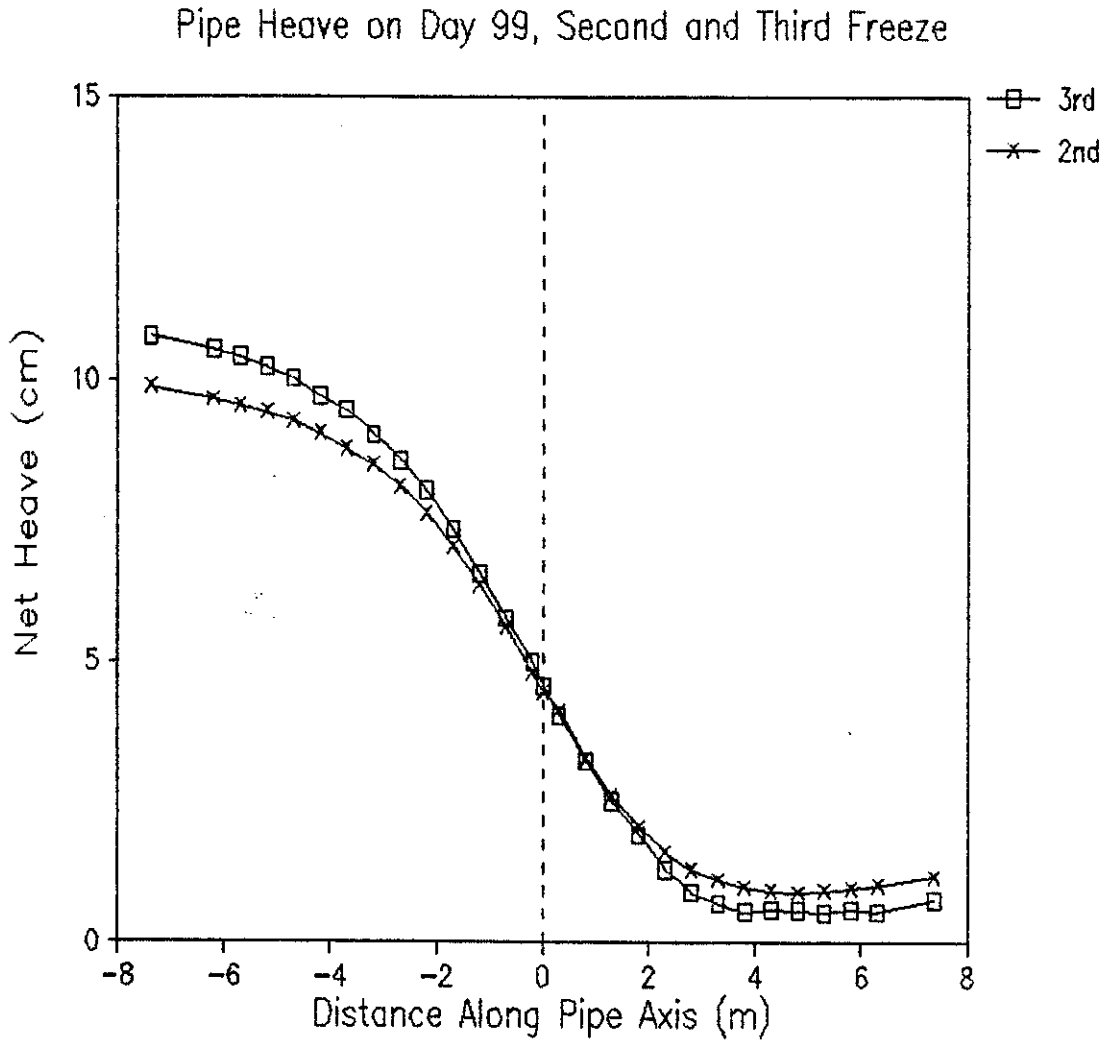

Figure 6.10 Pipe heave comparison, day 99, second and third freeze: pipe elevations

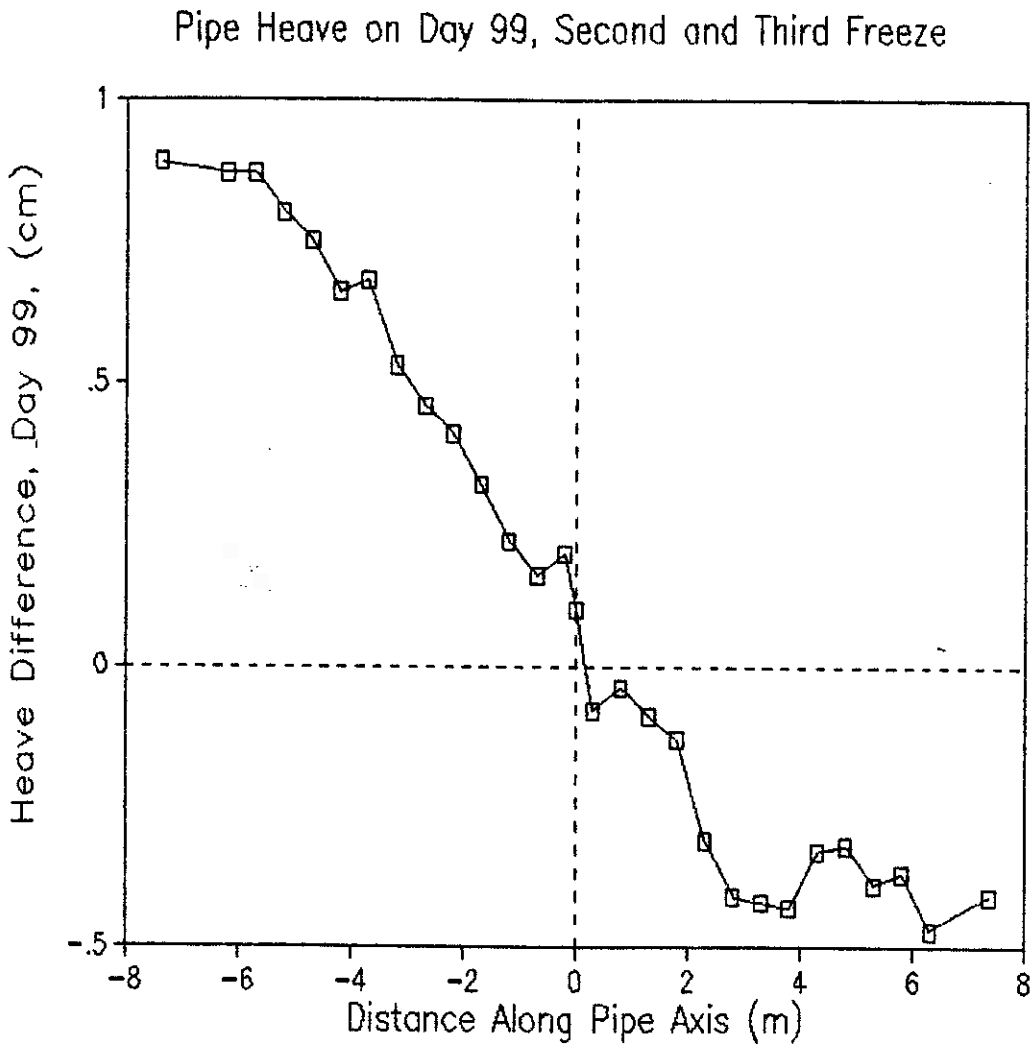

Figure 6.11 Pipe heave comparison, day 99, second and third freeze: difference in elevation

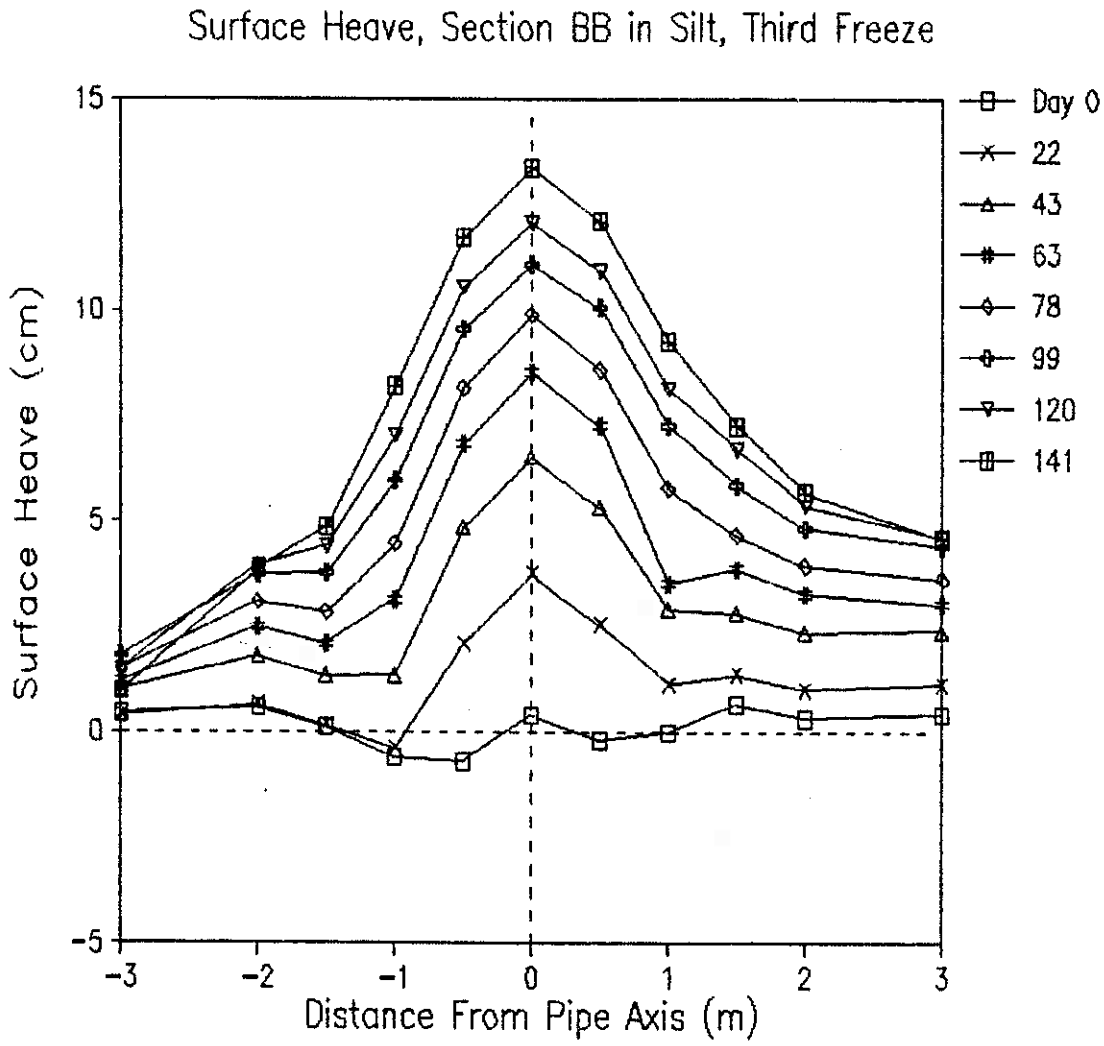

Figure 6.12 Surface heave, section BB in silt, third freeze

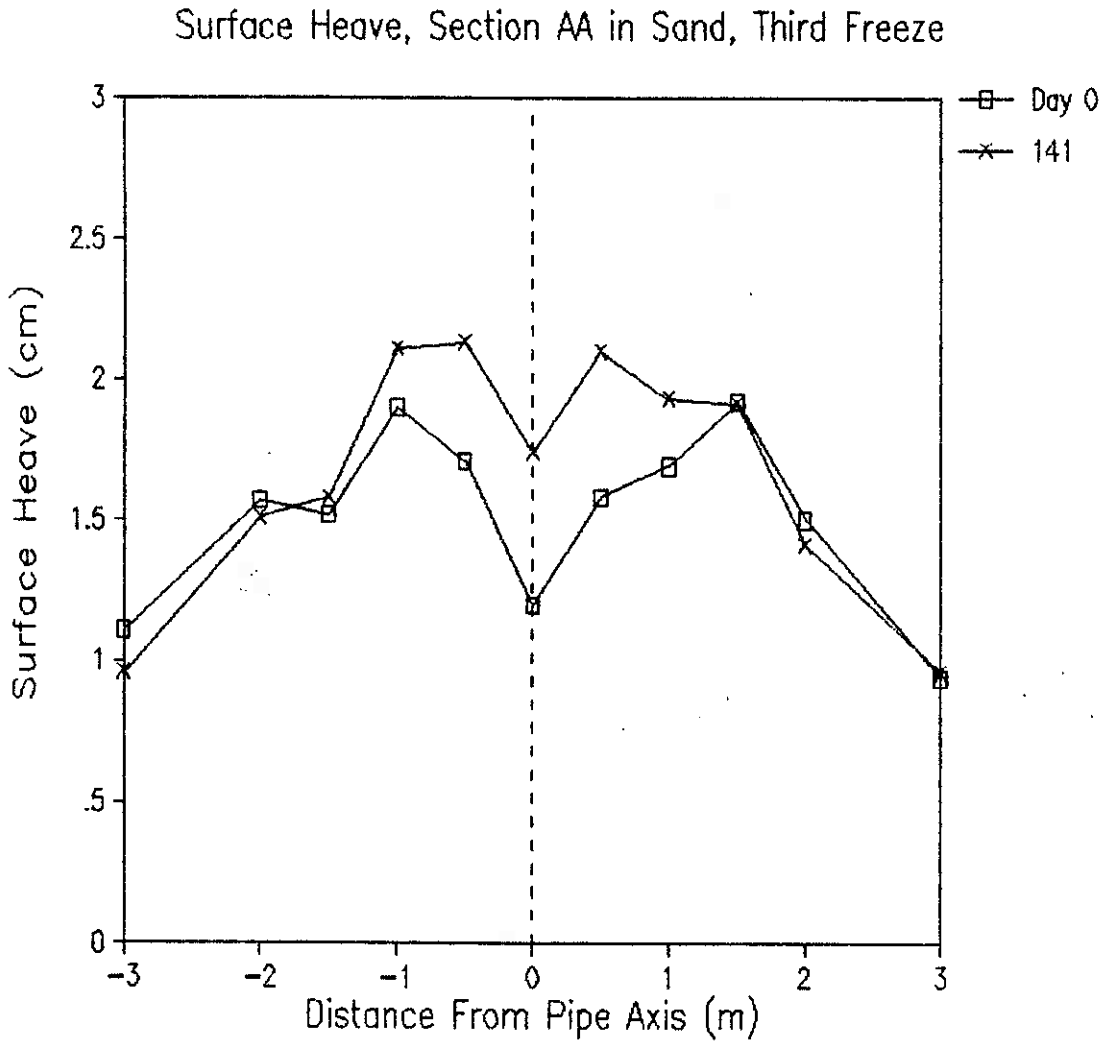

Figure 6.13 Surface heave, section AA in sand, third freeze

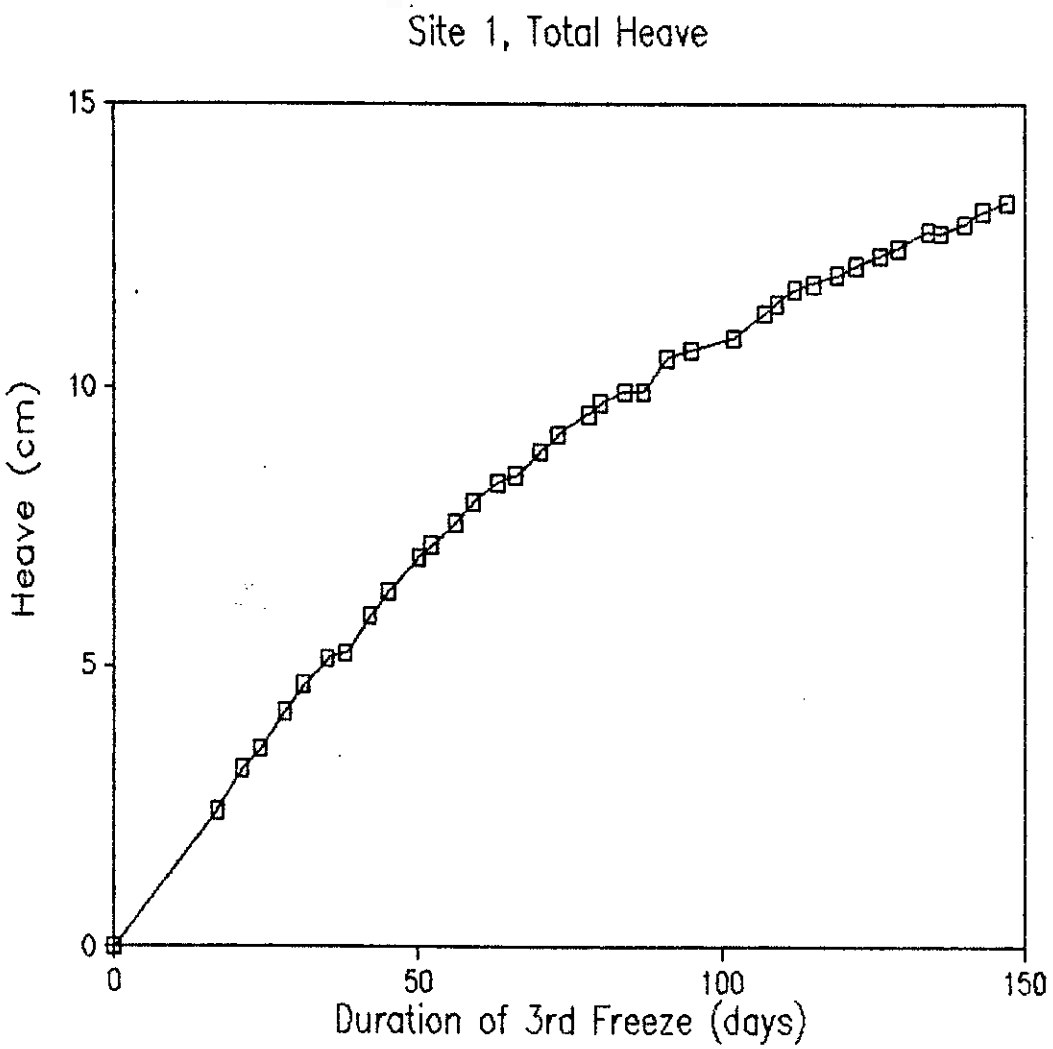

6.14 Total heave at site 1 in silt, third freeze

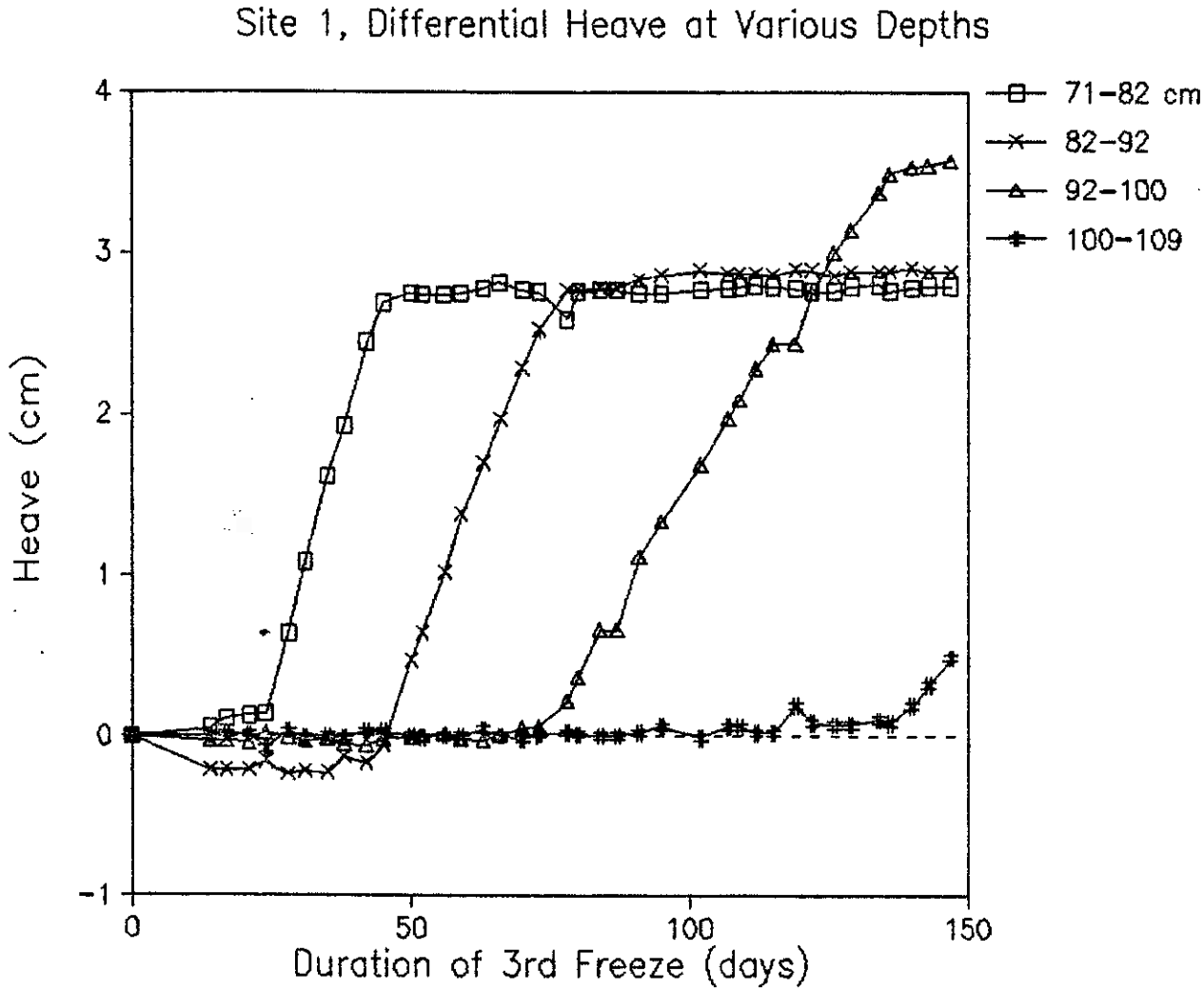

Figure 6.15 Differential heave at various depths, site 1, third freeze

approximately the same (2.7 cm) however, the rate of heave is much greater in the upper zone reflecting the greater rate of frost penetration. The 92-100 cm layer (initial depth) begins to heave on about day 70. The freezing rate was lower than found in the previous layers but the amount of heave in this layer was about 3.6 cm by day 147. It should be noted here that even though heave began in this layer on about day 70, the soil layer above continued to heave, albeit slowly, an additional 4 mm. This is attributed to secondary heave in already frozen ground. This aspect will be examined in detail at the end of the third freeze cycle when the freezing front has progressed further into the soil.

6.6 Surface Expression of Frost Heave

Figure 6.16 shows the surface elevations determined by optical levelling on day 116 of the third freeze cycle. As has been noted in previous freeze cycles, the maximum surface deflection occurs along the pipe axis in the silt section with decreasing heave as one moves laterally from the pipe axis or into the sand section.

6.7 Pipe Stress

Figure 6.17 shows pipe stress for selected dates during the third freeze cycle. As observed during previous freeze cycles, the stress levels build up quite rapidly during the onset of freeze when frost heave and pipe displacement is quite rapid and large. As noted in section 3.4, two gauges broke during the second thaw period resulting in an unfortunate loss of data for the third freeze period. Fortunately, the gauges where maximum

Day 116 Third Freeze

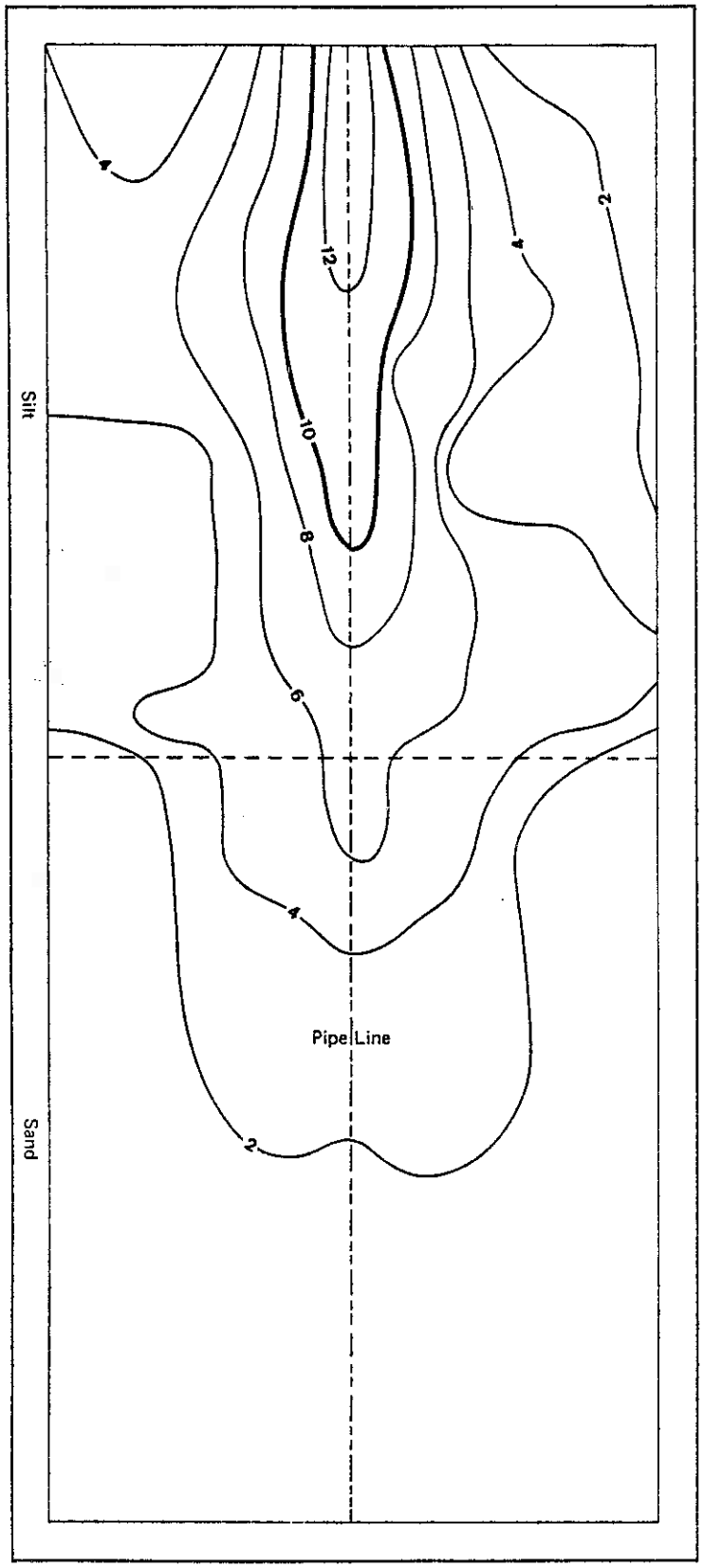

Contour Interval - 2 cm.

Drawn by Kevin Roberts
October 1986

Figure 6.16 urface elevation during third freeze, day 116

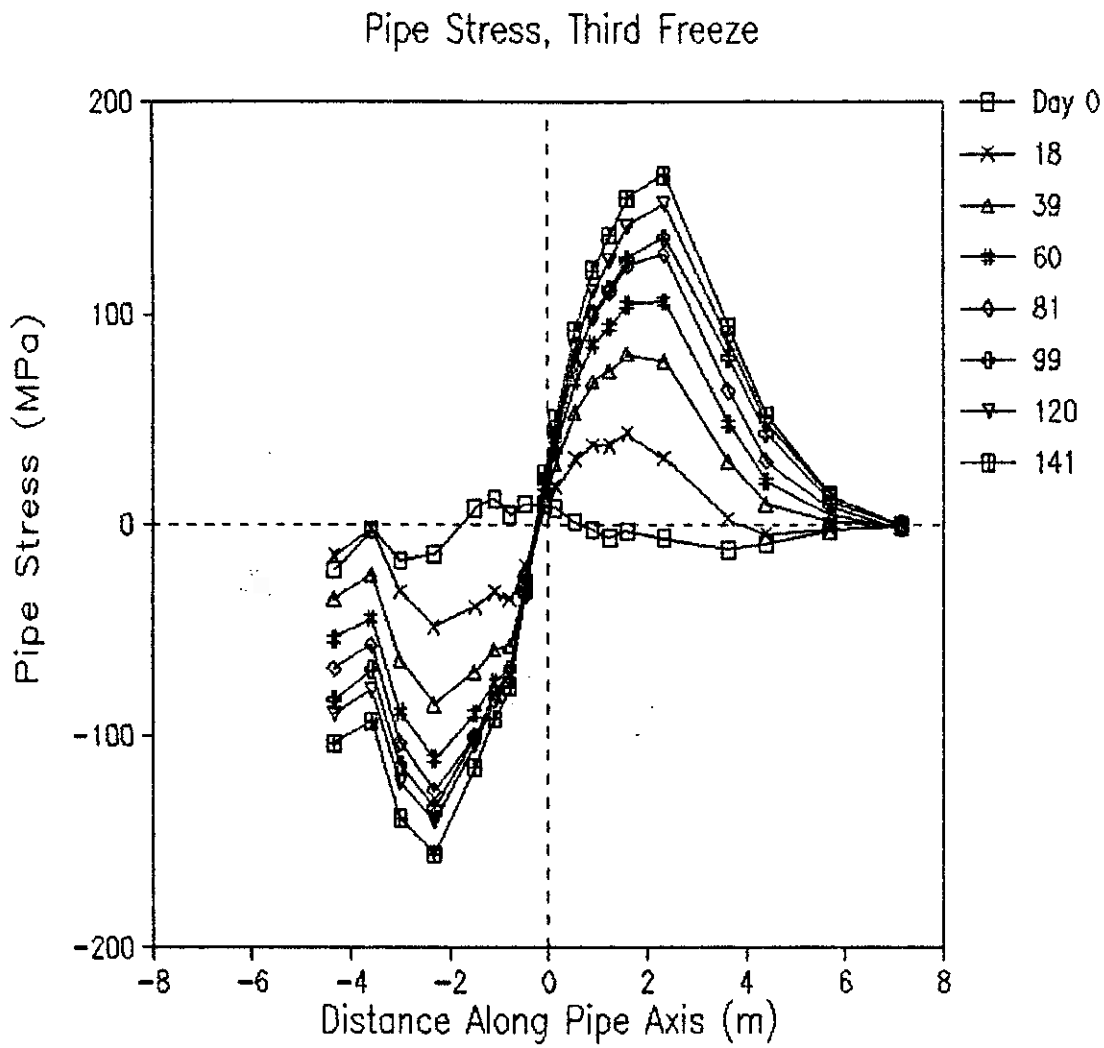

Figure 6.17 Pipe stress, third freeze

stress occurs in the pipe are still operational.

Figure 6.18 shows the pipe stress values for day 0 during the first, second and third freeze. This figure shows the residual stresses in the pipe following each thaw. Figure 6.19 presents the values noted on day 99 for the second and third freeze; these data show that higher values of pipe stress are being recorded during the third freeze cycles than were noted during the second.

6.8 Stress in the Ground

As noted previously, the Petur cells failed to operate successfully, hence information on stress in the ground was obtained only from the Glotzl cells.

Figure 6.20 shows the pressures recorded at the °BB' transition near the middle of the silt section. As is shown, the Glotzl cell at 10 cm shows a general rise in pressure as soil freezing progresses while the other gauges at 46 and 86 cm have remained relatively unaffected. The sudden drop in the recorded pressure from day 96 to day 103 occurred during a breakdown of the compressors which lasted from day 96 to day 98.

Figure 6.21 shows the pressures recorded at the °AA° transition near the middle of the sand section. The pressures recorded at 10 cm rise more steeply than those in the silt section and attain a higher level since soil freezing is quicker and more complete. The pressure at 46 cm also begins to rise sharply at about day 38 when the freezing front passes this depth. The effect of the compressor shut down is also clearly seen in the data from day 96 to day 103.

Figure 6.18

Pipe Stress at the Start of the Three Freeze Cycles

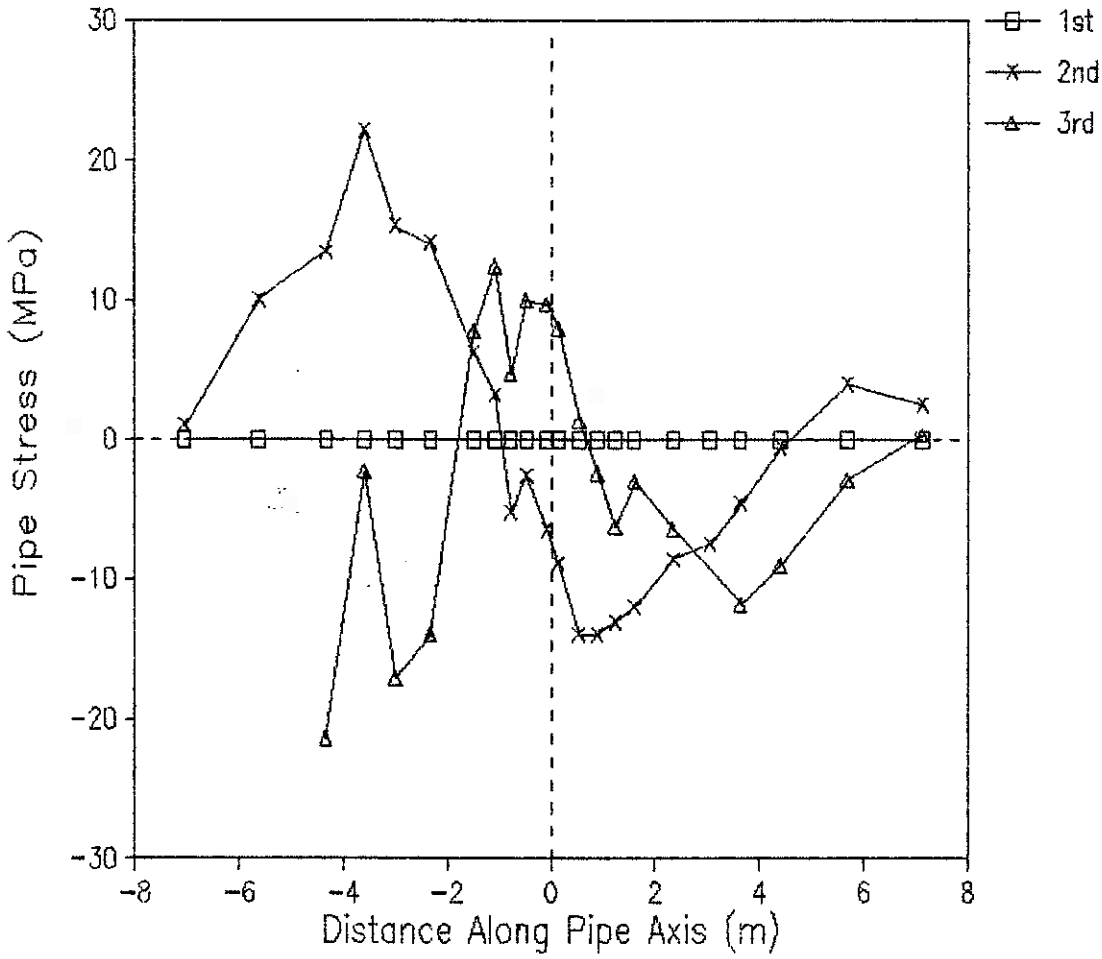

small door

large door

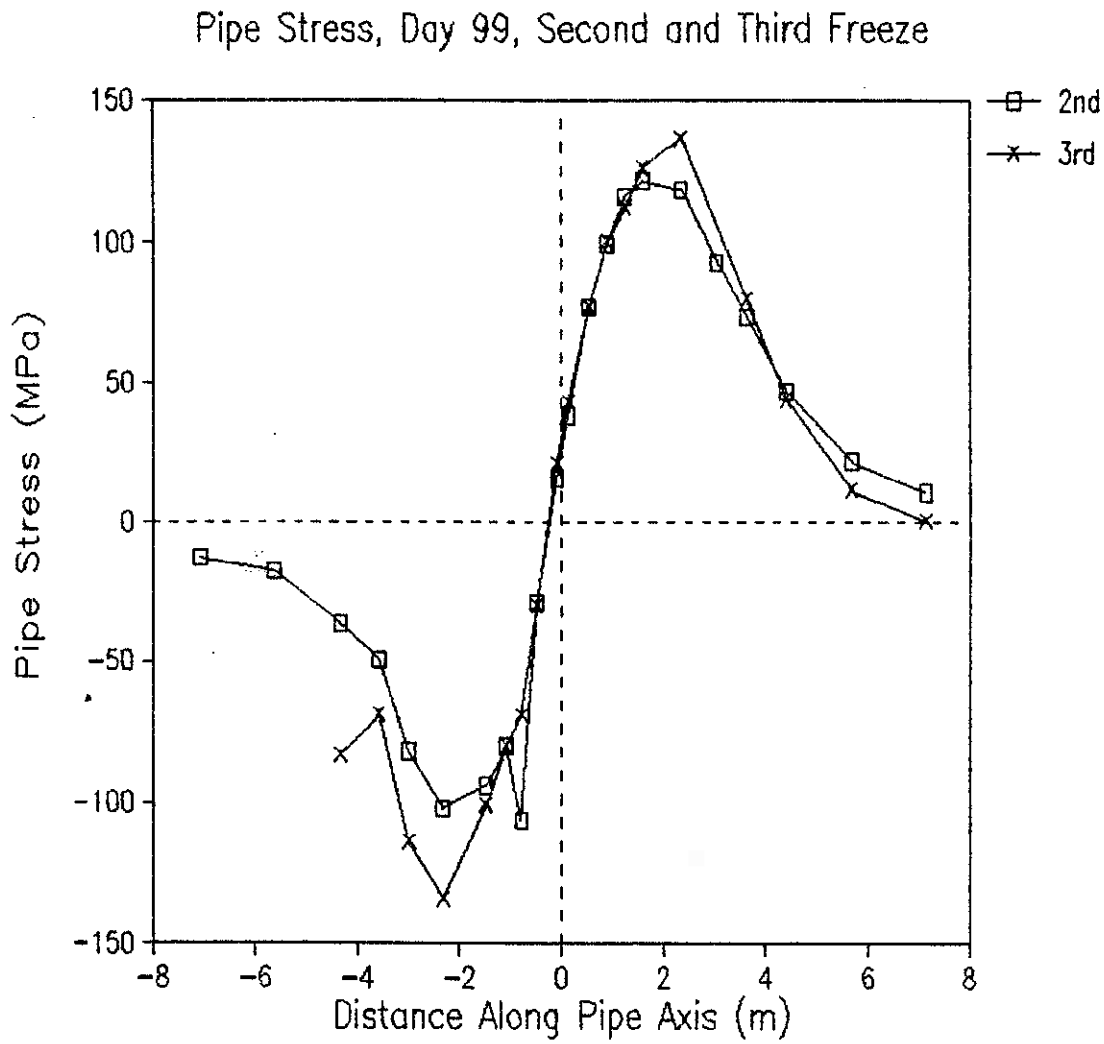

Figure 6.19 Pipe stress comparison, day 99 during second and third freeze

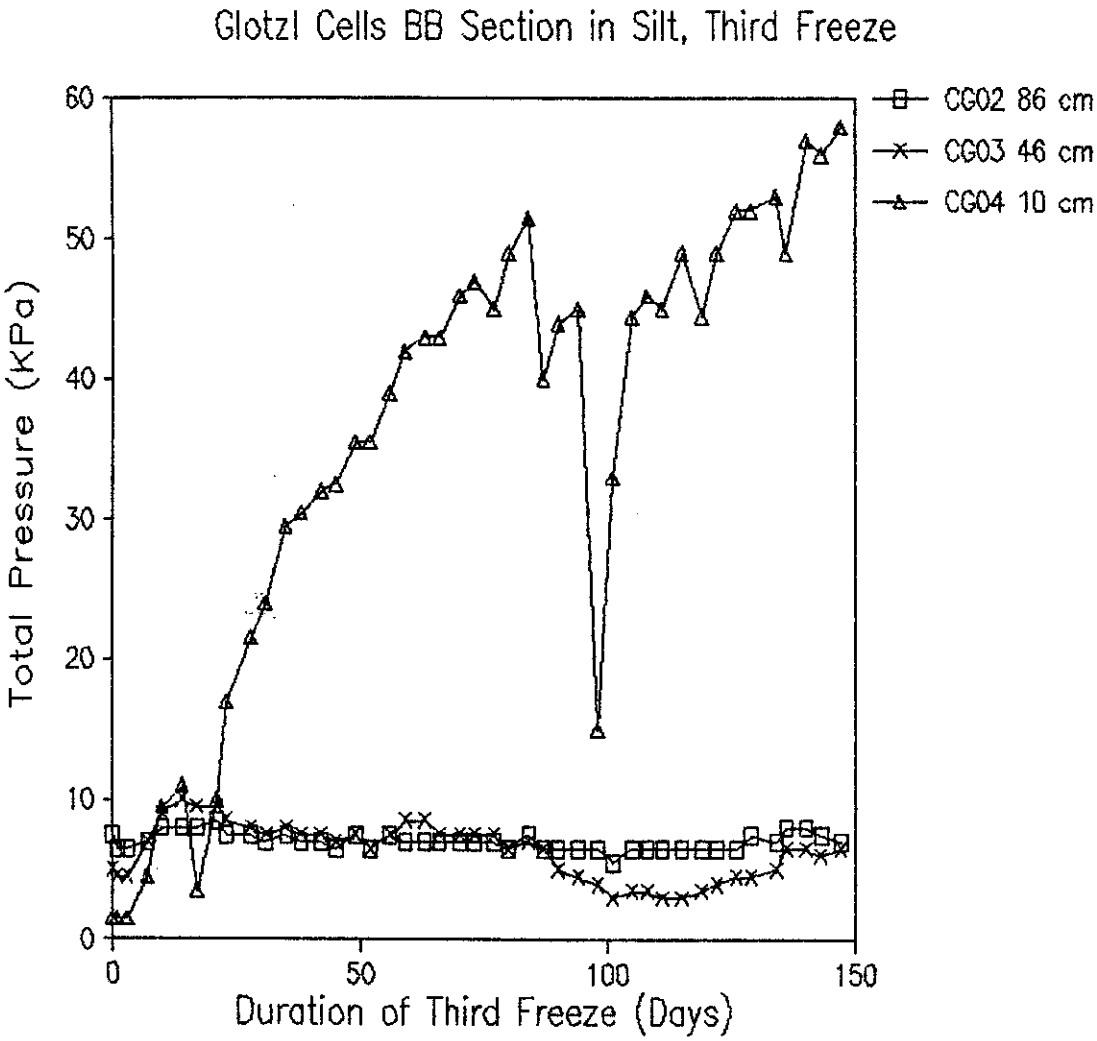

Figure 6.20 Soil pressures at section BB in silt, third freeze

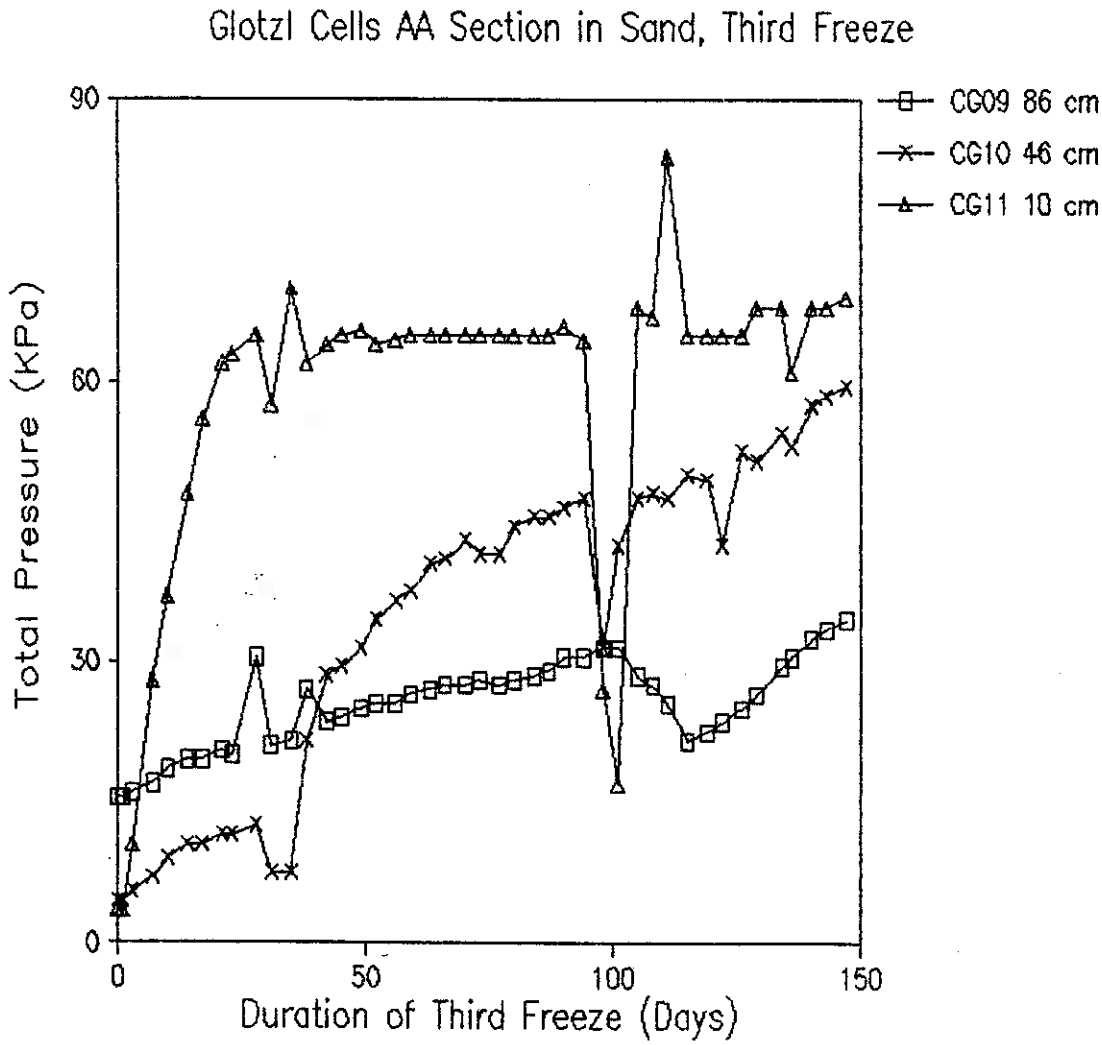

Figure 6.21 . Soil pressures at section AA in silt, third freeze

VII EXAMINATION OF SOIL BEHAVIOUR MADE OFF-SITE

7.1 Strain-Rate-Controlled Uniaxial Compression Tests with the Caen Silt

A major experimental investigation on this topic has been carried out in 1985, by B. Ladanyi and J. F. Morel, in the laboratories of the Northern Engineering Centre of Ecole Polytechnique, Montreal.

7.2 Introduction

The knowledge of the mechanical properties of the two frozen soils in which the experimental pipe is buried, is essential for mathematical modelling of soil-pipe interaction during the periods of freezing and thawing included in the testing programme in Caen.

In a previous report (Ladanyi and Lauzon, in Geotechnical Science Laboratories, 1985), we have presented the preliminary results of a study which included both soils used in the Caen experiment: the SNEC Sand and the Caen Silt. The first study involved two kinds of uniaxial and triaxial compression tests: stress-controlled (creep tests), and strain-rate-controlled tests. All these tests were made at a temperature of -2 C.

The purpose of the present study, which is a continuation of the first one, was to enlarge the scope of temperatures and strain rates, in order to get a more complete picture of one of the two soils, the Caen Silt, with a particular emphasis on temperatures close to the melting point.

7.3 Sample Preparation

For performing the tests, a sufficient quantity of the Caen Silt, shipped earlier from France to Montreal, was available at our laboratories. Figure 7.1 shows a typical grain size distribution curve of the silt, as received. From this, only the fraction passing a No. 40 sieve was used in the tests.

The samples were prepared by compacting the soil at optimum water content in plexiglass moulds, in 25 mm thick layers, with 25 blows per layer. The samples were then saturated by circulating distilled de-aerated water through them. Each mould had an overflow tube for evacuating excess water during freezing. The mould, laterally insulated, was then placed in a cold cabinet and frozen from below at -27 C, for at least 2 days. After freezing, the samples, which were about 37.5 mm in diameter, were cut by a diamond saw to the desired length of about 77.5 mm. The cuttings from each sample were used for water content and degree of saturation determinations.

Altogether, 41 samples of the Caen Silt were prepared in this manner and tested. Their main physical characteristics (water content, void ratio, and degree of saturation) are shown in Table 7.1. It is noted that the first 12 samples contained thin ice lenses, because they were frozen deliberately more slowly, at a higher temperature.

7.4 Test Equipment and Procedure

Each sample was mounted in a triaxial cell, protected by a latex membrane, and enclosed in a thick layer of insulating material. The temperature in the cell was maintained by

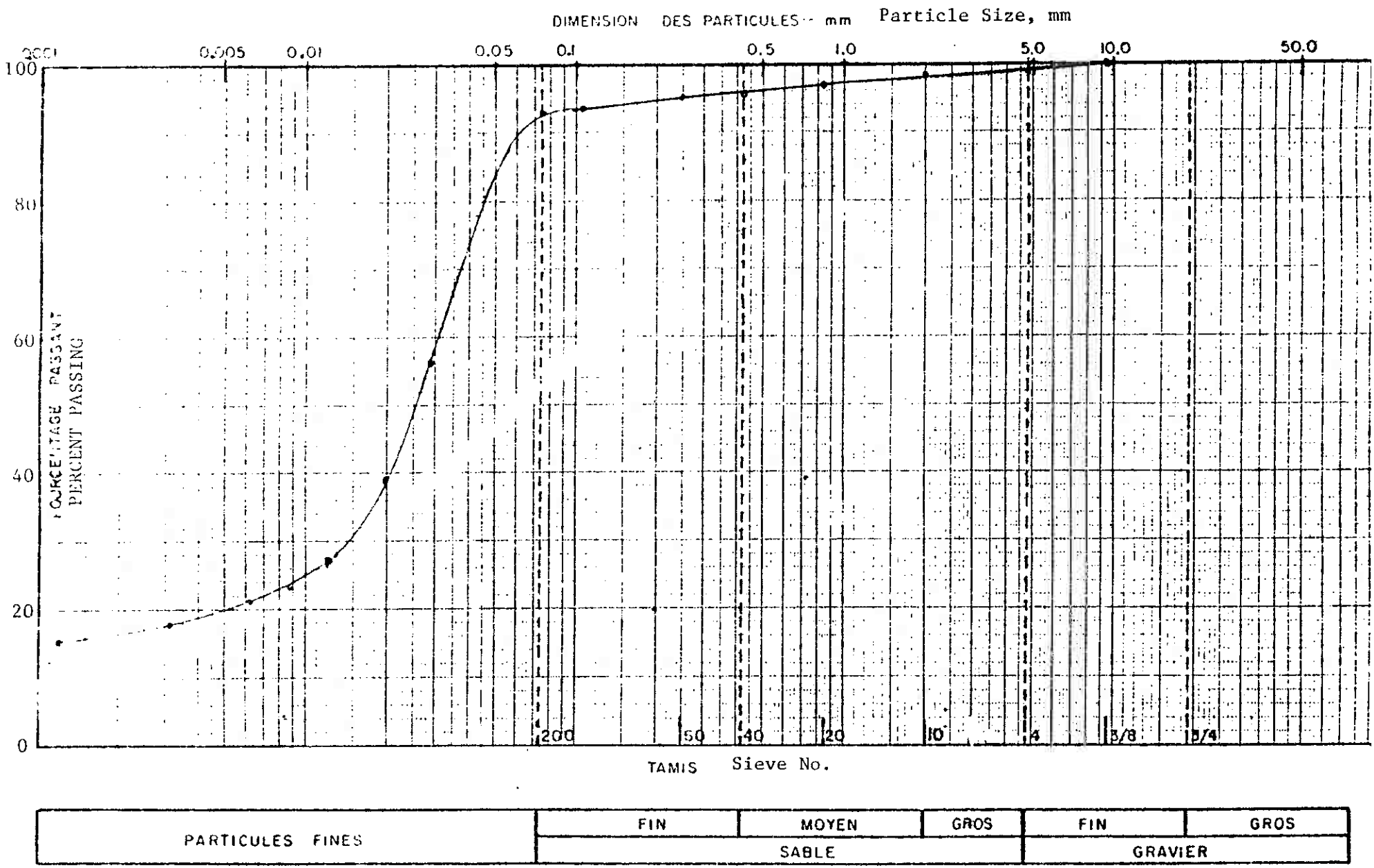

Figure 7.1 - Caen Silt: Grain Size Distribution Curve.

TABLE

PHYSICAL AND MECHANICAL PROPERTIES OF TESTED SAMPLES

SAMPLE No.	WATER CONTENT w(%)	VOID RATIO e	DEGREE OF SATURATION S_r(%)	TEMPERATURE (°C)	PEAK OR YIELD STRENGTH (MPa)	AXIAL STRAIN RATE AT PEAK OR YIELD (min^{-1})
1*	16.7	0.563	79.5	-2	1.259	5.428(-3)**
2*	16.9	0.547	82.8	-2	1.418	4.909(-3)
3*	17.9	0.582	82.4	-2	1.195	5.074(-3)
4*	18.0	0.584	82.5	-2	0.375	1.574(-4)
5*	18.5	0.562	88.1	-2	0.654	1.635(-4)
6*	18.7	0.591	84.5	-2	0.561	1.605(-4)
7*	19.2	0.593	86.8	-5	1.585	1.626(-4)
8*	18.7	0.597	84.0	-5	1.639	1.608(-4)
9*	19.4	0.619	84.0	-5	1.530	1.597(-4)
10*	18.2	0.576	84.7	-5	2.467	5.074(-3)
11*	18.2	0.574	85.0	-5	2.467	4.931(-3)
12*	17.3	0.559	82.9	-5	2.463	4.945(-3)
13	18.7	0.563	89.0	-2	1.102	4.956(-3)
14	17.3	0.541	85.6	-2	1.266	4.901(-3)
15	18.1	0.539	90.1	-2	1.267	4.831(-3)
16	17.1	0.547	83.7	-1	0.691	4.963(-3)
17	18.3	0.544	90.1	-1	0.625	5.022(-3)
18	17.7	0.542	87.5	-1	0.777	4.921(-3)
19	17.7	0.527	90.0	-2	0.921	1.585(-4)
20	17.6	0.515	91.5	-2	0.942	1.572(-4)
21	17.0	0.535	85.1	-2	0.686	1.575(-4)
22	17.1	0.545	84.0	-1	0.251	1.665(-4)
23	16.6	0.538	82.7	-1	0.261	1.545(-4)
24	18.1	0.546	88.8	-1	0.321	1.574(-4)
25	18.3	0.559	87.8	-2	1.932	5.585(-2)
26	18.1	0.549	88.3	-2	1.706	5.490(-2)
27	19.1	0.554	92.4	-2	1.691	5.505(-2)
28	18.7	0.546	91.8	-1	0.864	5.503(-2)
29	20.0	0.586	91.4	-1	0.846	5.713(-2)
30	18.4	0.562	87.7	-1	0.715	5.414(-2)
31	19.1	0.539	95.0	-2	0.780	2.905(-5)
32	18.2	0.533	91.5	-2	0.823	2.870(-5)
33	19.2	0.557	92.3	-2	0.677	2.868(-5)
34	19.5	0.542	96.5	-1	0.344	2.932(-5)
35	19.1	0.541	94.7	-1	0.297	2.942(-5)
36	17.8	0.536	89.0	-1	0.265	2.960(-5)
37	18.6	0.543	91.6	-1	0.217	5.460(-6)
38	18.9	0.547	92.6	-1	0.221	5.690(-6)
39	17.6	0.536	87.9	-1	0.337	9.245(-4)
40	18.0	0.530	91.0	-1	0.376	9.342(-4)
41	17.8	0.552	86.3	-1	0.314	9.198(-4)

NOTE: 1* = sample with ice lenses;

** 5.428(-3) denotes 5.428×10^{-3}.

circulating a coolant through a tube spiralling around the sample. The tube was connected to a cooling bath with a temperature control of +/- 0.01 C. The strain-rate-controlled tests were carried out in an electrically operated 50-ton testing machine, enabling one to control the velocity of movement of its loading plattens.

During the tests, the axial stress in the samples was recorded by means of a force transducer. Overal volume changes of the samples were recorded by a burette connected to the liquid in the cell surrounding the sample.

From the recorded vertical displacements, the natural axial strains were determined by the usual procedure. The axial stress was calculated by taking into account the variation of the sample diameter and the volume changes that occurred during the test.

7.5 Testing Programme and Results

Before the tests, the samples were stabilized at 3 different temperatures: -1 C, -2 C, and -5 C, respectively. Of the 41 samples, 17 were tested at -1 C, 18 at -2 C (6 of which had ice lenses), and 6 at -5 C (all of which had ice lenses).

As shown in Table 7.1, the testing machine construction, and the size of samples, enabled only 6 different axial strain rates to be applied during the tests, i.e., about: 5.5×10^{-6}, 2.9×10^{-5}, 1.6×10^{-4}, 9.2×10^{-4}, 5.0×10^{-3}, and 5.5×10^{-2} min^{-1}.

For each test a complete set of stress-strain and volume-strain curves were computer-plotted. Some typical results are shown in Figures 7.2 to 7.13. The peak or the yield strengths, determined from each stress-strain curve, are shown in Table 7.1.

For comparison purposes, two sets of typical selected stress-strain curves, for -1 C and -2 C, respectively, are shown in Figures 7.14 and 7.15.

Finally, Figure 7.16 shows a whole set of rheological curves obtained in the tests. The curves relate the peak or yield stresses with the corresponding applied axial strain rates, enabling the determination of the values of creep parameters n and σ_c in the power-law creep equation:

$$\dot{\varepsilon} = \dot{\varepsilon}_c(\sigma / \sigma_c)^n \qquad 1$$

mentioned in the previous report (Ladanyi and Lauzon, in Geotechnical Science Laboratories, 1985).

7.6 Discussion of Test Results

On the basis of test results obtained in this investigation, several aspects of the behaviour of the frozen Caen Silt have become evident. A review of some principal findings is given below.

7.6.1 Stress-strain Behaviour

As seen in Figures 7.2 to 7.13, the compacted frozen silt (with an average void ratio of 0.540), shows a non-linear stress-strain behaviour in the pre-peak region. After the peak, or the yield point, (which occurs at strains between 4% and 8%), there is a more or less pronounced drop of strength ("brittleness"). Comparing the stress-strain curves for different temperatures and strain rates, it is found that the "brittleness" (post-peak drop of strength) increases with increasing strain rate and decreasing

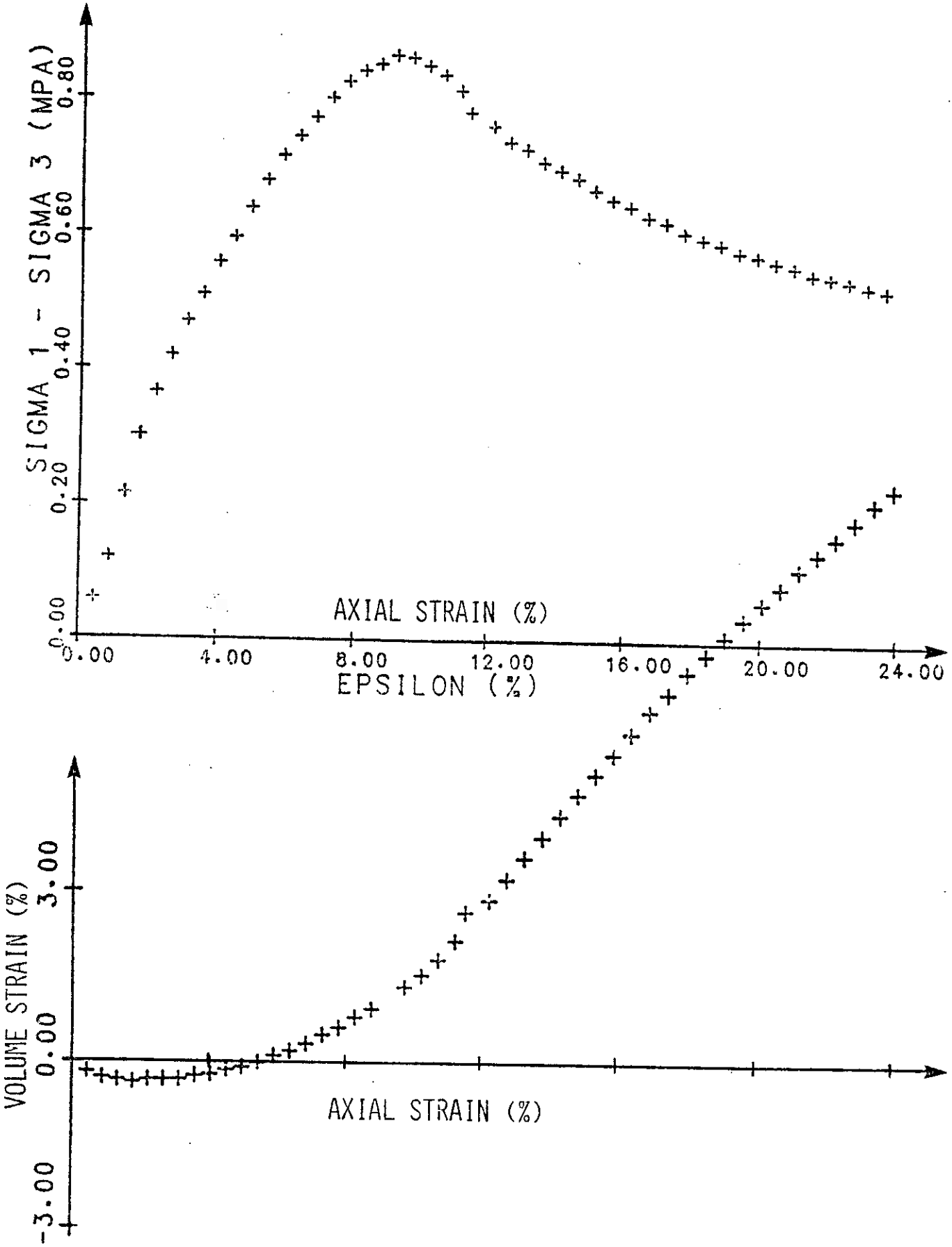

Figure 7.2 - Caen Silt: Test 28. Stress-strain curves at $-1^{\circ}C$ and at 5.52×10^{-2} min^{-1}.

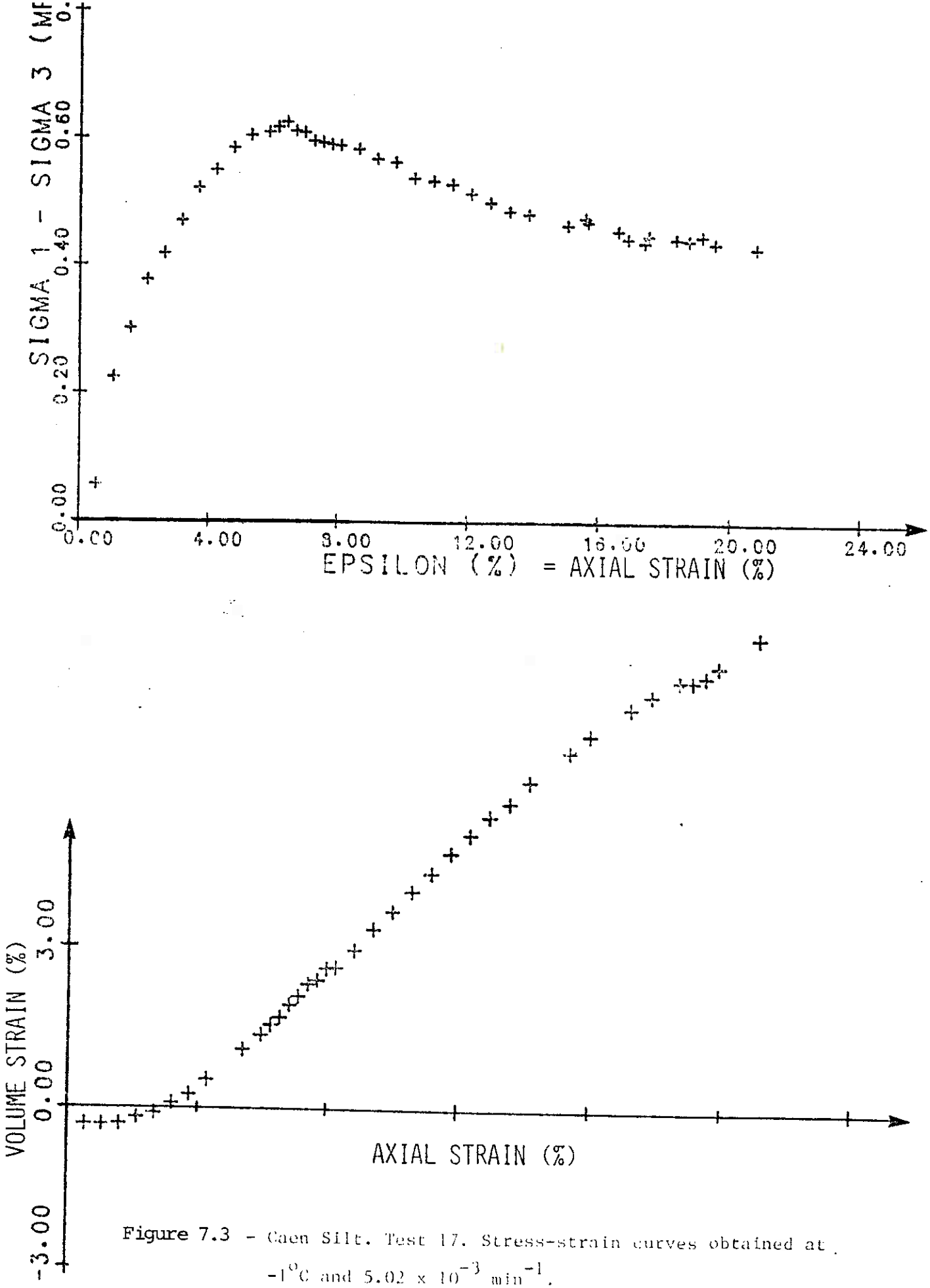

Figure 7.3 - Caen Silt. Test 17. Stress-strain curves obtained at $-1^{o}C$ and 5.02×10^{-3} min^{-1}.

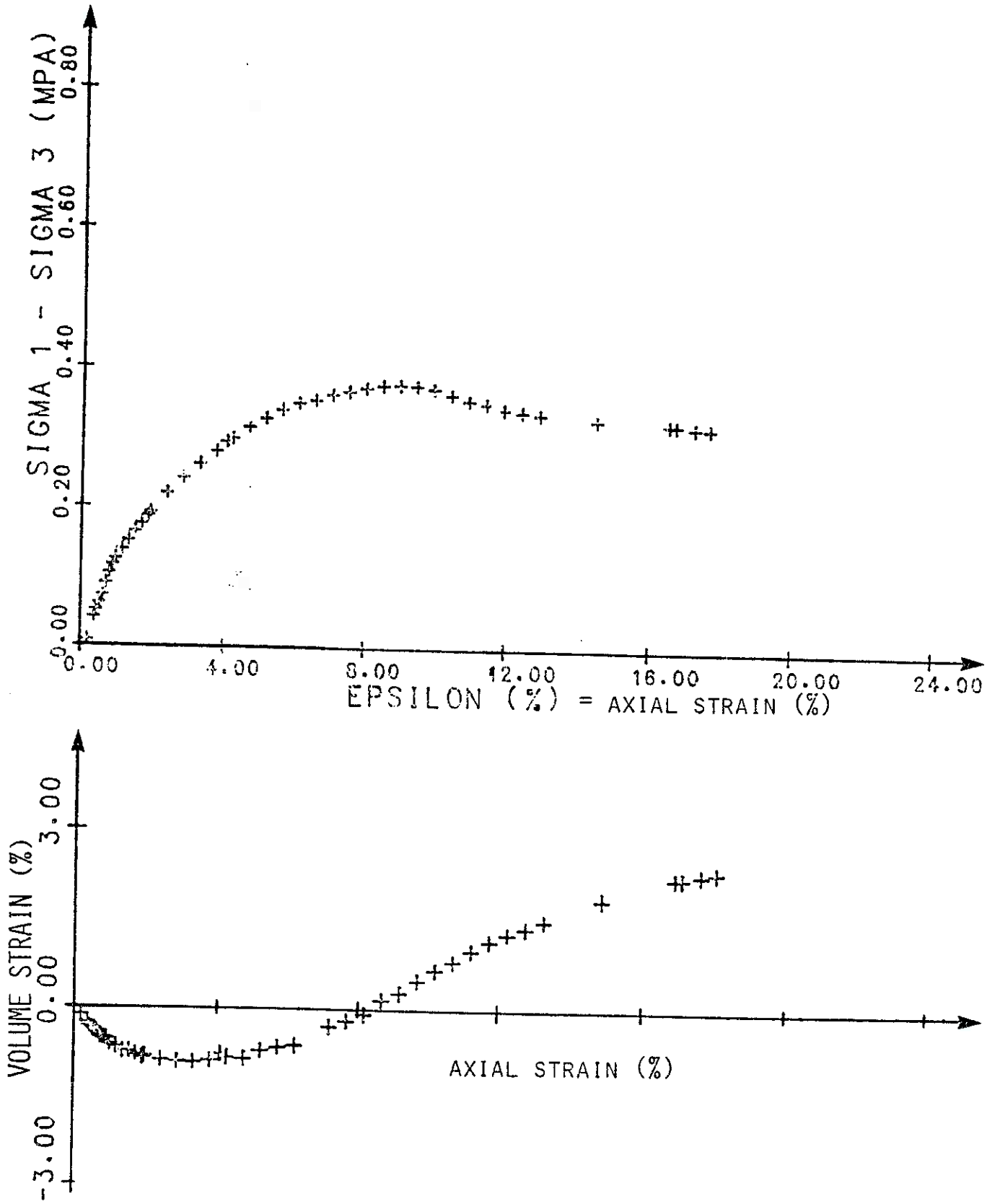

Figure 7.4 - Caen Silt. Test 39. Stress-strain curves obtained at $-1^{o}C$ and 9.25×10^{-4} min^{-1}.

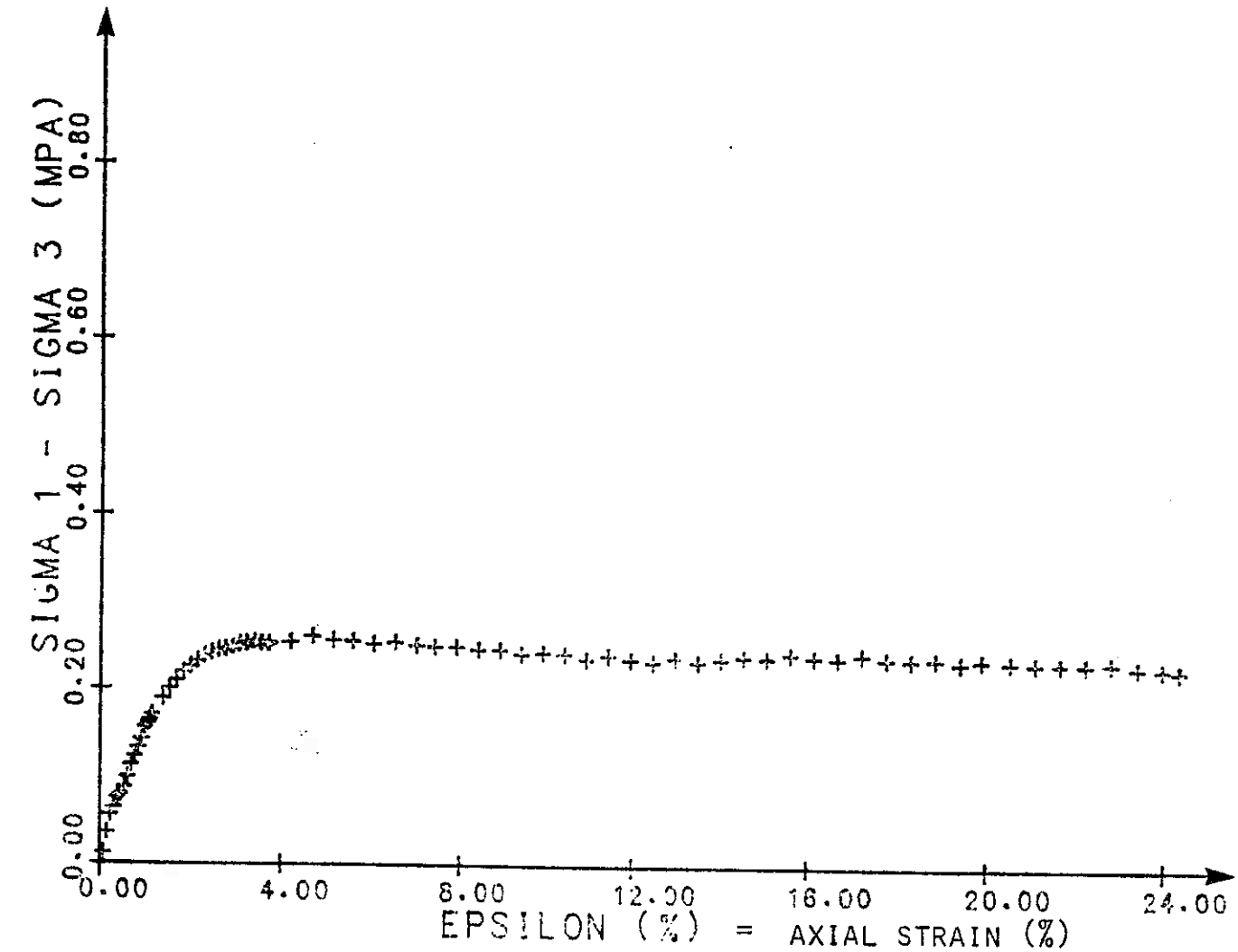

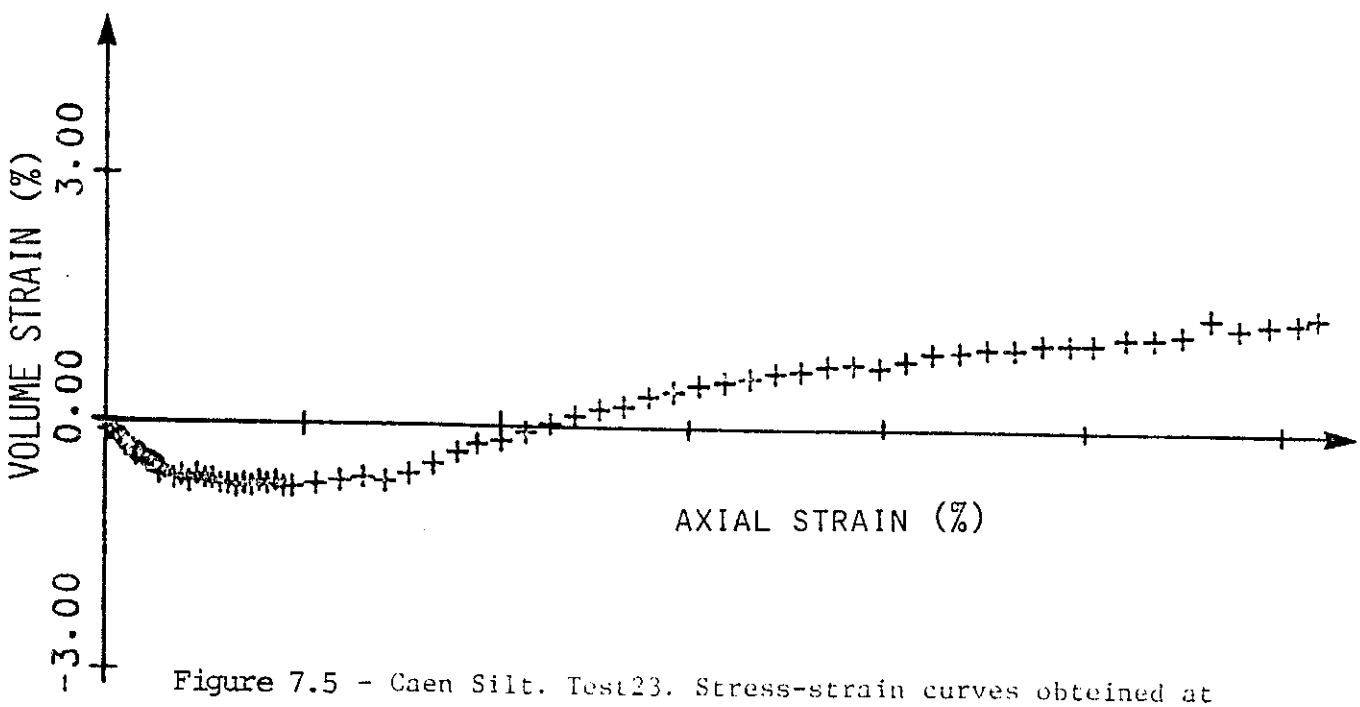

Figure 7.5 - Caen Silt. Test23. Stress-strain curves obtained at $-1^{o}C$ and 1.55×10^{-4} min^{-1}.

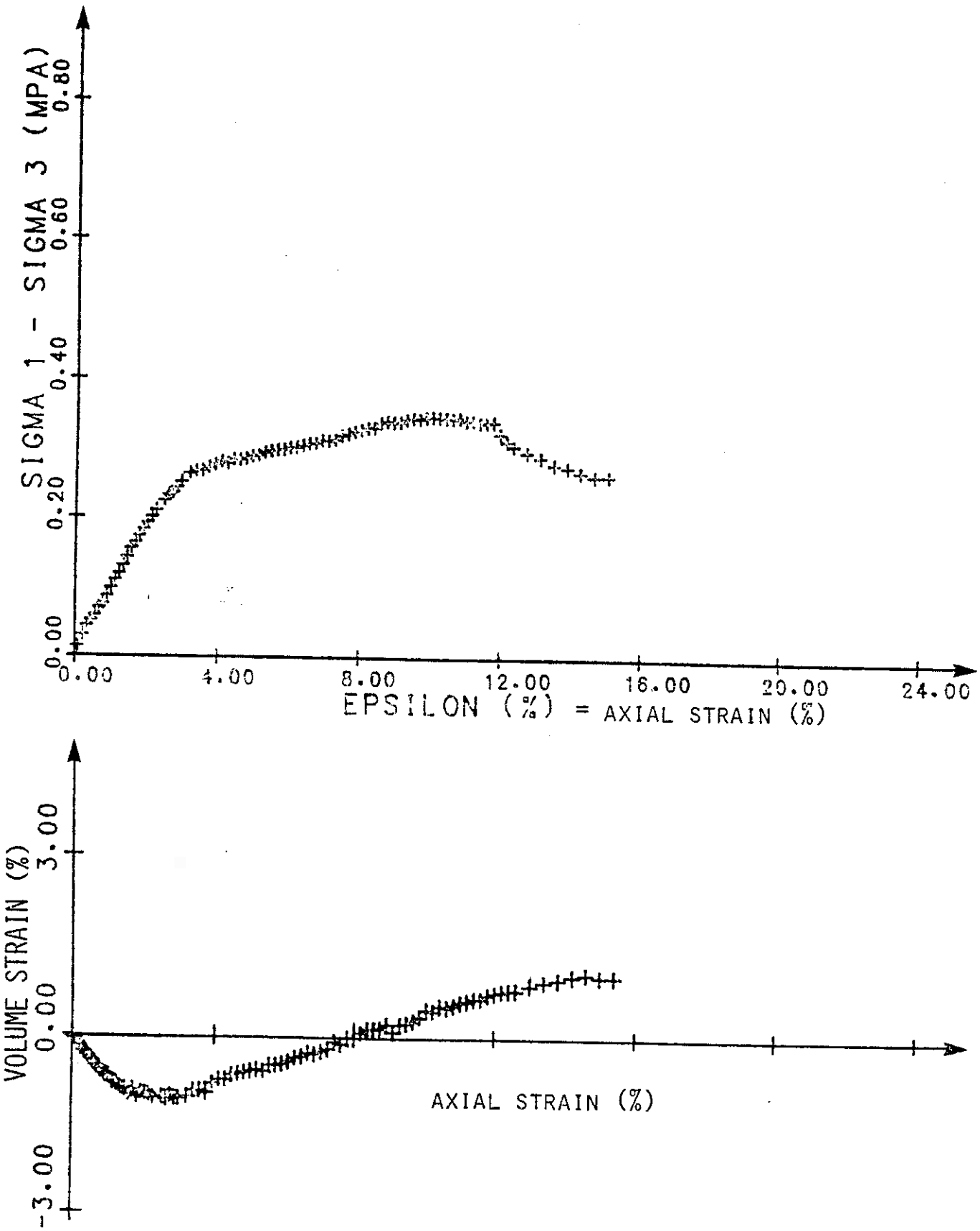

Figure 7.6 - Caen Silt. Test 36. Stress-strain curves obtained at $-1^{o}C$ and 2.86×10^{-5} min^{-1}.

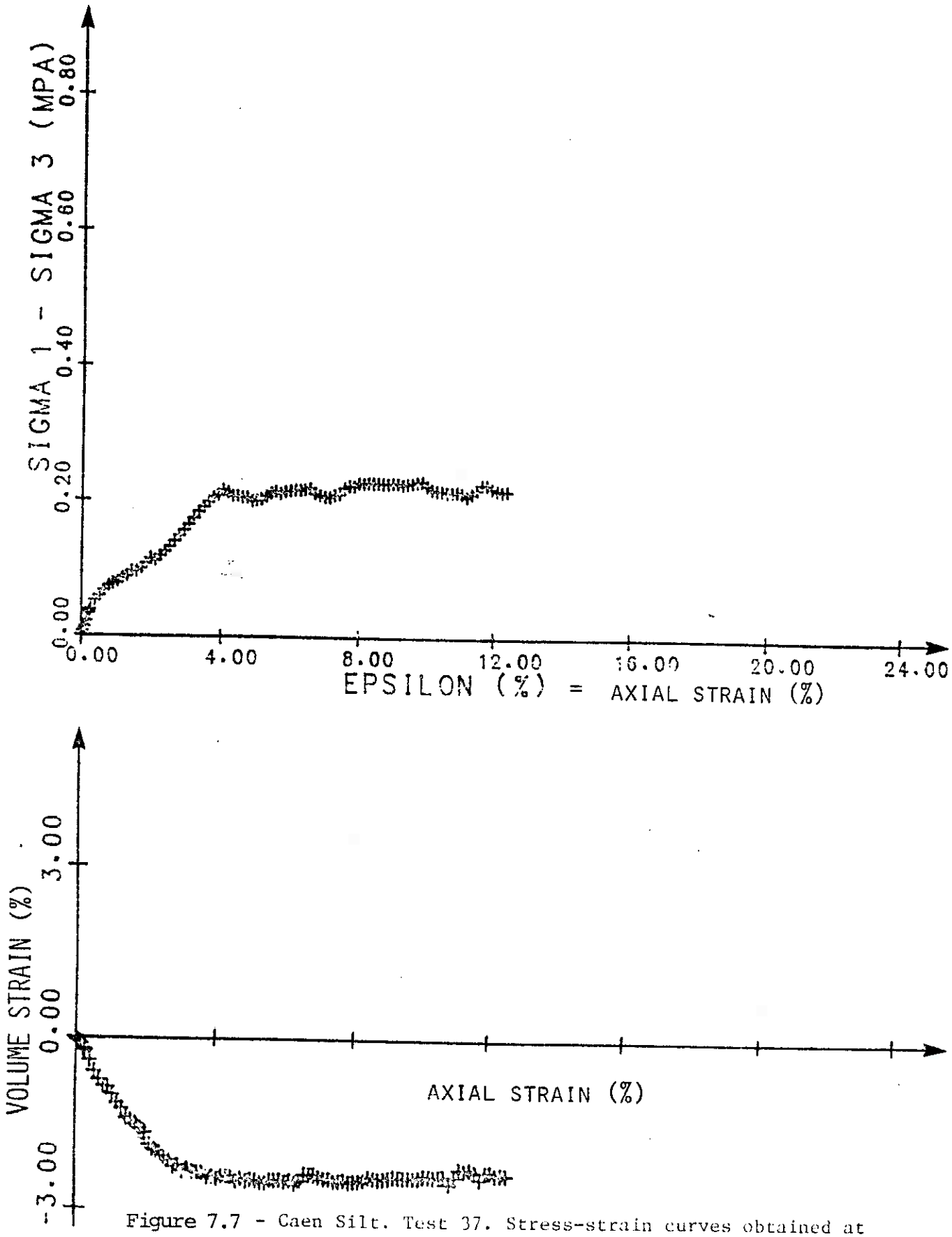

Figure 7.7 - Caen Silt. Test 37. Stress-strain curves obtained at $-1^{o}C$ and 5.64×10^{-6} min^{-1}.

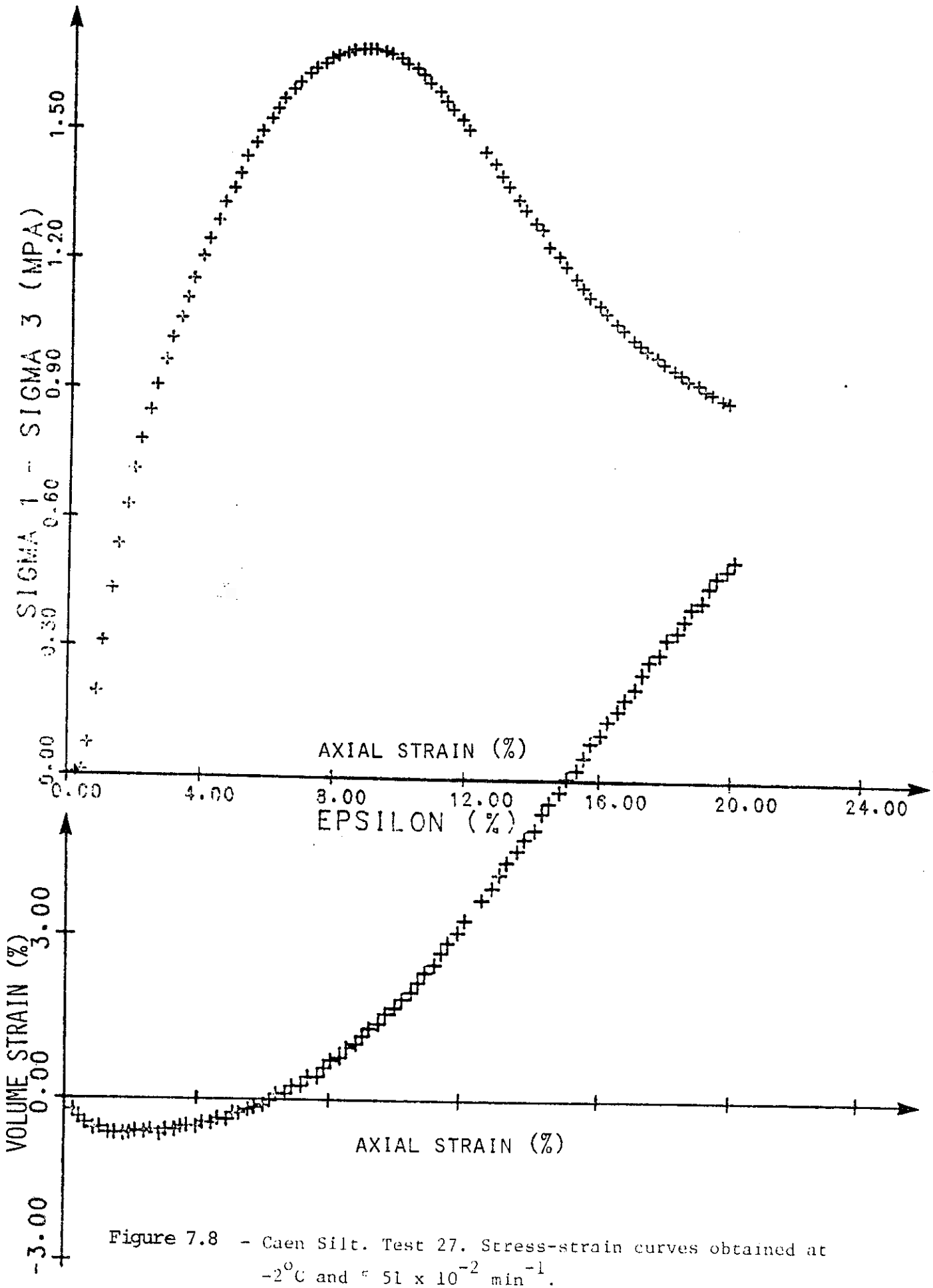

Figure 7.8 - Caen Silt. Test 27. Stress-strain curves obtained at $-2^{o}C$ and $\dot{\varepsilon}$ 51 x 10^{-2} min^{-1}.

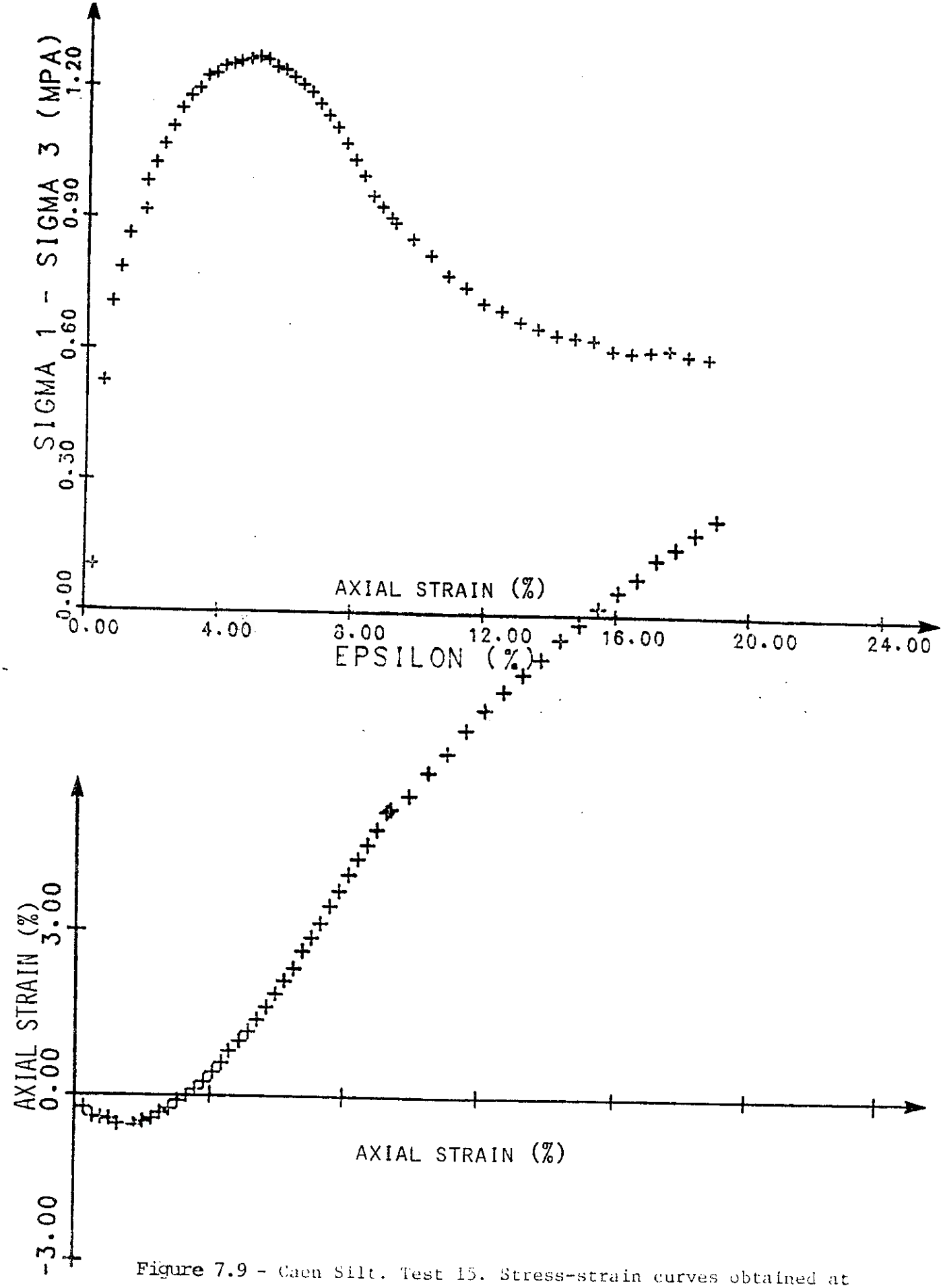

Figure 7.9 - Caen Silt. Test 15. Stress-strain curves obtained at $-2^{o}C$ and 4.83×10^{-3} min^{-1}.

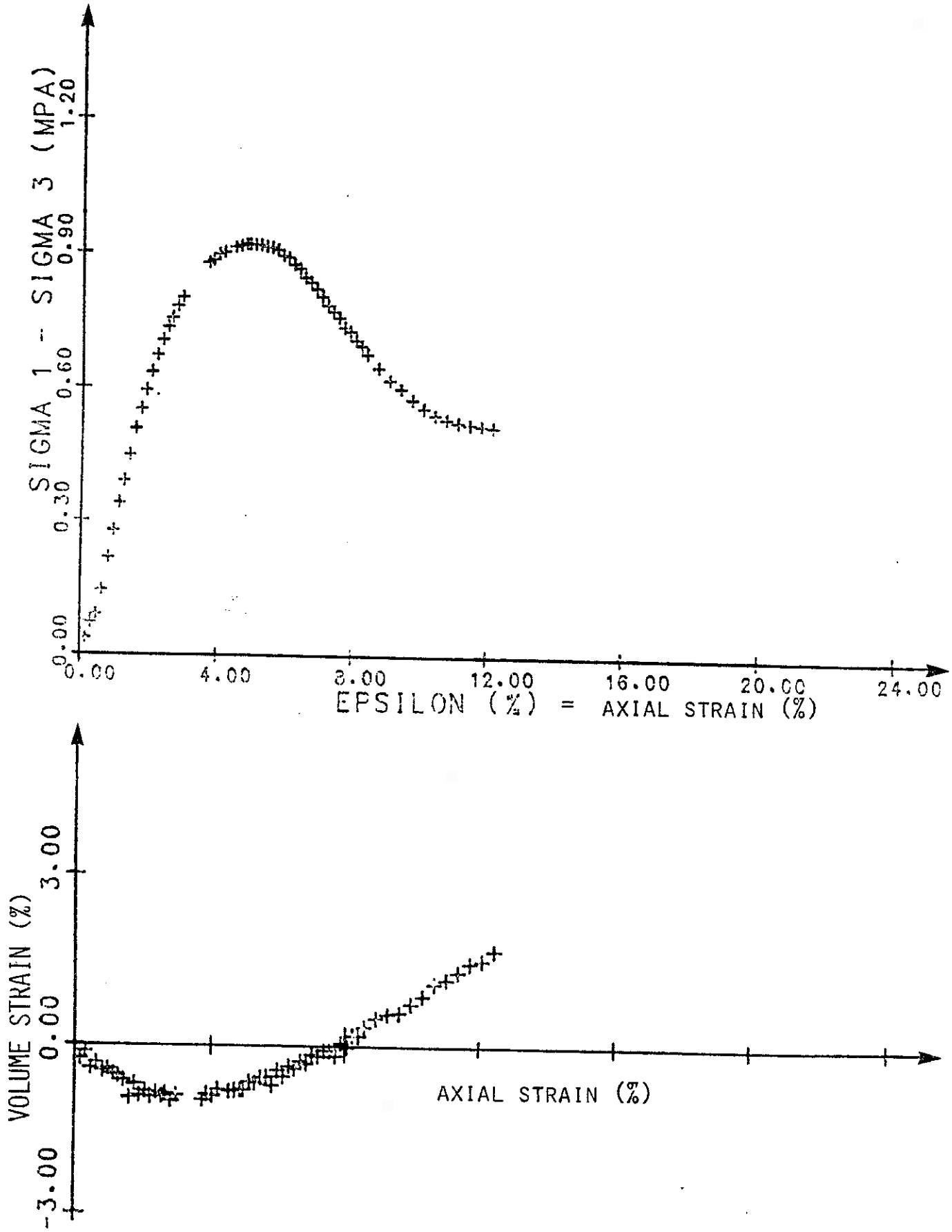

Figure 7.10- Caen Silt. Test 19. Stress-strain curves obtained at $-2^{o}C$ and 1.59×10^{-4} min^{-1}.

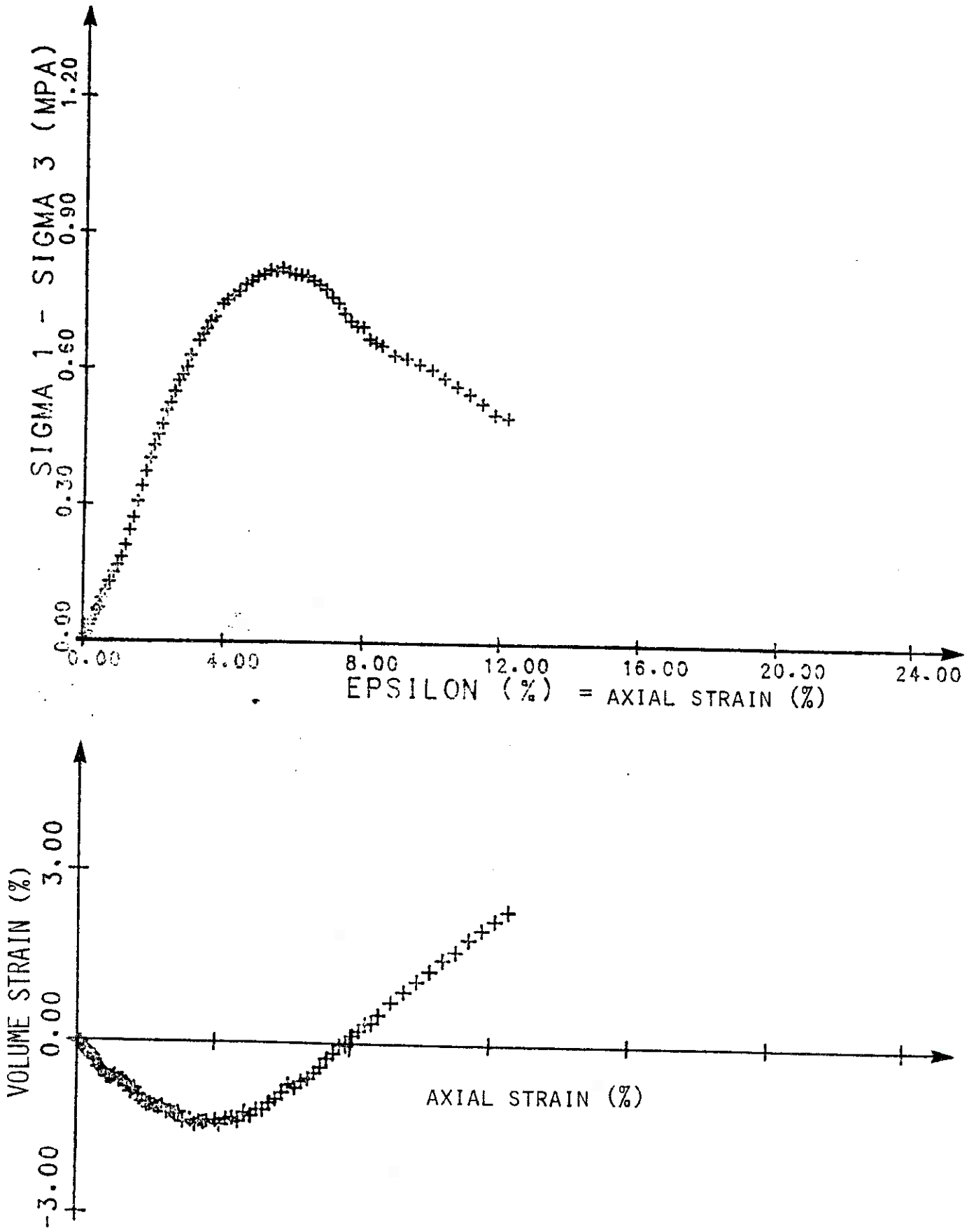

Figure 7.11 - Caen Silt. Test 32. Stress-strain curves obtained at $-2^{o}C$ and 35×10^{-5} min^{-1}.

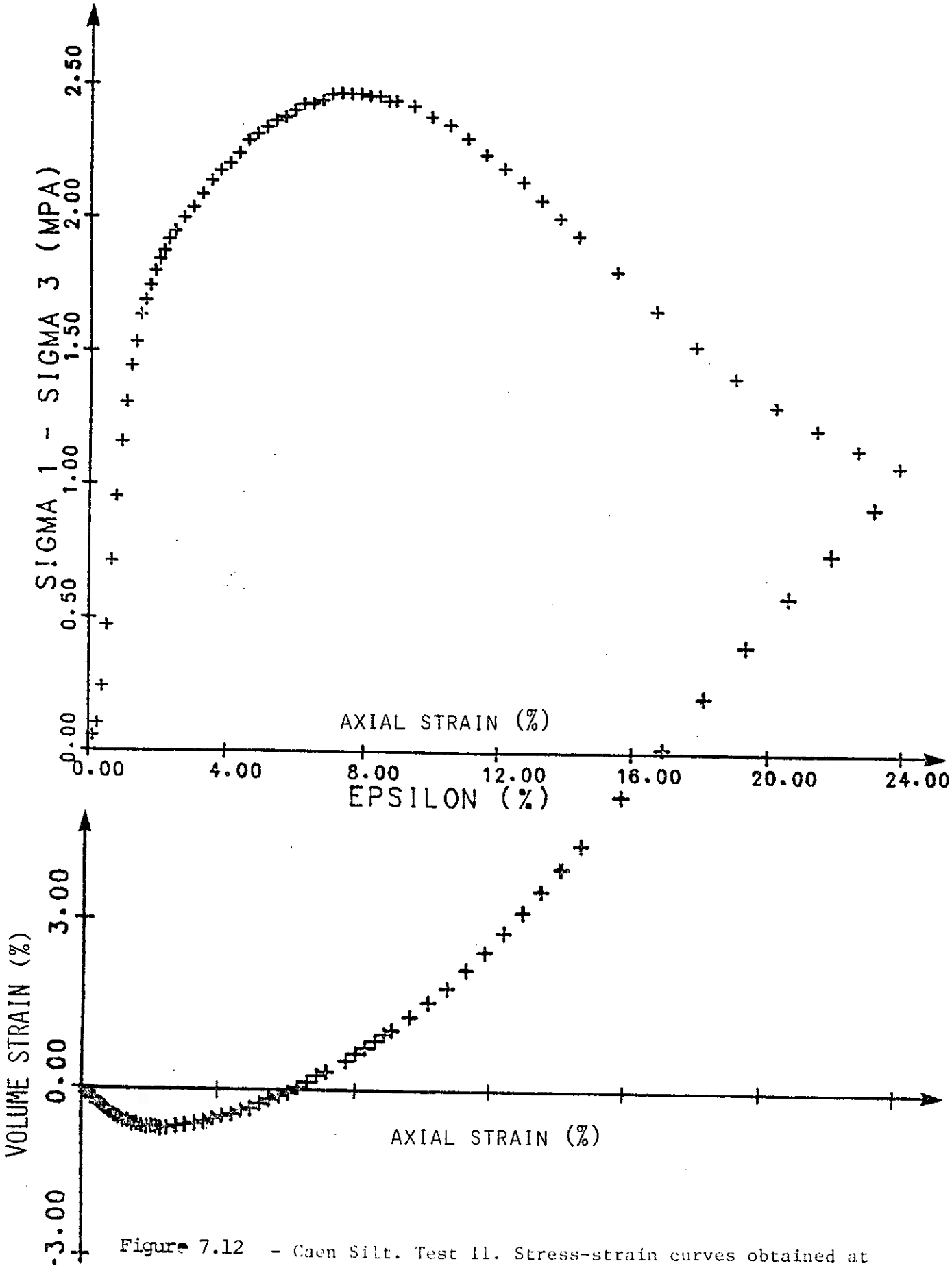

Figure 7.12 - Caen Silt. Test 11. Stress-strain curves obtained at $-5^{o}C$ and 4.93×10^{-3} min^{-1}. (Sample with ice lenses)

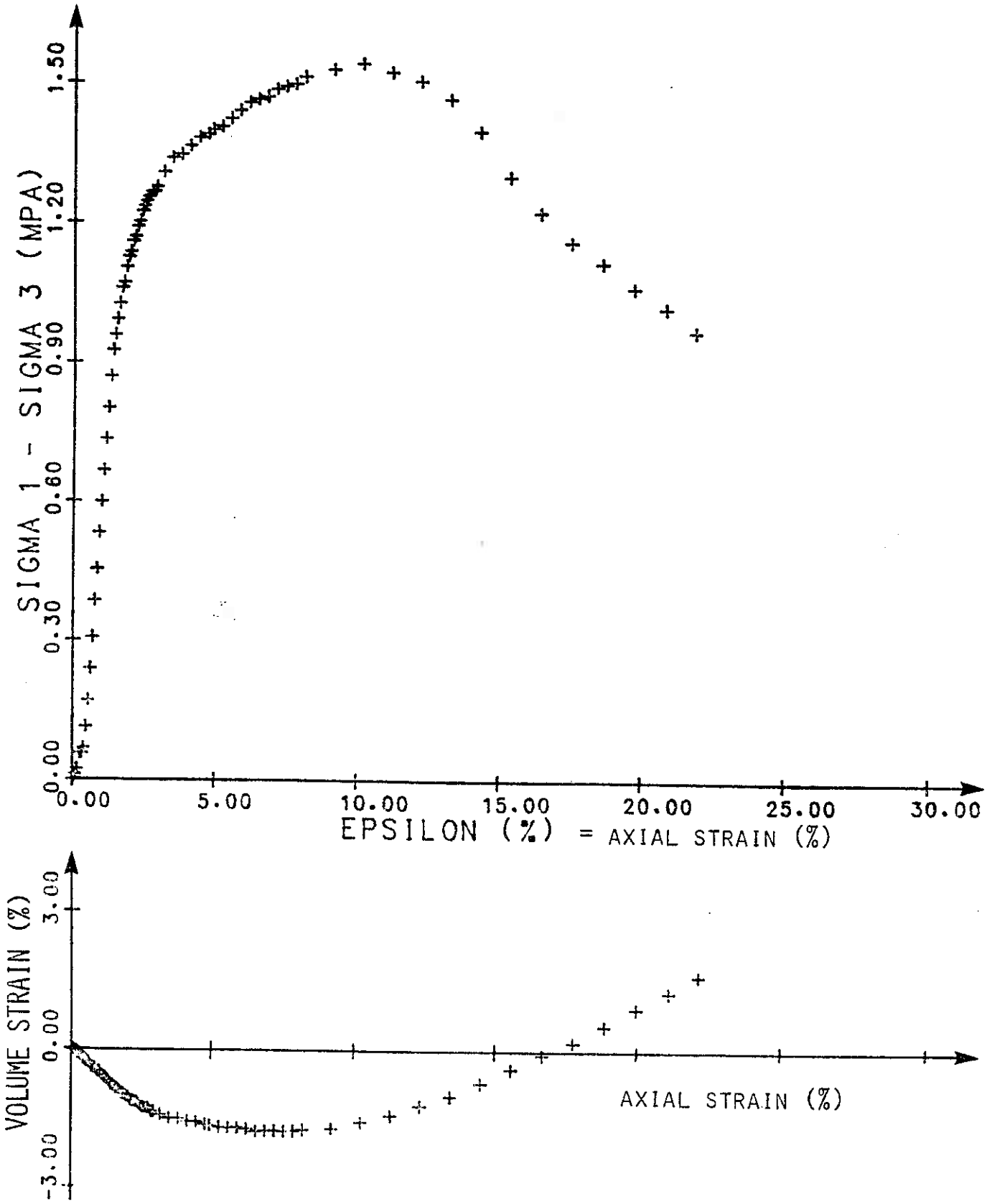

Figure 7.13 - Caen Silt. Test 9. Stress-strain curves obtained at $-5^{o}C$ and 1.60×10^{-4} min^{-1}. (Sample with ice lenses).

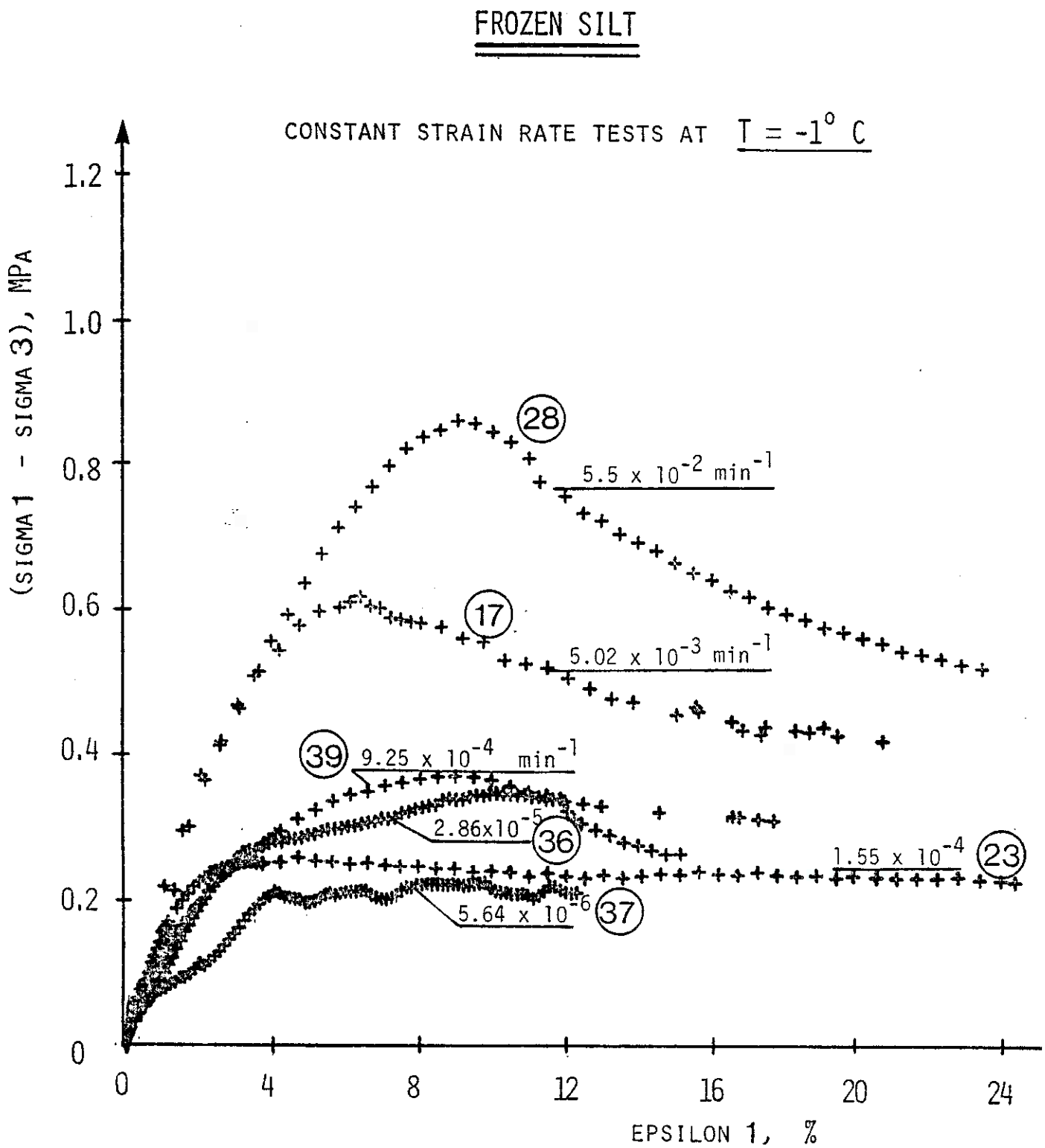

Figure 7.14 - Caen Silt. Stress-strain curves in uniaxial compression obtained at -1°C and at different strain rates.

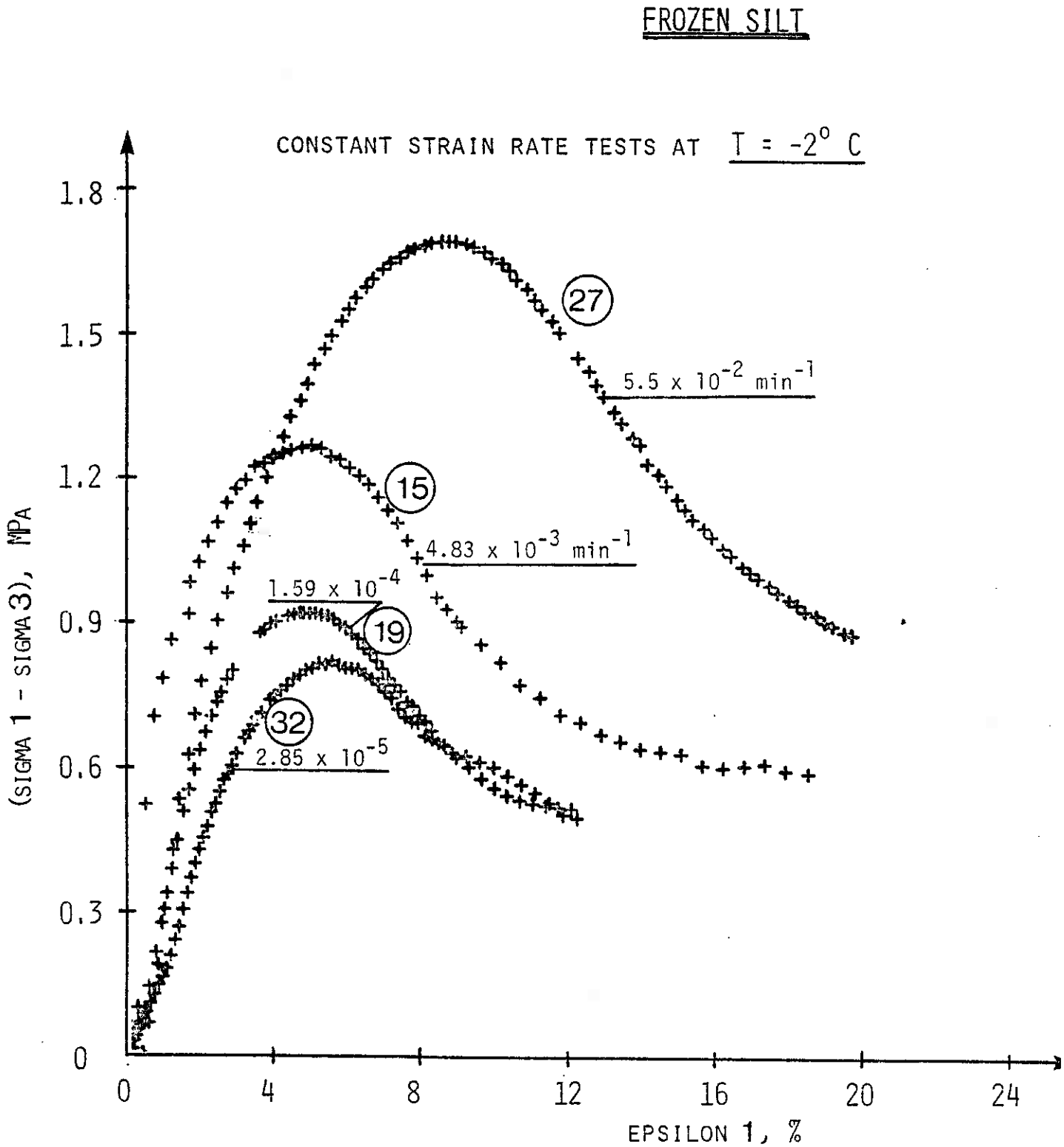

Figure 7.15 - Caen Silt. Stress-strain curves in uniaxial compression, obtained at -2°C and at different strain rates.

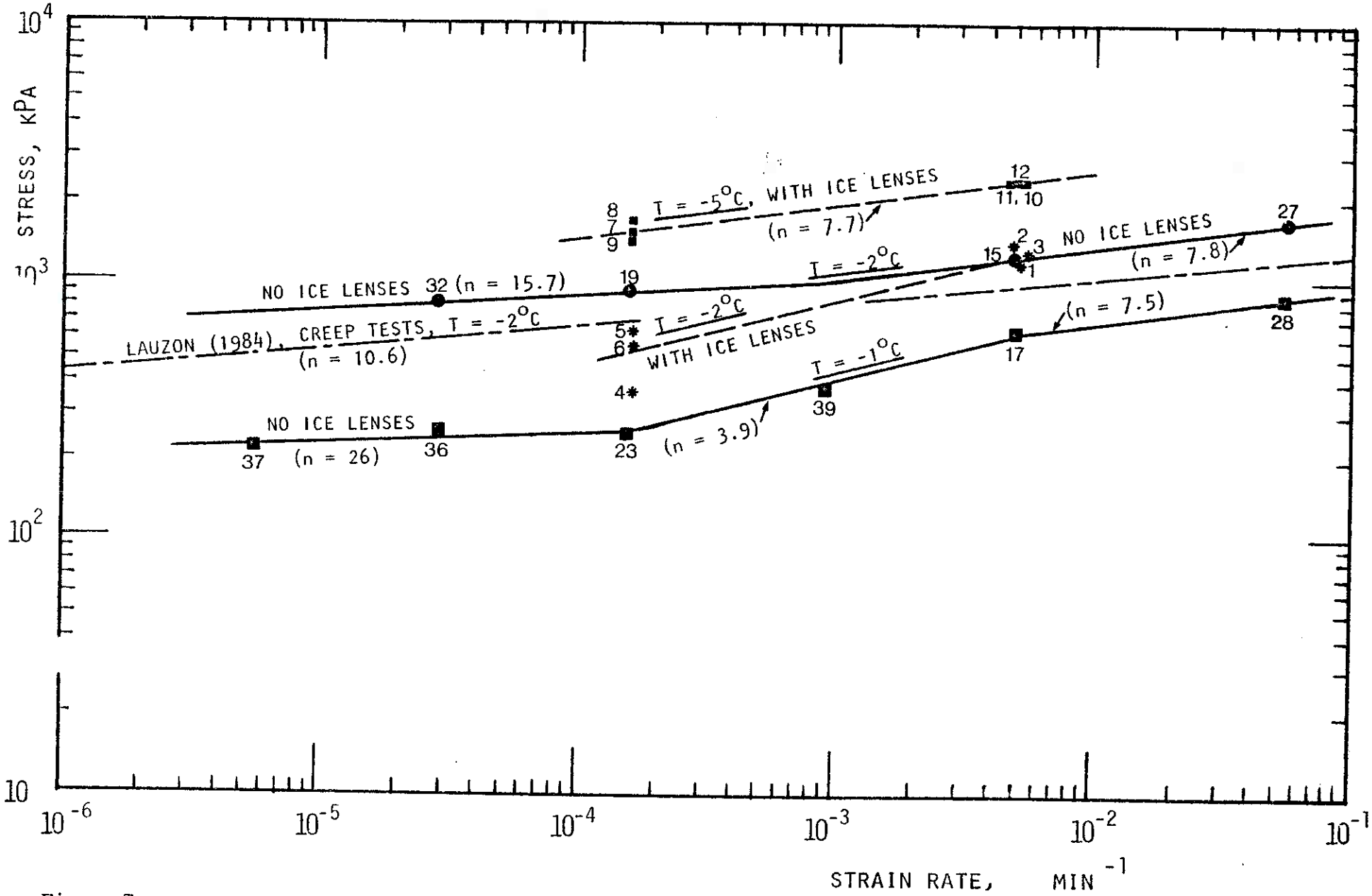

Figure 7.16 -CAEN SILT: RHEOLOGICAL CURVES FOR TEMPERATURES OF -1, -2, AND -5° C.

temperature (Figures 7.14 and 7.15). At -1 C, and strain rates below about 10^{-5} min^{-1}, the behaviour becomes practically plastic, without strength loss after failure.

7.6.2 Dilatancy

This relatively dense frozen silt (void ratio of about 0.540) shows generally a dilatant character at failure. Comparison of volume strain versus axial strain curves in Figures 7.2 to 7.13, shows that the dilatancy rate at failure $(d[V/V]/d_1)_{max}$, increases with increasing strain rate and decreasing temperature. It disappears only at high temperatures and very low strain rates (Figure 7.7). It is known that the dilatancy can also be suppressed by increasing the confining pressure, which was not included in this series of tests.

7.6.3 Strength versus Strain Rate Curves ("Rheological Curves")

The slope of the log-log plot of these curves in Figure 7.16, gives the value of the stress exponent n in the power-law creep equation (1). The value of n characterizes the strain rate sensitivity of strength. For example, in ice and ice-rich frozen soils, n has a value of about 3, while it usually exceeds 25 in unfrozen soils.

In the present experience with the dense frozen silt, it was found that n has a value of 7.5 to 7.18 at rates of about 10^{-4} min^{-1}, but it increases sharply to values over 15 or 25 at lower rates. This behaviour, which is contrary to that of frozen sand, can be explained by the fact that, at lower strain rates and temperatures close to zero, the behaviour of the silt is affected more by the unfrozen water than by the pore ice. In other words,

a fine-grained frozen soil at a high temperature and a very low strain rate, behaves very similarly to an unfrozen soil of the same geotechnical characteristics.

7.6.4 Effect of Ice Lens on Strength

From the tests performed at -2 C (Figure 7.16), it appears that thin ice lenses in the sample, oriented normally to the force application, have the effect of reducing the compression strength, but only at strain rates lower than about 10^{-2} min^{-1}. No strength reduction was noted at higher rates of strain.

7.6.5 Comparison with Previous Test Results

The dash-dotted line in Figure 7.16 presents the rheological curve drawn on the basis of a previous study of the frozen Caen Silt at -2 C (Ladanyi and Lauzon in Geotechnical Science Laboratories, 1985). The line is seen to follow the same general trend as the one obtained presently for -2 C, but the strengths are everywhere slightly lower. This difference can be easily explained by the fact that, in the previous study, the density of the samples was systematically lower than in the present study (average void ratio 0.624 before and 0.538 now). On the other hand, the average degree of saturation was higher in the previous study (S_r = 96.8% before and 91.0% now), which may have also affected the results.

7.7 Conclusions

This new study of the mechanical properties of the frozen compacted Caen Silt has furnished a very clear picture of its stress-strain and strength behaviour in a wide range of strain

rates, and at temperatures close to the melting point. This information was required as input into the numerical simulation of the behaviour of the buried chilled pipe involved in the Caen Project.

VIII STATUS OF CANADA-FRANCE PROJECT

The present phase of the project is planned to continue under a contract to July 1, 1987. Currently (October 1986) freezing is continuing around the pipe and will extend into the New Year. The date for termination of this freezing period will be assessed in December during a visit by the Co-principal Investigator.

The observations of internal pressures in the frozen annulus and of secondary heave, in particular, lead to a new concept of the pipe annulus interaction which is outlined in the general conclusions (chapter 9). The mathematical modelling procedures, the studies of creep properties and of the phase relations in the soil are being brought together. Additional personnel with special expertise are needed for these aspects.

To this end Dr. Ghani Razaqpur of the Faculty of Engineering at Carleton has joined the Canadian participants as a consultant. Negotiations are in progress to involve Mr. Laurel Goodrich, National Research Council Institute of Research and Construction, a French-speaking specialist in numerical simulation of thermal problems in frozen ground. Mr. Goodrich's role will be to integrate the numerical modelling techniques of Michel Fremond with the experimental and theoretical findings of the Canadian team.

The collaboration of scientists not directly funded by the project has also introduced the technique for preservation of frozen soils. Largely developed by Brigitte van Vliet Lanoe of the C.N.R.S. at Caen, the technique has potential for establishing the micromorphological changes associated with

secondary frost heave and creep (see frontispiece). In addition D.E. Lawrence, project manager, December 1985 to June 1986, is continuing studies in Ottawa, arising from his work with the project, on a part-time basis and by agreement with the National Energy Board.

The concept of internal pressure in the frozen annulus as being the origin of stresses on the pipe is a new hypothesis requiring testing by experimental and theoretical procedures. It is, therefore, pleasing that a continuation of this co-operative project beyond 1987 is envisaged by both Canadian and French agencies responsible for the funding. A review of the specific requirements for the continuation will be undertaken during the coming year.

IX SUMMARY OF CONCLUSIONS

During this phase of the contract, thawing was maintained around the pipe for an initial period, followed by refreezing. The observations made during this period coupled with continuing theoretical studies lead to the following conclusions in particular:

1. Observations with the glotzl total pressure cells during and subsequent to the thaw showed these to behave normally. The observations of elevated pressures when the cells were enclosed in the frozen ground are, therefore, almost certainly valid. The elevated pressures are probably related to the internal stresses in frozen ground that are also being measured in small scale laboratory tests.

2. The presence of elevated pressures in the frozen annulus and the absence of other than overburden pressures in underlying unfrozen material during the freezing period, leads to a novel concept for the deformation of the pipe. According to conventional approaches a pipe being deformed by frost heave is jacked up and reactive stresses are developed in the unfrozen ground below. The stresses observed suggest rather that the pipe is deformed by differential movements within the annulus. The stresses responsible for the deformation are similarly found only within the annulus.

This hypothesis, formulated over a year ago on the basis of the then available observations, will be emphasised in future investigation. If proven, the hypothesis alters the basis for analysis and design for chilled (freezing) pipelines.

3. Secondary frost heave, the accumulation of ice in

already frozen ground can now be precisely monitored. In some layers the rate of secondary heave is several millimeters per year.

4. Samples of the frozen soil showing morphological changes due to differential heave have been preserved and will permit study microscopically. The particle displacements and orientation of ice inclusions provide information on the nature of heave and deformation and origin of frost-heave induced stresses.

5. Finally certain general conclusions from the accumulated data can be drawn which have a broad practical significance.

The nature and magnitude of the stresses observed in the pipe are now such that they would be very serious were this a real pipeline. The varied natural conditions make prediction of pipe behaviour in the field (and whether or not ameliorative design and construction are required) extremely difficult.

There are several points to be considered:

(a) For a given pipe diameter the same imposed curvature gives the same longitudinal stress regardless of wall thickness (other conditions being equal).

(b) Greater wall thickness allows a greater operating gas pressure. The permissible operating pressure depends on both wall thickness and imposed curvature.

(c) Where the predicted curvature (due to frost heave) gives rise to high longitudinal pipe stresses, a thicker pipe wall would have to be used if the design gas pressure is not to be reduced. This is costly, and an

alternative procedure would be to adopt geotechnical constructions to limit the heave.

(d) An added advantage of thicker-walled pipe is the increased resistance to deformation (curvature). However, the creep and heave behaviour of the soils is not yet sufficiently understood that a prediction can be made of the reduction of curvature that follows from the greater resistance of the pipe.

It is clear, therefore, that financially acceptable design solutions will depend on sufficient information on the creep and thermodynamic properties of the soils as well as on a satisfactory model of the deformation of a pipe by frost heave. Ultimately the use of thermal-mechanical-hydrological numerical models, together with firm knowledge of the soil and site behaviour and conditions, should allow the most reliable, cost-effective designs. These conclusions govern the current design of the experiment.

REFERENCES

Burgess, M., G. Lemaire, M.W. Smith and P.J. Williams, 1982. Etude du gel sols autour d'une conduite refroidie enterree dans une station experimentale-Phase I. Pour Le Ministere d'Energie, Mines et Ressources, Direction de la Physique du Globe, 62 pp.

Geotechnical Science Laboratories, 1982. Feasibility studies for stresses in a pipeline buried in freezing soil. Report to Energy, Mines and Resources, Canada, Earth Physics Branch. 36 pp.

Geotechnical Science Laboratories, 1983. Investigation of soil freezing in association with a buried chilled pipeline in a large-scale test facility, Phase 2. 41 pp.

Geotechnical Science Laboratories, 1984a. Analysis of stresses developed in pipelines buried in freezing ground. Report to Energy, Mines and Resources, Canada, Earth Physics Branch, 59 pp.

Geotechnical Science Laboratories, 1984b. Experimentation sur le gel d'un sol et d'une canalisation enterree et refroidie dans une installation d'essai de grandes dimensions 3^{e} phase. Rapport pour le Ministere de l'Energie, Mines et Ressources, Direction de la Physique du Globe. 73 pp.

Geotechnical Science Laboratories, 1985. Analyses of stresses developed in pipelines buried in freezing ground. Final report for Earth Physics Branch, Energy, Mines and Resources, 39pp.

Williams, P.J. and J.A. Wood, 1986. "Internal stresses in frozen ground", Canadian Geotechnical Journal, Vol. 22, pp. 413-416.

Appendix I

Selected Temperature Data

The thermistors are coded in such a manner that the first two digits indicate the position of the cable in the facility and the last two indicate the depth within the profile. The following table will serve as a guide.

First Digits	Distance along axis	Distance off axis	
T1	5.6 m	0.25 m	in silt
T2	4.4	0.25	
T3	4.4	0.65	
T4	4.4	1.00	
T5	4.4	2.00	
T6	3.3	0.25	
T7	2.1	0.25	
T8	1.1	0.25	
T9	0.6	0.25	
TS	0.5	0.25	in sand

Second Digits	Depth (cm)
01	0
02	15
03	30
04	45
05	60
06	75
07	90
08	105
09	120
10	135
11	160

The actual depth of any thermistor is calculated by adding the heave of the access tube at that site to the initial depth. A complete summary of the data and methods will be submitted as a companion to the final report at the end of the third freeze cycle.

Day

therm.	10	21	31	42	52	59	70	80	91	100	112
T101	-.19	-.89	-.97	-1.03	-1.17	-.91	-.69	-1.32	-1.41	-1.37	-1.76
T102	-.38	-1.28	-1.48	-1.59	-1.78	-1.75	-1.91	-2.02	-2.09	-2.08	-2.17
T103	-.59	-1.45	-1.81	-2.00	-2.20	-2.20	-2.28	-2.42	-2.51	-2.44	-2.57
T104	-.50	-1.25	-1.66	-1.87	-2.06	-2.17	-2.22	-2.35	-2.43	-2.42	-2.52
T105	.31	-.45	-.93	-1.22	-1.44	-1.55	-1.67	-1.77	-1.90	-1.91	-2.00
T106	1.21	-.98	-.03	-.33	-.58	-.73	-.90	-1.03	-1.21	-1.24	-1.32
T107	2.26	1.12	.72	.33	.12	.00	-.20	-.33	-.51	-.53	-.65
T108	1.81	.92	.53	.25	.09	.09	-.01	-.16	-.10	-.05	-.12
T109	3.28	2.11	1.62	1.27	.98	.90	.71	.61	.49	.39	.32
T110	3.81	2.61	1.98	1.60	1.37	1.26	1.11	1.01	.89	.81	.75
T111	4.31	2.98	2.43	2.00	1.76	1.66	1.51	1.42	1.32	1.25	1.22
T201	-.63	-1.01	-.98	-1.15	-1.12	-.93	-.32	-1.21	-1.31	-1.34	-1.69
T202	.09	-.62	-.59	-1.02	-1.34	-1.22	-1.23	-1.74	-1.86	-1.86	-1.96
T203	-.10	-.05	-.78	-1.30	-1.80	-1.87	-2.09	-2.31	-2.42	-2.37	-2.46
T204	-.62	-1.36	-1.76	-2.01	-2.16	-2.19	-2.31	-2.43	-2.51	-2.45	-2.56
T205	.51	-.12	-.44	-.94	-1.24	-1.44	-1.59	-1.78	-1.88	-1.84	-1.98
T206	2.12	.92	.56	.10	-.22	-.40	-.56	-.87	-.96	-1.21	-1.14
T207	1.80	.86	.52	.19	-.01	-.13	-.29	-.45	-.57	-.57	-.68
T208	1.22	.13	.05	-.35	-.38	-.54	-.75	-.44	-.50	-.51	-.45
T209	3.20	2.62	2.17	1.61	1.34	.98	.85	.64	.51	.45	.36
T210	3.80	2.60	2.05	1.62	1.26	1.18	1.06	.89	.80	.75	.68
T211	4.12	2.85	2.32	1.90	1.72	1.61	1.47	1.31	1.22	1.16	1.09
T301	-.14	-.16	-.29	-.33	-.46	-.36	-.29	-.79	-.90	-.93	-.94
T302	.17	-.02	-.15	-.36	-.53	-.55	-.67	-.83	-.91	-1.00	-1.02
T303	.74	.38	.25	.01	-.18	-.23	-.43	-.55	-.65	-.65	-.73
T304	1.13	.58	.36	.13	.00	-.05	-.24	-.34	-.44	-.43	-.52
T305	1.46	.78	.50	.25	.09	.07	-.07	-.16	-.24	-.25	-.35
T306	2.02	1.21	.92	.61	.47	.41	.27	.18	.10	.11	.05
T307	2.20	1.30	.87	.53	.43	.39	.18	.12	.10	-.01	-.09
T308	3.35	1.35	1.47	1.10	.90	.83	.57	.51	.44	.38	.36
T309	3.42	2.23	1.73	1.35	1.17	1.09	.91	.84	.77	.72	.68
T310	3.77	2.72	2.17	1.77	1.58	1.49	1.33	1.25	1.17	1.13	1.08
T311	4.17	2.94	2.44	2.00	1.83	1.77	1.64	1.53	1.45	1.44	1.39

Day

therm.	10	21	31	42	52	59	70	80	91	100	112
T401	-.21	-.26	-.31	-.36	-.36	-.17	.00	-.46	-.51	-.55	-.55
T402	.32	.13	.05	-.02	-.06	-.05	-.07	-.17	-.25	-.32	-.37
T403	.80	.47	.28	.18	.10	-.03	.02	-.07	-.10	-.14	-.18
T404	1.34	.81	.58	.41	.36	.45	.27	.27	.22	.17	.14
T405	1.83	1.11	.83	.62	.54	.55	.43	.39	.34	.30	.26
T406	2.30	1.45	1.11	.86	.73	.67	.59	.54	.49	.45	.40
T407	2.72	1.75	1.35	1.06	.92	.85	.76	.70	.66	.62	.57
T408	3.20	2.15	1.70	1.37	1.20	1.16	1.09	.99	.95	.92	.88
T409	3.54	2.41	1.93	1.60	1.48	1.39	1.30	1.22	1.17	1.12	1.10
T410	3.89	2.73	2.18	1.84	1.69	1.62	1.51	1.44	1.39	1.35	1.31
T411	4.24	3.07	2.54	2.15	1.99	1.91	1.81	1.73	1.68	1.64	1.60
T501	-.21	-.27	-.29	-.36	-.38	-.17	.06	-.38	-.39	-.45	-.40
T502	.49	.27	.19	.12	.08	.09	.09	.03	.01	-.04	-.03
T503	1.08	.72	.58	.44	.37	.38	.33	.30	.28	.27	.28
T504	1.58	1.04	.81	.64	.55	.53	.47	.45	.44	.42	.40
T505	2.10	1.42	1.13	.93	.82	.79	.73	.70	.68	.66	.64
T506	2.69	1.87	1.52	1.26	1.15	1.11	1.04	1.01	.99	.98	.96
T507	3.07	2.19	1.77	1.51	1.37	1.32	1.25	1.22	1.20	1.17	1.15
T508	3.55	2.60	2.14	1.83	1.69	1.63	1.55	1.53	1.51	1.50	1.19
T509	3.85	2.85	2.39	2.05	1.90	1.84	1.76	1.72	1.70	1.67	1.66
T510	4.04	2.99	2.47	2.13	1.98	1.90	1.81	1.75	1.72	1.69	1.67
T511	4.52	3.45	2.95	2.59	2.42	2.34	2.26	2.21	2.18	2.16	2.13
T601	-.70	-1.23	-1.25	-1.43	-1.35	-1.11	-.78	-1.50	-1.59	-1.56	-1.53
T602	-.79	-1.50	-1.70	-1.88	-1.97	-1.93	-1.92	-2.13	-2.19	-2.14	-2.21
T603	-1.17	-1.95	-2.15	-2.32	-2.44	-2.38	-2.49	-2.68	-2.69	-2.61	-2.70
T604	-.75	-1.44	-1.82	-2.10	-2.24	-2.34	-2.36	-2.49	-2.55	-2.52	-2.60
T605	.14	-.59	-1.00	-1.34	-1.54	-1.65	-1.75	-1.87	-1.95	-1.91	-2.04
T606											
T607	1.80	.81	.40	.10	-.08	-.19	-.35	-.48	-.58	-.59	-.74
T608	2.53	1.41	.97	.61	.41	.33	.18	.10	.01	-.03	-.11
T609	2.94	1.75	1.22	.88	.69	.60	.47	.37	.29	.25	.17
T610	3.53	2.25	1.69	1.31	1.12	1.02	.89	.79	.72	.67	.60
T611	3.98	2.70	2.12	1.71	1.52	1.42	1.29	1.20	1.12	1.07	.99
T701	-.50	-1.04	-1.09	-1.33	-1.14	-.92	-.61	-1.42	-1.52	-1.49	-1.48
T702	-.49	-1.29	-1.48	-1.71	-1.80	-1.72	-1.76	-1.96	-2.01	-1.95	-2.02
T703	-.60	-1.36	-1.72	-1.92	-2.04	-2.06	-2.14	-2.25	-2.31	-2.25	-2.34
T704	-.51	-1.19	-1.60	-1.84	-2.01	-2.07	-2.15	-2.26	-2.37	-2.32	-2.43
T705	.36	-.35	-.78	-1.07	-1.27	-1.39	-1.51	-1.62	-1.70	-1.65	-1.80
T706	1.17	.38	.01	-.28	-.51	-.64	-.79	-.91	-1.02	-.99	-1.15
T707	1.94	.93	.51	.21	.03	-.09	-.22	-.33	-.44	-.47	-.59
T708	2.43	1.33	.84	.49	.33	.24	.10	.03	-.07	-.10	-.17
T709	3.06	1.88	1.36	.99	.81	.72	.59	.49	.41	.36	.29
T710	3.48	2.23	1.67	1.29	1.10	1.00	.88	.78	.69	.64	.59
T711	3.94	2.66	2.06	1.93	1.47	1.37	1.25	1.15	1.06	1.31	.94

Day

therm.	10	21	31	42	52	59	70	80	91	100	112
T801	-.29	-.82	-.82	-.97	-.49	-.05	.16	-1.03	-1.38	-1.08	-.84
T802	-.09	-.94	-1.06	-1.37	-1.39	-1.23	-1.35	-1.64	-1.94	-1.63	-1.69
T803	-.55	-1.35	-1.55	-1.87	-1.98	-1.94	-1.94	-2.21	-2.57	-2.16	-2.30
T804	-.45	-1.32	-1.49	-1.89	-2.04	-2.14	-2.17	-2.46	-2.60	-2.43	-2.60
T805	-.07	-.82	-1.22	-1.48	-1.43	-1.44	-1.51	-1.89	-2.05	-2.18	-2.14
T806	.93	.10	-.40	-.72	-.89	-1.01	-1.07	-1.25	-1.30	-1.35	-1.43
T807	1.66	.72	.22	-.03	-.17	-.32	-.43	-.60	-.70	-.77	-.84
T808	2.56	1.41	.77	.54	.34	.33	.22	-.04	-.22	-.19	-.30
T809	2.95	1.74	1.20	.82	.64	.55	.46	.31	.24	.18	.09
T810	3.33	2.10	1.63	1.23	1.06	.93	.95	.76	.48	.60	.48
T811	3.84	2.85	2.21	1.76	1.60	1.47	1.34	1.16	.84	.93	.89
T901	-.38	-1.00	-.97	-1.17	-.86	-.59	-.40	-1.30	-.93	-1.30	-1.22
T902	-.42	-1.19	-1.15	-1.65	-1.71	-1.63	-1.70	-1.87	-1.34	-1.85	-1.93
T903	-.82	-1.62	-1.45	-2.16	-2.30	-2.29	-2.38	-2.50	-2.03	-2.47	-2.59
T904	-.57	-1.32	-1.76	-2.01	-2.17	-2.20	-2.31	-2.41	-2.20	-2.41	-2.54
T905	.09	-.68	-1.76	-1.46	-1.66	-1.74	-1.87	-1.97	-1.77	-1.96	-2.14
T906	1.01	.15	-1.09	-.58	-.81	-.94	-1.08	-1.21	-1.25	-1.25	-1.42
T907	1.74	.76	-.31	.02	-.19	-.32	-.48	-.61	-.66	-.68	-.85
T908	2.36	1.24	.27	.46	.28	.18	.05	-.06	-.03	-.19	-.31
T909	2.81	1.59	.67	.73	.55	.45	.33	.23	.14	.11	.02
T910	3.26	1.96	1.10	1.06	.87	.78	.65	.56	.72	.44	.37
T911	3.76	2.39	1.56	1.44	1.25	1.16	1.04	.94	1.12	.81	.74
T801	-.77	-1.12	-1.09	-1.25	-1.04	-.80	-.71	-1.33	-1.39	-1.34	-1.22
T802	-.88	-1.30	-1.42	-1.59	-1.63	-1.53	-1.59	-1.77	-1.82	-1.76	-1.81
T803	-1.01	-1.50	-1.72	-1.91	-2.01	-1.94	-2.05	-2.15	-2.21	-2.14	-2.22
T804	-.74	-1.36	-1.63	-1.86	-2.01	-1.85	-2.11	-2.19	-2.24	-2.15	-2.23
T805	-.10	-.87	-1.16	-1.44	-1.61	-1.61	-1.75	-1.83	-1.88	-1.79	-1.90
T806	.56	-.19	-.56	-.85	-1.02	-1.06	-1.20	-1.29	-1.36	-1.28	-1.38
T807	1.23	.34	.02	-.29	-.47	-.56	-.67	-.77	-.84	-.79	-.91
T808	1.84	.80	.42	.12	-.04	-.14	-.26	-.37	-.45	-.43	-.53
T809	2.30	1.19	.77	.47	.30	.21	.11	.01	-.09	-.07	-.16
T810	2.81	1.54	1.06	.73	.56	.48	.38	.28	.22	.19	.14
T811	3.32	1.93	1.43	1.08	.91	.82	.71	.63	.56	.52	.47

Appendix II

Summary of Heave Data Obtained Via the Magnetic Heave Device

The position of each magnetic assembly uses the same coding format as that used for the thermistor locations (see Appendix I). The depth of each magnet is indicated by the values ascribed to them on Day 0 in the raw data tables. Differential heave is also calculated by subtracting the difference between two successive magnets on a given day from the difference which existed on Day 0. It should be noted that consolidation of the soil is evident in some of the soil layers after the onset of freeze (see M111-M112 on the differential heave table for site 1). In order to separate primary heave from secondary heave, the data must be referenced to temperature.

Heave at Site # 1 Raw Data (cm)

Magnetic Number

Day	M101	M102	M103	M104	M105	M106	M107	M108	M109	M110	M111	M112
0	20.23	30.48	40.87	53.04	60.85	71.6	82.01	91.65	100.35	109.2	120.38	130.15
14	20.78	31.11	41.51	53.97	62.2	74.27	84.73	94.16	102.83	112.67	123.79	133.53
17	20.7	31.14	41.52	53.92	62.26	74.26	84.78	94.21	102.88	111.74	122.83	132.56
21	20.73	31.17	41.56	53.95	62.28	74.98	85.52	94.95	103.61	112.47	123.56	133.3
24	20.71	31.06	41.48	53.85	62.2	75.34	85.89	95.37	104.09	112.86	123.97	133.66
28	20.71	31.12	41.51	53.95	62.27	75.44	86.49	95.89	104.59	113.46	124.62	134.32
31	20.71	31.19	41.58	54	62.32	75.54	87.04	96.46	105.13	113.97	125.08	134.81
35	20.66	31.13	41.5	53.91	62.26	75.48	87.51	96.92	105.6	114.45	125.55	135.29
38	20.41	30.88	41.3	53.69	62.04	75.29	87.63	97.14	105.79	114.63	125.7	135.38
42	20.55	31	41.36	53.79	62.2	75.37	88.23	97.7	106.34	115.22	126.35	136.06
45	20.61	31.09	41.47	53.89	62.22	75.43	88.53	98.11	106.79	115.67	126.77	136.49
50	20.67	31.14	41.51	53.92	62.26	75.44	88.6	98.71	107.4	116.25	127.36	137.1
52	20.72	31.17	41.57	53.98	62.27	75.49	88.64	98.92	107.62	116.46	127.57	137.32
56	20.65	31.16	41.55	53.97	62.27	75.49	88.64	99.3	108.01	116.86	127.96	137.72
59	20.72	31.17	41.56	53.97	62.26	75.46	88.62	99.64	108.32	117.17	128.34	138.09
63	20.72	31.17	41.56	53.97	62.3	75.5	88.69	100.03	108.7	117.59	128.69	138.44
66	20.63	31.03	41.43	53.83	62.13	75.35	88.58	100.19	108.89	117.74	128.81	138.57
70	20.68	31.14	41.53	53.93	62.27	75.46	88.64	100.57	109.32	118.15	129.25	139.01
73	20.69	31.15	41.53	53.95	62.27	75.49	88.66	100.83	109.59	118.45	129.56	139.31
78	20.66	31.13	41.53	53.96	62.3	75.65	88.65	101.06	109.98	118.85	129.95	139.67
80	20.69	31.15	41.54	53.95	62.29	75.51	88.68	101.09	110.16	119.02	130.14	139.87
84	20.61	31.07	41.43	53.85	62.19	75.4	88.58	101	110.36	119.21	130.31	140.07
87	20.21	31.07	41.43	53.85	62.19	75.4	88.58	101	110.36	119.21	130.31	140.07
91	20.72	31.17	41.52	53.92	62.26	75.47	88.63	101.1	110.92	119.79	130.9	140.67
95	20.66	31.12	41.49	53.85	62.21	75.39	88.55	101.05	111.09	120	131.07	140.81
102	20.68	31.15	41.51	53.83	62.18	75.36	88.54	101.07	111.46	120.3	131.15	141.03
107	20.68	31.13	41.5	53.91	62.24	75.42	88.61	101.12	111.8	120.71	131.78	141.47
109	20.68	33.15	41.49	53.91	62.26	75.44	88.64	101.15	111.94	120.85	131.93	141.64
112	20.66	31.17	41.57	53.96	62.3	75.51	88.72	101.23	112.22	121.09	132.19	141.89
115	20.66	31.1	41.49	53.91	62.24	75.47	88.67	101.17	112.31	121.18	132.27	141.99

Differential Heave (cm) at Site 1

Magnet Number

Day	M101 M102	M102 M103	M103 M104	M104 M105	M105 M106	M106 M107	M107 M108	M108 M109	M109 M110	M110 M111	M111 M112	Total Heave
0	0	0	0	0	0	0	0	0	0	0	0	0
21	.08	.01	.29	.42	1.32	.05	-.21	-.03	0	-.06	-.03	
24	.19	-.01	.23	.53	1.25	.11	-.21	-.03	.01	-.09	-.04	2.41
28	.19	0	.22	.52	1.95	.13	-.21	-.04	.01	-.09	-.03	3.15
31	.1	.03	.2	.54	2.39	.14	-.16	.02	-.08	-.07	-.08	3.51
35	.16	0	.27	.51	2.42	.64	-.24	-.01	.03	-.02	-.07	4.17
38	.23	0	.25	.51	2.47	1.09	-.22	-.03	-.01	-.07	-.04	4.66
42	.22	-.02	.24	.54	2.47	1.62	-.23	-.02	0	-.08	-.03	5.14
45	.22	.03	.22	.54	2.5	1.93	-.13	-.05	-.01	-.11	-.09	5.23
50	.2	-.03	.26	.6	2.42	2.45	-.17	-.06	.03	-.05	-.06	5.91
52	.23	-.01	.25	.52	2.46	2.69	-.06	-.02	.03	-.08	-.05	6.34
56	.22	-.02	.24	.53	2.43	2.75	.47	-.01	0	-.07	-.03	6.95
59	.2	.01	.24	.48	2.47	2.74	.64	0	-.01	-.07	-.02	7.17
63	.26	0	.25	.49	2.47	2.74	1.02	.01	0	-.08	-.01	7.57
66	.2	0	.24	.48	2.45	2.75	1.38	-.02	0	-.01	-.02	7.94
70	.2	0	.24	.52	2.45	2.78	1.7	-.03	.04	-.08	-.02	8.29
73	.15	.01	.23	.49	2.47	2.82	1.97	0	0	-.11	-.01	8.42
78	.21	0	.23	.53	2.44	2.77	2.29	.05	-.02	-.08	-.01	8.86
80	.21	-.01	.25	.51	2.47	2.76	2.53	.06	.01	-.07	-.02	9.16
84	.22	.01	.26	.53	2.6	2.59	2.77	.22	.02	-.08	-.05	9.52
80	.21	0	.24	.53	2.47	2.76	2.77	.37	.01	-.06	-.04	9.72
84	.21	-.03	.25	.53	2.46	2.77	2.78	.66	0	-.08	-.01	9.92
87	.61	-.03	.25	.53	2.46	2.77	2.78	.66	0	-.08	-.01	9.92
91	.2	-.04	.23	.53	2.46	2.75	2.83	1.12	.02	-.07	0	10.52
95	.21	-.02	.19	.55	2.43	2.75	2.86	1.34	.06	-.11	-.03	10.66
102	.22	-.03	.15	.54	2.43	2.77	2.89	1.69	-.01	-.33	.11	10.98
107	.2	-.02	.24	.52	2.43	2.78	2.87	1.98	.06	-.11	-.08	11.32
109	2.22	-2.05	.25	.54	2.43	2.79	2.87	2.09	.06	-.1	-.06	11.49
112	.26	.01	.22	.53	2.46	2.8	2.87	2.29	.02	-.08	-.07	11.74
115	.19	0	.25	.52	2.48	2.79	2.86	2.44	.02	-.09	-.05	11.84

Heave at Site #2, Raw Data (cm)

	Magnet Number											
Day	M201	M202	M203	M204	M205	M206	M207	M208	M209	M210	M211	M212
0	21.72	31.45	43.39	51.39	61.42	72.79	81.24	92.97	102.84	112.87	127.19	135.93
14	21.99	31.76	43.73	52.13	62.88	74.18	82.7	94.48	103.26	115.25	127.41	135.8
17	21.1	31.82	43.77	52.36	63.52	74.71	83.21	94.97	104.7	115.44	129.22	137.34
21	22.13	31.77	43.76	52.41	64.07	75.43	83.93	95.68	105.43	116.16	129.94	138.05
24	22.12	31.92	43.88	52.45	64.27	75.91	84.36	96.12	105.89	116.62	130.4	138.49
28	22.22	31.87	43.86	52.5	64.38	76.51	84.99	96.72	106.49	117.22	131	139.12
31	22.13	31.85	43.83	52.41	64.36	76.86	85.38	97.09	106.84	117.55	131.35	139.45
35	22	31.71	43.67	52.26	64.21	77.16	85.7	97.42	107.18	117.89	131.66	139.8
38	21.97	31.63	43.6	52.25	64.13	77.44	86.01	97.77	107.53	118.24	131.98	140.12
42	21.91	31.6	43.55	52.21	64.09	77.68	86.52	98.29	108.05	118.76	132.52	140.7
45	21.97	31.76	43.67	52.26	64.18	77.77	86.9	98.66	108.38	119.11	132.86	140.99
50	22.06	31.76	43.73	52.33	64.26	77.93	87.52	99.26	109.02	119.77	133.53	141.76
52	22.08	31.79	43.72	52.39	64.28	77.98	87.75	99.52	109.24	120	133.74	
56	22.01	31.65	43.6	52.25	64.15	77.89	88.02	99.77	109.5	120.25	134.01	
59	21.99	31.73	43.67	52.27	64.19	77.84	88.32	100.1	109.8	120.54	134.31	
63	22.01	31.69	43.65	52.3	64.19	77.88	88.56	100.45	110.21	120.94	134.67	
66	21.57	31.34	43.26	51.88	63.7	77.42	88.19	100.31	110.11	120.85	134.44	
70	21.91	31.65	43.57	52.2	64.1	77.81	88.59	100.97	110.71	121.44	135.13	
73	21.94	31.56	43.56	52.2	64.1	77.83	88.66	101.29	111.03	121.76	135.47	
78	21.06	30.87	42.8	51.41	63.2	76.92	87.73	100.76	110.57	121.27	134.92	
80	22.06	31.87	43.73	52.35	64.29	77.98	88.78	101.93	111.68	122.43	136.16	
84	22.28	32.03	43.98	52.61	64.41	78.22	89.04	102.46	112.3	122.99		
87	22.28	32	43.93	52.6	64.39	78.18	89	102.65	112.45	123.15		
91	22.25	31.99	43.93	52.59	64.38	78.16	89	102.97	112.76	123.46		
95	22.24	31.99	43.97	52.55	64.43	78.21	89.05	103.19	112.97	123.64	137.32	
102	22.26	32	43.96	52.53	64.51	78.25	89.09	103.24	113.02	123.68		
107	22.25	31.99	43.93	52.59	64.4	78.17	89.08	103.9	113.7	124.36	138	
109	22.28	32.01	43.99	52.63	64.42	78.22	89.1	104.05	113.89	124.54	138.16	
112	22.26	32.98	43.96	52.57	64.37	78.11	89.01	104.17	114.01	124.7	138.33	
115	22.16	31.86	43.81	52.46	64.23	78.06	88.9	104.12	114.05	124.75	138.34	

Differential Heave (cm) at Site 2

Magnetic Number

Day	M201 M202	M202 M203	M203 M204	M204 M205	M205 M206	M206 M207	M207 M208	M208 M209	M209 M210	M210 M211	M211 M212	Total Heave
0	0	0	0	0	0	0	0	0	0	0	0	0
21	.04	.03	.4	.72	-.07	.07	.05	-1.09	1.96	-2.16	-.35	.22
24	.99	.01	.59	1.13	-.18	.05	.03	-.14	.71	-.54	-.62	2.03
28	-.09	.05	.65	1.63	-.01	.05	.02	-.12	.7	-.54	-.63	2.75
31	.07	.02	.57	1.79	.27	0	.03	-.1	.7	-.54	-.65	3.21
35	-.08	.05	.64	1.85	.76	.03	0	-.1	.7	-.54	-.62	3.81
38	-.01	.04	.58	1.92	1.13	.07	-.02	-.12	.68	-.52	-.64	4.16
42	-.02	.02	.59	1.92	1.58	.09	-.01	-.11	.68	-.55	-.6	4.47
45	-.07	.03	.65	1.85	1.94	.12	.03	-.11	.68	-.58	-.6	4.79
50	-.04	.01	.66	1.85	2.22	.39	.04	-.11	.68	-.56	-.56	5.33
52	.06	-.03	.59	1.89	2.22	.68	.03	-.15	.7	-.57	-.61	5.67
56	-.03	.03	.6	1.9	2.3	1.14	.01	-.11	.72	-.56	-.51	6.34
59	-.02	-.01	.67	1.86	2.33	1.32	.04	-.15	.73	-.58		6.55
63	-.09	.01	.65	1.87	2.37	1.68	.02	-.14	.72	-.56		6.82
66	.01	0	.6	1.89	2.28	2.03	.05	-.17	.71	-.55		7.12
70	-.05	.02	.65	1.86	2.32	2.23	.16	-.11	.7	-.59		7.48
73	.04	-.02	.62	1.79	2.35	2.32	.39	-.07	.71	-.73		7.25
78	.01	-.02	.63	1.87	2.34	2.33	.65	-.13	.7	-.63		7.94
80	-.11	.06	.64	1.87	2.36	2.38	.9	-.13	.7	-.61		8.28
84	.08	-.01	.61	1.76	2.35	2.36	1.3	-.06	.67	-.67		7.73
88	.08	-.09	.62	1.91	2.32	2.35	1.42	-.12	.72	-.59		8.97
94	.02	.01	.63	1.77	2.44	2.37	1.69	-.03	.65			
87	-.01	-.01	.67	1.76	2.42	2.37	1.92	-.07	.67			
91	.01	0	.66	1.76	2.41	2.39	2.24	-.08	.67			
95	.02	.04	.58	1.85	2.41	2.39	2.41	-.09	.64	-.64		10.13
102	.01	.02	.57	1.95	2.37	2.39	2.42	-.09	.63			
107	.01	0	.66	1.78	2.4	2.46	3.09	-.07	.63	-.68		10.81
109	0	.04	.64	1.76	2.43	2.43	3.22	-.03	.62	-.7		10.97
112	.99	-.96	.61	1.77	2.37	2.45	3.43	-.03	.66	-.69		11.14
115	-.03	.01	.65	1.74	2.46	2.39	3.49	.06	.67	-.73		11.15

APPENDIX III

FURTHER INFORMATION ON INSTRUMENTATION FOR THE THIRD FREEZE PERIOD

III.1 Petur Pressure Meters

III.1.1 Assembly

All transducers were placed in a silicon oil bath for a minimum of 48 hours prior to joining to the brass coupling and pressure sensitive rubber bulb. Degassing of both parts was ensured prior to assembly. Particular care must be taken to ensure that no air is trapped within the components. Important areas to check are:

1. the space between the brass casting and rubber bulb
2. within the brass casting
3. within the threads of the casting and coupling
4. within the nylon pressure fittings
5. within the pressure transducer, particularly the wire mesh protection filter.

There is no way to visually inspect the interior of the pressure transducer so there is no absolute assurance that no air bubbles remain within the apparatus. Purging should continue periodically over at least 24 - 48 hours.

The assembly and tightening were carried out while all the components were submerged in the silicon oil to ensure that all spaces were filled with oil. An attempt was made to tighten all units in the same manner. All were handtightened follwed by a further tightening with wrenches of between 1 1/4 to 1 1/2 turns

of the brass coupling.

Units were then removed from the bath, cleaned and inspected for leaks. Of the 20 assemblies 6 were found to be defective because of leaks:

1. no leaking was observed at the couplings
2. all leaks involved perforation of the pressure sensitive rubber bulb

III.1.2 Leak Detection, Repair and Modification to the Sensors

Minute holes, most likely caused by pinching were found generally in two locations (see also Figure III.1):

1. where the collar holding the bulb in place and been drawn tight
2. where the bulb passes over the edge of the casting

A third location which did not cause leaking was at the base of the bulb. This was probably caused by finger nails or a hard object used to push the bulb in place (see #3 on Figure III.1). With case #1 the holes were probably caused when a hard object (not necessarily sharp) hit the edge of the casing thus pinching the rubber. Tests in the lab at Caen showed that a firm but light tap was sufficient to puncture the rubber. Holes at location #2 (Figure III.1) were caused either by the collar itself or the tightening tool. This problem is more severe in the castings for the omni-directional units since the notch for the collar is much deeper than the uni-directional units. Over tightening of the collars could also contribute to the problem.

III.1.2 Modifications Being Investigated for Future Installations

These findings by the Caen staff and the tests in Ottawa in light of these, have necessitated a redesign of the bulb fitting of the pressure sensors. Not only were the rubber bulbs more sensitive to installation procedures than originally perceived but the rubber appears to degenerate when left in contact with water. This latter aspect was not anticipated given the description and composition of the bulb material. Subsequently a suitable rubber bulb has been located which is more robust in nature and does not degrade in contact with soil water.

The brass fittings are being redesigned to remove any design flaws which may lead to inadvertent puncture. Also the use of silicon grease and silicon rubber are being investigated as possible replacements for the use of silicon oil to fill the bulb cavity. Silicon rubber appears to be a suitable alternative and further developments will be reported in subsequent reports.